

eman ta zabal zazu



Universidad del País Vasco Euskal Herriko Unibertsitatea

Design and energy consumption of invariant based shortcuts to adiabaticity

Ander Tobalina

Supervisors:

Prof. J. Gonzalo Muga

Dr. Ion Lizuain

Departamento de Química-Física
Facultad de Ciencia y Tecnología
Universidad del País Vasco/Euskal Herriko Unibertsitatea
(UPV/EHU)

Leioa, January 2021

**TESI ZUZENDARIAREN BAIMENA TESIA
AURKEZTEKO**

**AUTORIZACIÓN DEL/LA DIRECTORA/A
DE TESIS PARA SU PRESENTACIÓN**

Zuzendariaren izen-abizenak /Nombre y apellidos del/la director/a: **Juan Gonzalo Muga Francisco**

IFZ /NIF: **30553396N**

Tesiaren izenburua / Título de la tesis: **Design and energy consumption of invariant based shortcuts to adiabaticity**

Doktorego programa / Programa de doctorado: **Doctorado en Láseres y Aplicaciones en Química (Quimiláser)**

Doktoregaiaren izen-abizenak / Nombre y apellidos del/la doctorando/a: **Ander Tobalina Novo**

Unibertsitateak horretarako jartzen duen tresnak emandako ANTZEKOTASUN TXOSTENA ikusita, baimena ematen dut goian aipatzen den tesia aurkez dadin, horretarako baldintza guztiak betetzen baititu.

Visto el INFORME DE SIMILITUD obtenido de la herramienta que a tal efecto pone a disposición la universidad, autorizo la presentación de la tesis doctoral arriba indicada, dado que reúne las condiciones necesarias para su defensa.

Tokia eta data / Lugar y fecha: **Leioa, 25 de enero de 2020**

Sin. / Fdo.: Tesiaren zuzendaria / El/La director/a de la tesis

J. Gonzalo Muga

**TESI ZUZENDARIAREN BAIMENA TESIA
AURKEZTEKO**

**AUTORIZACIÓN DEL/LA DIRECTORA/A
DE TESIS PARA SU PRESENTACIÓN**

Zuzendariaren izen-abizenak /Nombre y apellidos del/la director/a: **Ion Lizuain Lilly**

IFZ /NIF: **35778769S**

Tesiaren izenburua / Título de la tesis: **Design and energy consumption of invariant based shortcuts to adiabaticity**

Doktorego programa / Programa de doctorado: **Doctorado en Láseres y Aplicaciones en Química (Quimiláser)**

Doktoregaiaren izen-abizenak / Nombre y apellidos del/la doctorando/a: **Ander Tobalina Novo**

Unibertsitateak horretarako jartzen duen tresnak emandako ANTZEKOTASUN TXOSTENA ikusita, baimena ematen dut goian aipatzen den tesia aurkez dadin, horretarako baldintza guztiak betetzen baititu.

Visto el INFORME DE SIMILITUD obtenido de la herramienta que a tal efecto pone a disposición la universidad, autorizo la presentación de la tesis doctoral arriba indicada, dado que reúne las condiciones necesarias para su defensa.

Tokia eta data / Lugar y fecha: **Leioa, 25 de enero de 2020**

Sin. / Fdo.: Tesiaren zuzendaria / El/La director/a de la tesis



Ion Lizuain Lilly

AUTORIZACIÓN DE LA COMISIÓN ACADÉMICA DEL PROGRAMA DE DOCTORADO

La Comisión Académica del Programa de Doctorado en

Láseres y Aplicaciones en Química (Quimiláser)

en reunión celebrada el día 26 de enero de 2020, ha acordado dar la conformidad a la presentación de la Tesis Doctoral titulada:

Design and energy consumption of invariant based shortcuts to adiabaticity

dirigida por el/la Dr/a. **Juan Gonzalo Muga Francisco** y por el/la Dr/a **Ion Lizuain Lilly**

y presentada por Don/Dña. **Ander Tobalina Novo**

adscrito o adscrita al Departamento de **Química-Física**

En Leioa a 26 de enero de 2020

EL/LA RESPONSABLE DEL PROGRAMA DE DOCTORADO



Fdo.: Francisco J. Basterretxea

AUTORIZACIÓN DEL DEPARTAMENTO

El Consejo del Departamento de **Química-Física**

en reunión celebrada el día 27 de enero de 2020 ha acordado dar la conformidad a la admisión a trámite de presentación de la Tesis Doctoral titulada:

Design and energy consumption of invariant based shortcuts to adiabaticity

dirigida por el/la Dr/a. **Juan Gonzalo Muga Francisco** y por el/la Dr/a **Ion Lizuain Lilly**

y presentada por Don/ña. **Ander Tobalina Novo**


ante este Departamento.

En Leioa a 27 de enero de 2020

VºBº DIRECTOR/A DEL DEPARTAMENTO


SECRETARIO/A DEL DEPARTAMENTO

Fdo.:


Fdo.: **José Luis Vilas**

Fdo.:




Fdo.: **Leyre Pérez**

ACTA DE GRADO DE DOCTOR O DOCTORA
ACTA DE DEFENSA DE TESIS DOCTORAL

DOCTORANDO/A DON/DÑA. **ANDER TOBALINA NOVO** _____

TITULO DE LA TESIS: **DESIGN AND ENERGY CONSUMPTION OF INVARIANT BASED SHORTCUTS TO ADIABATICITY** _____

El Tribunal designado por la Comisión de Postgrado de la UPV/EHU para calificar la Tesis Doctoral arriba indicada y reunido en el día de la fecha, una vez efectuada la defensa por el/la doctorando/a y contestadas las objeciones y/o sugerencias que se le han formulado, ha otorgado por _____ la calificación de:
unanimidad ó mayoría

--

SOBRESALIENTE / NOTABLE / APROBADO / NO APTO

Idioma/s de defensa (en caso de más de un idioma, especificar porcentaje defendido en cada idioma):

Castellano _____

Euskera _____

Otros Idiomas (especificar cuál/cuales y porcentaje) _____

En _____ a _____ de _____ de _____

EL/LA PRESIDENTE/A,

EL/LA SECRETARIO/A,

Fdo.:

Fdo.:

Dr/a: _____

Dr/a: _____

VOCAL 1º,

VOCAL 2º,

VOCAL 3º,

Fdo.:

Fdo.:

Fdo.:

Dr/a: _____ Dr/a: _____ Dr/a: _____

EL/LA DOCTORANDO/A,

Fdo.: _____

“I did it my way”

Acknowledgements

El trabajo de investigación puede ser tan gratificante en algunas ocasiones, como frustrante en otras. Es en esos momentos no tan buenos en los que es vital contar con gente en la que apoyarse. Si bien es probable que nunca me hayáis escuchado decirlo, espero que seáis conscientes de lo importantes que sois para mí.

Gonzalo, Ion, confiasteis en mí cuando ni siquiera yo lo hacía, me habéis brindado la oportunidad de mi vida. Mikel, Sofía, Miguel, compartirlo con vosotros ha hecho que recorrer este camino haya sido un verdadero placer. Aita, Ama, Marcos, no he recibido otra cosa que no fuera apoyo por vuestra parte, sobra decir que si hoy estoy aquí es gracias a vosotros. Kuadrilla, le alegráis a uno la vida, espero que siempre sigáis ahí. Sara, iba a decir que deberías ser la persona que menos necesita oír lo importante que es para mí, a lo que probablemente contestarías que aun así quieres escucharlo. Sencillamente me haces feliz.

Sabed que este trabajo hubiera sido inviable sin vuestra presencia. Gracias de todo corazón.

Esta Tesis ha sido financiada a través de una beca predoctoral concedida por el Ministerio de Economía, Industria y Competitividad.

Contents

Acknowledgements	xv
List of publications	xix
1 Introduction	1
2 Scientific Context. Shortcuts to Adiabaticity	7
2.1 Introduction	7
2.2 Control of elementary motion operations	9
2.3 STA in quantum thermal machines	12
3 Summary of the Research	17
3.1 Goals	17
3.2 Results in energy consumption	19
3.2.1 Energy consumption for shortcuts to adiabaticity	19
3.2.2 Energy consumption for ion-transport in a segmented Paul trap .	20
3.2.3 Vanishing efficiency of a speeded-up ion-in-Paul-trap Otto engine	21
3.3 Discussion of the results in energy consumption	23
3.4 Results on the design of basic operations	25
3.4.1 Fast atom transport and launching in a nonrigid trap	25
3.4.2 Fast state and trap rotation of a particle in an anisotropic potential	26
3.4.3 Invariant-based inverse engineering of time-dependent, coupled harmonic oscillators	27
3.4.4 Time-dependent harmonic potentials for momentum or position scaling	28
3.5 Discussion of the results on the design of basic operations	29
3.6 Prospects for future research	31
4 Conclusions	33
Bibliography	35

Original publications 45

Please note that the numbers in this table may not coincide with the page numbers in the articles, as each of them retains its original numbering given by the corresponding journal.

Fast atom transport and launching in a nonrigid trap	45
Energy consumption for shortcuts to adiabaticity	57
Energy consumption for ion-transport in a segmented Paul trap	65
Vanishing efficiency of a speeded-up ion-in-Paul-trap Otto engine	77
Fast state and trap rotation of a particle in an anisotropic potential	85
Invariant-based inverse engineering of time-dependent, coupled harmonic oscillators	105
Time-dependent harmonic potentials for momentum or position scaling	113

List of publications

I) This thesis is composed by the following articles

1. A. Tobalina, M. Palmero, S. Martínez-Garaot, and J.G. Muga
Fast atom transport and launching in a nonrigid trap
Scientific Reports **7**, 5753 (2017) DOI: 10.1038/s41598-017-05823-x
2. E. Torrontegui, I. Lizuain, S. González-Resines, A. Tobalina, A. Ruschhaupt, R. Kosloff, and J.G. Muga
Energy consumption for shortcuts to adiabaticity
Phys. Rev. A **96**, 022133 (2017). DOI: 10.1103/PhysRevA.96.022133.
3. A. Tobalina, J. Alonso, and J. G. Muga
Energy consumption for ion-transport in a segmented Paul trap
New Journal of Physics **20**, 065002 (2018). DOI: 10.1088/1367-2630/aac685.
4. A. Tobalina, I. Lizuain, and J. G. Muga
Vanishing efficiency of a speeded-up ion-in-Paul-trap Otto engine
EPL (Europhysics Letters) **127**, 20005 (2019). DOI: 10.1209/0295-5075/127/20005.
5. I. Lizuain, A. Tobalina, A. Rodríguez-Prieto, and J. G. Muga
Fast state and trap rotation of a particle in an anisotropic potential
Journal of Physics A: Mathematical and Theoretical **52**, 465301 (2019). DOI: 10.1088/1751-8121/ab4a2f.
6. A. Tobalina, E. Torrontegui, I. Lizuain, M. Palmero, and J.G. Muga
Invariant-based inverse engineering of time-dependent, coupled harmonic oscillators
Phys. Rev. A **102**, 063112 (2020). DOI: 10.1103/PhysRevA.102.063112

7. J.G. Muga, S. Martínez-Garaot, M. Pons, M. Palmero, and A. Tobalina

Time-dependent harmonic potentials for momentum or position scaling

Phys. Rev. Research **2**, 043162 (2020). DOI: 10.1103/PhysRevResearch.2.043162

II) Other articles produced during the Thesis period

8. J.G. Muga, M.A. Simn, and A. Tobalina
How to drive a Dirac system fast and safe
New Journal of Physics **18**, 021005 (2016).
9. S. Gonzalez-Resines, D. Gury-Odelin, A. Tobalina, I. Lizuain, E. Torrontegui, and J. G. Muga
Invariant-Based Inverse Engineering of Crane Control Parameters
Phys. Rev. Applied **8**, 054008 (2017).
10. R. Dann, A. Tobalina, and R. Kosloff
Shortcut to Equilibration of an Open Quantum System
Phys. Rev. Lett. **122**, 250402 (2019).
11. I. Lizuain, A. Tobalina, A. Rodriguez-Prieto, and J.G. Muga
Invariant-based inverse engineering for fast and robust load transport in a double pendulum bridge crane
Entropy **22**, 350 (2020).
12. R. Dann, A. Tobalina, and R. Kosloff
Fast route to equilibration
Phys. Rev. A **101**, 052102 (2020).

1. Introduction

Technology began as long as 2.5 million years ago, by the time not a single *homo sapiens* had yet set a foot on the planet Earth, when early hominids, somewhere in east Africa, started manufacturing stone tools for hunting and food preparation. Someone may get confused by the use of the term technology here, used as we are nowadays to relate such term to the latest commercialized self phone or any other electronic device. However, technology is not only embedded in modern machinery, it also relates to knowledge. Knowledge of skills, methods and techniques that have allowed early and modern humans to interpret and control the world around them. Even if it does not sound as much for the present human, imagine the immense difference the use of tools would had constituted compared with hunting and manipulating food with your bare hands.

Over the years, the effort of countless individuals, some boosted by a welcoming atmosphere, others in lone endeavour, sometimes even against the prevailing wisdom and the prejudices of their times, has pushed the boundaries that limit our collective technological knowledge further and further. We, as a species, have come a long way from the control of the fire to the advent of the internet, through the early uses of metals, the development of agriculture, the invention of the wheel and the production of electricity. Nowadays technology has reached a level of sophistication unforeseeable for a person living at the turn of the XIX century. Humanity has taken a giant technological step in a ridiculously short period compared with the time humans have populated this planet (not to mention compared with the other cosmic time scales like the age of our planet or even the age of the universe). In few centuries we have provided our cities with light and our houses with running water and heating, we have developed self-propelled vehicles that take us wherever we want to go and established communication systems that allow us to be in direct contact with anyone around the globe.

One might wonder, however, if those technologies, that seem so liberating at first sight, do not hide an enslaving angle. Aside from the obvious fact that the intensive use of polluting machinery will cause (if it is not already causing) huge environmental issues, and the evidence that a large percentage of the global population takes close to none advantage of the technological improvements but gets their same ill consequences, it might be sound to ask ourselves whether we are relying too much on machines. Whether the offload in the every day duties provided by the beautiful pieces of technology we have today, will not lead to a demise of skills and techniques, technological knowledge after all, that humans have gathered during millennia. These issues, as relevant as they might be for the future of humanity, lay beyond the scope of this work, that, instead, is directed towards expanding our technological knowledge with the hope that future generations will make a good use of them. Namely, that they will provide ways to a more sustainable way of living without resulting in a loss of happiness. On the contrary, that they facilitate and extend the possibility to pursue happiness to the totality of human beings.

The latest step in our technological journey compels us to explore the bizarre quantum world. Bizarre in the sense that the behavior of microscopic objects, dictated by the laws of quantum mechanics, is hardly related to our everyday intuition of the physical world. As Richard Feynman once said, “it is very hard to imagine all the crazy things that things really are like”. The essence of quantum physics is probably best described by the double slit experiment. It consists on separating a wave, making it pass through a wall with two distant slits on it, and letting the two resulting wavefronts interact before measuring them. It was first performed by Thomas Young in 1801 with a beam of light [1], and then replicated by Davisson and Germer in 1927 for a beam of electrons [2]. In both demonstrations the results were well predicted by assuming that the beams behaved like waves. Despite these results, one could still support the idea that the wave-like behavior is due to the particles that form the beams, photons in the first experiment and electrons in the second, interacting between the wall and the measurement apparatus in some way that they resemble the dynamics of a wave, but that there is nothing fundamental behind it. The surprising thing is that, even when electrons are sent one by one, with no time to interact with one another, the result of the measurement suggests that they are behaving like waves [3]. This sets the ground for the concept of particle-wave duality, and demonstrates the fundamental probabilistic

nature of quantum mechanics.

The understanding of the discretized structure of energy levels and the wave-particle duality at the turn of the last century led to the first quantum revolution. It allowed for the development of most of the technology that underpins modern society. Every electronic device or modern communication system is based on quantum effects. The same is true for the GPS system and for medical applications such as the nuclear magnetic resonance. Today, we are in the midst of a second quantum revolution, devoted to take advantage of fundamental quantum phenomena such as superposition, tunneling, entanglement or coherence [4]. Almost every relevant device invented through the XXth century was based on some kind of knowledge of quantum properties, but they lacked the technology to alter quantum systems and engineer those properties at will. Today we are able to address individual quantum degrees of freedom and actively manipulate them. In the words of Dowling and Milburn, “The difference between science and technology is the ability to engineer your surroundings to your own ends, and not just explain them” [4], so we may state that the first quantum revolution was scientific in essence, while the second one will be, or it is already being, fundamentally technological.

Scientists envision huge possibilities in terms of increased precision and computing power, and the interest to develop quantum technologies is common for governments and companies all over the globe. Quantum metrology [5] and quantum communication [6], for example, are already a reality. The former employs quantum resources, such as entanglement, to increase the resolution on measurements of physical properties. The detection of gravitational waves in LIGO, a work that yielded Rainer Weiss, Barry Barish and Kip Thorne the 2017 Nobel prize in physics, probably constitutes the most sound example of metrology, and even though it was not based on quantum physics, there are proposals to implement quantum metrology in LIGO [7]. The latter studies the transmission of information encoded in quantum bits, also called qubits, and usually translates into protocols that apply some form of quantum cryptography to protect information channels against unwanted eavesdropping.

Possibly the less advanced branch of quantum technology, and, at the same time, the one that sparks the biggest interest, is quantum computation. The use of superposition and entanglement to perform computations promises to deliver a computer able to solve computational problems that a classical device would take an infinite amount of time

to solve. Many physical platforms pose as candidates to implement a working quantum computer (trapped ions and superconducting circuits for instance). Google's group lead by John Martinis claimed last year, not without certain controversy, to have achieved "quantum supremacy" (which means to solve a problem that no classical computer can solve) with their superconducting qubit processor [8]. More recently, the group lead by Jian-Wei Pan has claimed to have demonstrated the quantum computational advantage by implementing boson sampling in a photonic quantum computer [9]. Nevertheless, there are still some issues to be figured out and lot of work to be done in the road towards a useful quantum computer [10].

Technology, as we have just portrayed, has a history of its own, but, at the same time, it has shared most of its path with another brilliant human enterprise, Science. As the practical knowledge allowed for the rise of the first civilizations in the ancient near East, more fundamental questions about the nature of things arose and drew the interest of some curious minds. The development of advanced mathematics, for example, aside from the bare practice of counting, followed the necessity of distributing crop fields. The first insights of astronomy stemmed from the inability to navigate at night, when the absence of the sun made it impossible to discern the cardinal points. Even one of the most relevant human abilities, writing, unique among any other animal and what structures our conception of history, arose from the need of keeping track of commercial exchanges. The advent of technology based on quantum properties makes this relation stronger than ever.

Science and technology have, in principle, disparate goals. Science builds and organizes knowledge, but, importantly, it does so with no particular goal in mind other than pure curiosity on the behavior of the world around us. This statement, of course, does not mean that science is useless, it rather means that, in principle again, it has no practical application as a direct objective. In fact, history has proven over and over again that science makes the perfect travel companion for technology. Isn't it true, by any chance, that the developments of wireless telegraphy, a technological breakthrough that shapes the world today and for what Guglielmo Marconi and Karl Ferdinand Braun won the 1909 physics Nobel Prize, would not have been possible without the previous research on electromagnetic waves carried out by James Clerk Maxwell and Heinrich Rudolf Hertz? A work, must be emphasized, inspired only by the will of satisfying a purely theoretical curiosity.

The clear distinction drawn in the previous paragraph between science and technology is, to say the least, blurred nowadays. The basic logic of our market driven societies, that is, the pursue of economic benefits over any other considerations, has also reached the academic sphere and purely abstract theoretical research is hard to justify (even harder to fund) within that framework. Inevitably, as the popular saying goes, we are all children of our own time, and so, the research carried out for this Thesis has a technological prospect throughout. Nonetheless, we hope to have made a contribution, however small, to fundamental science. The main topic of research is the behavior and control of microscopic objects, what constitutes simultaneously one of the current frontiers of physics and one of the greatest avenues for developing new technologies. Thus, I cannot help feeling as a part of the long human effort to both understand and govern the Universe.

The work done during the last four years is contained in seven articles, already published in various scientific journals and provided here in the last section of the Thesis. This first part is thought as an introductory guide to my work. In section 2 explains the state of the art of the field in which this Thesis is inscribed, introducing the reader to the concept of Shortcuts to adiabaticity (STA) and its intersection with the ever growing field of quantum thermodynamics. Section 3 summarizes the research: it sets the research goals, outlines the obtained results and discusses them briefly. For a more complete display of the results I refer the reader to the original articles, which constitute the core of this Thesis. Finally, section 4 contains some general conclusions. Inevitably, the exploratory nature of our work has caused some deviations from the original goals established back in 2017, but the overall tone of the research has followed the initial plan.

2. Scientific Context. Shortcuts to Adiabaticity

2.1 Introduction

The topic that wraps this Thesis and provides a common framework for the research that I have carried out for the last four years is "Shortcuts to Adiabaticity". In order to dig into this concept, it seems appropriate to begin with the definition of adiabaticity. Let us start by mentioning that the traditional notion of adiabaticity, used in thermodynamics to describe processes in which no heat exchange takes place, is not the meaning we will be using here. Our research applies mainly (but not exclusively) to microscopic objects that obey quantum mechanics. The meaning of adiabaticity in this context is encapsulated in the adiabatic theorem, that, as stated by Max Born and Vladimir Fock back in 1928, and translated here from the original German, declares that *a physical system remains in its instantaneous eigenstate if a given perturbation is acting on it slowly enough and if there is a gap between the eigenvalue and the rest of the Hamiltonian's spectrum* [11]. Thus, here we understand adiabatic processes as those for which some dynamical properties remain invariant as a consequence of the slow changes of the controls. Examples of those properties, referred to as adiabatic invariants, are the quantum number in quantum systems or the phase-space area in classical systems.

In the quantum case, the fact that the populations -for instantaneous Hamiltonian eigenstates that adapt to control changes- remain constant over time is a key feature to attain exhaustive control over microscopic systems. Adiabatic processes are thus specially well suited to provide the fundamental operations needed to develop quantum technologies. However, they come with a downside. In practice, they could imply really

long times (compared to other relevant scales), which may induce decoherence and make the system prone to the noise present in the environment and in the control elements. Additionally, there are many interesting applications that require repetitive operations, such as information processing [12] or cyclic thermal devices [13], in which, obviously, long process times become an issue to be avoided.

Shortcuts to adiabaticity are fast routes that mimic the result of an adiabatic evolution. They procure the same benefits of adiabatic processes regarding controllability and avoid the drawbacks of the implied long times. STA methods were first applied in simple quantum systems: two and three-level systems [14] or a particle in a time-dependent harmonic oscillator [15, 16]. Since then, the concept of STA has been extended to various fields, facilitated by the widespread use of slow operations to avoid undesired excitation during the manipulation of a system and as state preparation in a broad domain of areas such as optics, solid state, chemistry and even classical mechanical systems and engineering. Another relevant aspect of STA is their flexibility. For a given system and operation, there are typically many different routes to implement the shortcut, which, aside from speeding up the process, allows to optimize physically relevant variables, for example, to minimize transient energy excitations and/or energy consumptions or to maximize robustness against perturbations.

A distinction can be made between (i) STA methods that keep the structure of some Hamiltonian form and design the time dependence of the control parameters, and (ii) techniques that add new terms to the original Hamiltonian. Both approaches may be useful in different scenarios. Structure-preserving methods usually allow for transient excitations, while the methods that require additional terms manage to follow the adiabatic path (defined with respect to the Hamiltonian without added terms) at all times. The first ones rely on the existence of non-trivial (non constant, time-dependent) operators whose expectation values remains constant for a given evolution, i.e., “invariants”, which are not always easy to find. In the other approach, a frequent problem with the additional terms is the difficulty to implement them in the experiments.

The work of this Thesis is divided into two main thematic areas, one is the STA control of basic motion operations relevant for the implementation of quantum technologies, and the other one is the assessment of the energy consumption in sped up operations and the implications of the use of STA in quantum thermal machines.

2.2 Control of elementary motion operations

There are many settings that benefit from a speedup of fundamental operations. In mechanical engineering setups, robotic arms or overhead cranes may implement STA to achieve accelerated and robust protocols that enhance accuracy and efficiency. In optics, where time usually translates into the size of the lenses and other devices, faster operations imply smaller, more compact gadgets. In quantum information processing STA fit smoothly within the two main paradigms. Adiabatic computing may become a reality by speeding up the transition from the initial to the final Hamiltonian, whereas the gate based paradigm could profit from faster state preparation and sped up fundamental operations that implement quantum gates. Besides fighting decoherence, STA may also help to find scalable architectures, since the need for error-correction codes, and therefore the amount of required qubits, gets reduced as decoherence is mitigated.

One of the legs of this Thesis focuses on designing protocols for basic operations through invariant-based shortcuts, a type of STA that preserves the structure of the Hamiltonian. In essence, it consists on deducing the required time dependence of the control parameters from a prescribed evolution of the system. In 1969, Lewis and Riesenfeld introduced a time-dependent hermitian operator whose expectation values for a state driven by a time-dependent harmonic oscillator Hamiltonian would remain constant in time [17]. This dynamical invariant was originally used to solve the dynamics of the system. In order to develop STA, Chen et. al. reversed this idea, setting first the desired evolution of the system and inferring the Hamiltonian from it [15]. The invariant operator, and consequently the evolution of the system, is defined in terms of an auxiliary time-dependent parameter, which obeys some equation that, crucially, depends on the control parameters in the Hamiltonian. Then, one may determine the desired evolution of the system by setting the shape of the auxiliary parameter, and inverse engineer the required controls, that is, solve the auxiliary equation to find the time-dependence of the control parameters that drives the intended evolution.

Many dynamical invariants exist for the same system. Depending on the operation and the system we could choose one or another to design the shortcut. A particularly fruitful one, related to a system subject to a specific form of potential, was introduced by Lewis and Leach in the context of classical Hamiltonians [18] and then extended to

quantum systems by Dhara and Lawande [19]. This quadratic-in-momentum invariant has been thoroughly exploited to speed up various operations such as cooling [15] or shuttling atoms in harmonic traps [16], and has been even extended to state transfer operations in two-level systems [20]. The idea of invariant-based inverse engineering applies as well to other systems and operations, and finding relevant invariants for larger sets of Hamiltonians -and systems- has been an important research task during the last ten years.

An area that could benefit from suitable invariant-based inversely engineered protocols is the control of few body systems described by multidimensional time-dependent Hamiltonians. Rooted partly in the foreseen potential of quantum information processing, there is widespread interest to achieve precise control over systems comprised of interacting particles. For instance, a proposal to accomplish large-scale quantum computation in the context of trapped ions, one of the most developed physical platforms to implement quantum technologies, relies on controlled multi-ion tasks [12]. The interest, however, is not just limited to trapped ion setups. In fact, cavity quantum electrodynamics setups [21] and optomechanical systems [22] are often governed by the same equations as interacting trapped ions [23] and could thus benefit from similar control protocols.

A crucial notion to address the extension of STA to systems formed by interacting parts is the concept of dynamical normal modes. A static Hamiltonian describing the coupled dynamics of two bodies may be rewritten in terms of different variables, in a way that, in the new frame, the dynamics may be seen as composed by independent motions (normal modes) of harmonic oscillators. If the Hamiltonian depends on time, however, the decoupling might be nothing but a mirage. In general, the transformation that leads to independent motions is only valid at a given instant of time, as the time-dependence of the Hamiltonian couples the evolutions of the instantaneous normal modes. In other words, the old Hamiltonian expressed in the new variables is not generally the Hamiltonian that describes the system in the new set of coordinates. The dynamical normal modes are a useful generalization of instantaneous, static normal modes that correspond to truly independent motions of (generally) time-dependent harmonic oscillators.

Recent efforts to extend invariant based STA to effective 2D systems have exploited this new concept. For example, certain manipulations of two ions interacting through

the Coulomb force are suitably described by independent dynamical normal modes, what allowed Palmero and collaborators to apply already existing inverse engineering techniques based on the Lewis-Leach invariant to rapidly shuttle [24, 25], squeeze [26] and separate [27] the ions. Following these works, Lizuain et al. [28] identified the general condition for which a point transformation of a two-dimensional Hamiltonian that evolves in time leads to decoupled dynamical modes: the potential should not rotate in the 2D space. Rotation thus stands as the paradigmatic problem to extend invariant based shortcuts beyond separable problems, amenable to well established inverse engineering techniques.

This Thesis goes beyond this state of the art in different ways: In a very practical vein, we design complex launching processes which may be of use, for example, to produce ion implantation with an accurately chosen energy spectrum. We also study how to manipulate the rotations of a trap so that a trapped particle ends up in a state which is simply a rotated copy of the original one, without further excitation, a much needed operation in some architectures. This goal is technically achieved by finding dynamical normal modes via variable transformations which are not point-transformations; we also treat the generic difficulty to deal with “coupled systems” -without dynamical normal modes- and put forward a new approach, namely, inverse engineering based on a 2D invariant. Finally we explore and use linear (rather than quadratic) invariants to implement a set of powerful robust scaling operations on simple harmonic systems.

2.3 STA in quantum thermal machines

Back in 1824, Sadi Carnot theorized the performance of heat engines in his book *Reflections on the Motive Power of Fire*, considered by many as the foundational work of thermodynamics, and introduced the first modern day definition of work: a weight lifted through a height. Before that, James Watt had already introduced his design of the steam engine, which was to become the driving force behind the industrial revolution, and Nicolaus Otto had built the first working four-stroke engine, what triggered the fabrication of automobiles. It was precisely the need to be consistent with thermodynamics what lead to Plank's ideas on the black body radiation [29] and Einstein's conclusion that light is quantized [30]. These works are the dawn of quantum theory, and granted their authors the Nobel prizes in Physics the years 1918 and 1921 respectively. Despite such early connection, thermodynamics and quantum theory evolved independently for several years.

The study of thermodynamics in the early XXth century was based on ideal, reversible processes. The assumption was that the system evolved through a series of equilibrium states, in which all macroscopic flows are zero, so even if the system changed in time, it was never out of equilibrium. The laws of thermodynamics were developed based on this assumption. It was not until the year 1975 when, being immersed in the study of the energy consumption of industrial processes and the consequent air pollution, Steve Berry was asked, "Why did you compare the actual energy with the ideal thermodynamic limits?... Who would wait for delivery of a car from a manufacturer who claimed to make his cars reversibly?" [31]. Soon after, when Peter Salamon, by then a freshman graduate student looking for an advisor, approached Berry and explained him his idea of exploring the differential geometry of thermodynamics, he answered "While youre at it, can you put time in?" [31]. That same year, Curzon and Ahlborn published their work on the efficiency of a Carnot engine operating at maximum power [32], which already considered a thermodynamic process at a finite rate, and two years later Berry, Salamon and collaborators published the first paper on finite-time thermodynamics [33].

Introducing time in thermodynamics created many new research avenues. Among them, the idea of optimizing the motion of the piston to improve the performance of an engine is particularly relevant for this Thesis. Mozurkevich and Berry used methods

from optimal control theory to optimize the maximum work per cycle of an internal combustion Otto engine [34, 35]. For fixed fuel consumption and cycle time, they optimized the engine by controlling the time-dependent volume of the gas inside the combustion chamber, which could be implemented, they claimed, by developing an alternative mechanism for connecting the piston to the crankshaft. However, this interesting idea was never fully developed, and, today, automobiles and other self propelled vehicles are driven by engines whose piston evolves as dictated by the evolution of the working fluid, with no special components intended to optimize its movement.

The paths of thermodynamics and quantum theory crossed again in 1959. Scovil and Schulz-DeBois explained the equivalence of a Carnot engine with a three level maser [13], setting the stage for new questions such as, what is the limit of miniaturization of a heat engine? or, can we build an engine that exploits quantum properties to surpass the classical thermodynamic limits? These and other similar ideas boosted the development of quantum thermodynamics [36, 37], a field that addresses the emergence of thermodynamic laws from quantum mechanics. Now we know that it is possible to build a heat engine whose working substance is a single atom [38], while the answer to whether there is quantum supremacy in the context of thermal machines remains a matter of debate.

The Otto cycle has been a historically useful tool to theorize thermodynamical processes. At a smaller scale, a quantum harmonic oscillator running an Otto cycle has been a fruitful model for a microscopic engine [39]. Compared to its macroscopic counterpart, the frequency acts as the inverse of the volume and the harmonic potential plays the role of the piston. Also, increasing the rate of the cycle enhances quantum friction the same way it increases dissipation in the classical case [40, 41]. Another relevant component of an operating engine is the mechanism to transfer the produced mechanical work to a system that either uses it to generate some dynamics, or stores it in a useful manner (battery). The original definition of work by Carnot can be adapted to a quantum context by understanding work as a state lifted from a lower to a higher discrete energy level, which could be seen as a quantum battery. The quantum harmonic oscillator that acts as the working medium of the engine should thus be coupled to an additional system in such a way that the work resulting from a completion of the cycle leads to a jump in the energy levels of the battery. Otherwise, the work generated by the cycle gets lost among the many degrees of freedom of the control fields. A particular proposal

considers another quantum harmonic oscillator, coupled to the working medium one, acting as the “flywheel” of the microscopic engine [42].

Connecting to Mozurkevich’s and Berry’s idea, STA have been used to optimize a quantum harmonic Otto engine by designing the evolution of the harmonic potential to produce “frictionless strokes” [43, 44]. STA reproduce the result of an adiabatic evolution in an arbitrary short time, so, at first sight, it seems that the use of STA in thermodynamic cycles provides increasing power without diminishing the efficiency of the device. STA community has nevertheless moved away from that perception. The existence of an energy “cost” inherent to STA is a widely accepted idea, but there is little agreement on the definition of such cost [45–49]. Those definitions are not contradictory, they rather address different energy flows or even different aspects of the system. Moreover, shortcuts to adiabatic expansions and compressions of single harmonic oscillators are well known, but, to the date, there are no devised shortcuts to adiabatic frequency change of coupled harmonic oscillators. Therefore, speeding up the cycle of a microscopic engine connected to a quantum flywheel so that the achieved work gets appropriately stored requires to develop new STA.

Another central debate within the field of quantum thermodynamics is the definition of work in the quantum realm. The fundamental reason is that work, unlike position or angular momentum, characterizes a process rather than a state, so there is no well defined operator that describes it, i.e., it is not an observable [50]. Attempts to define quantum work rely necessarily on some sort of measurement [51], so the definition of work depends on the particular type of measurement and on the resulting back-action. Further issues arise to define the work provided, or required, by a non-autonomous system, as we can define it inclusively or exclusively [52]. Moreover, a Hamiltonian that provides the correct equations of motion may not correspond to the energy of the system, since time-dependent Hamiltonians provide the physical energy of the system only if the appropriate gauge transformation has been applied [53]. Even more generally, the answer we get depends on the question we ask, so how we define the system of study, the choice of including certain elements and leaving some others out of it, shapes the results we obtain for the work produced or required by that system.

This Thesis contributes to reach some level of agreement regarding the cost of STA.

We advocate for a definition in terms of the total energy consumed to perform the operation, which, in most cases, includes the power required to generate the control fields. We assess the consumption of various operations in both classical and quantum systems, reaching some general conclusions and noticing that, indeed, this “cost” increases with the rate of the process. Our approach may also provide for a better understanding of more fundamental questions such as the role of external driving in the definition of work in microscopic systems and the suitability of quantum heat engines.

3. Summary of the Research

3.1 Goals

This Thesis, as said, comprises two general goals. As a consequence, the Thesis consists of two groups of publications, each addressing clearly distinguishable topics.

The first goal is to assess the energy cost of shortcuts to adiabaticity, quantifying the energy consumption of sped up operations in different setups to extract some general conclusions. It was first addressed in [54] and followed by [55, 56]. We aim to find a sensible definition of cost based on a fair assessment of all the energy flows required to perform a STA operation. We intend to start by quantifying the consumption of a classical mechanical system, and then extend the findings to quantum models, to end up analyzing the performance of a specific quantum engine taking account of the cost of STA. The fulfillment of this goal would entail a considerable step towards a general agreement on the definition of the cost of shortcuts. In fact, there is no need to have a single definition of cost. It is obvious by now that driving a system using STA implies many differences regarding transient excitations and fluctuations with respect to adiabatic manipulations or other simpler protocols. However, we aim to clarify that the intuitive idea that accelerating a process always leads to increasing dissipation and, in general, to a higher energy need, remains true in the context of STA applied to quantum systems when we consider a broader picture. Additionally, with this study we aim to shed some light on such a central concept in thermodynamics as work.

The second target is to extend the domain of systems amenable to invariant based inverse engineering STA and design operations that are relevant for the development of quantum technologies. It is undertaken in [57–60]. First we want to design STA to accelerate combined operations for which shortcuts have been already proposed. Then

we plan to speed up 2D anisotropic rotations, which, as explained in the introduction, constitutes the paradigmatic model for processes in which a point transformation does not provide independent normal modes. Additionally, we are open to the idea of finding new invariants that allow to address directly the 2D dynamics, instead of the separate 1D dynamics of the normal modes. The motivation behind this goal has been already hinted in the introduction: the huge interest on developing a working quantum processor draws forth the search of shortcuts to adiabatic manipulations of coupled systems that are not limited to decoupled dynamical normal modes. The case of coupled harmonic oscillators with controllable and dispare angular frequencies is of particular interest in this regard. The development of STA for this example would also allow to address more realistic quantum engines consisting of a cyclic working medium connected to a battery.

3.2 Results in energy consumption

3.2.1 Energy consumption for shortcuts to adiabaticity

The opening step towards the first goal was taken in [16]. Here we assess the energy consumption of an STA protocol implemented in an overhead crane. We model the system as a load hanging from an inelastic rope whose higher end is attached to a moving trolley. At a higher level of abstraction, the system can be seen as a rigid pendulum with moving swing point. We consider a transport operation that moves the swinging point of the pendulum, and design a STA so that the load ends up the process with the same energy it had at the beginning. We start by writing down all the energy flows of the system and derive the motion of each body (load and trolley) using the Euler-Lagrange equations. Dissipation, which in our case is due to mechanical friction, enters the description through a Rayleigh function. The dynamics of the load in the small oscillation regime resemble the motion of a forced harmonic oscillator, so we are able to inverse engineer the evolution of the system based on the Lewis-Leach invariant.

The energy required to perform the operation is injected to the system from the exterior, and modeled in our analysis as a force acting on the trolley. The power exerted by that force is compared with the rate of change of the load's mechanical energy. We see that they only agree when the trolley is massless and there is no friction on the system. We demonstrate that those conditions are either unattainable or undesirable. The whole point of STA is to perform fast operations, and we know that any process carried out at a finite rate incurs in some form of dissipation. Thus, even if the mechanical friction of our model could be diminished by reducing the rate of the process, this is definitely not the regime of interest throughout this Thesis. Moreover, a large trolley mass compared to the mass of the load decouples the external force from the dynamics of the load, as it makes the back-action from the swinging motion of the pendulum negligible. This is in line with the spirit of useful shortcuts, designed to drive the systems to the final configuration without final excitation regardless of the particular starting point. The limit of small trolley mass is therefore, undesirable, as it would force us to design a different shortcut for each initial condition.

The description of the load's motion as a forced harmonic oscillator that underpins the design of the STA is only valid in the small oscillation regime, so our protocol will not serve its purpose whenever the load deviates too much from the equilibrium axes. We exploit the mentioned flexibility of STA and, by minimizing the difference between the initial and final energies of the load, we redesign the protocol to suitably drive the system when the initial angle of the load lays beyond the small oscillation regime. Besides, we combine STA with optimal control theory to design a protocol that minimizes the energy consumption. We find out that, for fast transformations, the optimal protocol yields a lower bound for the total consumption that is inversely proportional to fifth power of the process time, implying a considerable growth in energy consumptions as we shorten operation times.

3.2.2 Energy consumption for ion-transport in a segmented Paul trap

In [55] we test the conclusions drawn in [54] in a quantum mechanical setup. We analyze the energy consumption of a shortcut to adiabatic transport of a single ion in a segmented Paul trap, which is modeled as a set of electric circuits composed by a resistance and a capacitor. We may as well add an inductance, but their effect in the resulting voltages is usually negligible. The potential that drives the ion evolves governed by the voltages in the electrodes, which are set by an external electromotive force applied to the circuits that form the trap. The evolution of the potential, and the subsequent time-dependence of the voltages, is designed using the compensating force approach [16]. In essence, this shortcut technique amounts to the trick a waiter uses when moving a tray with glasses full of water. If the waiter keeps the tray flat as he or she starts moving, some of the water will spill due to the inertia. Instead, if the waiter tilts the tray when moving, he or she creates a force that compensates the inertia and avoids the spilling of water.

We compute the power supplied by the electromotive force to generate the driving potential, and compare it with the energy consumed by the ion. As said, a time-dependent Hamiltonian gives the energy of the system up to a factor [53]. We find that, in our model, the factor that provides the physical energy for the ion depends on the properties of the trap. In fact, we notice that optimizing the protocol to reduce the energy consumed by the ion simultaneously decreases the energy required to manipulate

the control voltages only if the proper gauge is fixed. We also compute the total energy consumption and the power peaks of operations carried out in different times, and verify that both increase with the rate of the process. As expected, due to the scale difference, the energy consumed to set the desired voltages in the electrodes dominates by far the energy consumed during the operation. The scale difference also allows to describe the quantum system as governed by a semiclassical Hamiltonian with (classical) external time-dependent control parameters, as well as to design STA that are independent of the initial conditions and evolution of the ion.

3.2.3 Vanishing efficiency of a speeded-up ion-in-Paul-trap Otto engine

[56] improves the viewpoint in [55] by considering a more detailed Hamiltonian and studying the consumption of a new set of operations in Paul traps. Additionally, we use the concepts developed through the study of the previous models to examine how a fair assessment of the energy consumption affects the performance criteria of a sped up quantum engine. The study case is a quantum harmonic Otto engine with fast STA expansion/compression strokes implemented in an ion Paul trap setup.

We start by pointing out two aspects of work that lead to different definitions and thus to different results, and combine them to propose two definitions that we regard as useful in the context of externally driven microscopic engines. The first factor, which has been pointed out before, corresponds to the definition of work in externally driven systems. Consider a setting described by an unperturbed constant Hamiltonian plus an external driving potential. The exclusive definition computes the work done by the external driving by accounting only for the energy change of the static Hamiltonian. On the contrary, an inclusive definition evaluates work as the change of the total Hamiltonian, including the external influence. We combine this duality with the various boundaries one could consider to separate the system from the external world and define *microscopic work*, an inclusive definition that disregards the presence of a control system, and *total work*, an exclusive definition on the enlarged system.

By writing down the global Hamiltonian that encompasses both the ion and the control circuit, as well as their interaction, we verify that the time-dependent term that sets the gauge, otherwise neglected because it does not affect the dynamics of the

primary system, depends on the properties of the control apparatus. In fact, we see that once the specific gauge has been set, the evolution of the motional energy of the ion is the contrary to what we expect, namely, that it increases when the potential tightens and decreases when the potential expands. This is so because the gauge term induces an up and down movement with respect to a fixed zero energy point. To have a better intuition of what is going on, imagine a rope (the potential) laying horizontally with two fixing points and a ball (the ion) resting on it between the two fixing points. The weight of the ball curves the rope creating a well shape (the harmonic potential). Imagine also that someone (the control) holds the rope outside of the fixing points and can release it or pull it horizontally. If this person releases the rope, the ball will fall creating a deeper well. It will *feel* the rope tighter around it (compression), but altogether it has a lower potential energy. On the contrary, if the person pulls from the rope raising the ball, it will *feel* the rope more loose around it (expansion) but its potential energy has increased. This effect may be neglected in a cyclic process because the contributions of the gauge in the expansion and compression operations compensate each other.

Regarding the energy devoted to set the time-dependent driving of the primary system, i.e., the ion, we confirm the trend first seen in [54] and then supported by [55], namely, that the consumed energy is used to manipulate the inertia of the system and to fight dissipation losses. Following the mechanical-electrical analogy, the energy to manipulate the inertia of the control trolley in the crane amounts to the energy needed to charge the capacitor of the Paul trap, and the energy dissipated due to mechanical friction in the first case, corresponds to Ohmic dissipation in the second. A clear identification of the origin of the leading consumption terms opens the door to smart designs that might minimize them, and may even help develop STA that are not based in external, energy consuming driving. But for now, we must declare that the inclusion of the energy spent to generate the external driving in the debit of the operation, represented by the denominator in the expression for the efficiency, implies a vanishing energetic efficiency of the studied externally driven single ion engine. Accelerating the cycle via STA yields nevertheless increasing microscopic power and could benefit applications in which the energy expense is worth paying, as it is the case of the laser, a highly inefficient yet extremely useful device.

3.3 Discussion of the results in energy consumption

A system that starts and ends some transformation with the same energy necessarily incurs in some positive power segments, where it gains energy, and some negative power segments, where it losses it. The quantification of the energy consumed during the transformation depends crucially in the treatment of the negative power sections. Think of a car that starts at rest and ends, also at rest, in a different location. Down the road it accelerates gaining kinetic energy, and then brakes to slow down, loosing energy until it stops. The energy invested to move the car may be computed by integrating its power. However, compensating positive and negative power sections lead to the misleading result that no energy was needed. This is because the integral “sees” the energy that flows out of the system as recovered by the power source. This could be the case, to some extent, if the car of the example had some device able to recover the energy lost during the breaking, like Formula one cars do partially. For common cars however, the accumulated kinetic energy gets dissipated during the braking in the form of heat. This example illustrates a general feature of the definition of work as the integral of power, namely, that the assumption of energy recovery underlying the integral may not always be physically justified, and, in those cases, the computation must be adapted in order to find a realistic and pragmatic result, as has been done in this Thesis.

Compared with the example of the car, STA are even more demanding. They imply active control at all times, so they cannot let the system leak out its energy at some uncontrolled rate. For example, in the model studied in [54] the trolley would loose its energy in form of heat due to friction if the force stops acting on it. But, STA require to slow down the trolley in a predetermined way, so the force has to act on the system, in one direction or in the other, during the entire operation. Similarly, in the model addressed in [55, 56] if the electromotive force stops, the capacitor discharges at its natural rate. However, active driving at all times requires to reverse the direction of the current leading to a discharging process that involves as much energy consumption as the charging. We conjecture that the consuming character of the negative power sections, caused by the need of complete control over the evolution of the system, is a general feature in shortcuts to adiabatic transformations.

Roughly speaking, friction is the macroscopic reflection of interactions between individual microscopic subsystems. In general, any dissipative process is amenable to a similar microscopic interpretation. Therefore, the notion of dissipation in a setup that consists of an isolated single particle is irrelevant. There is, nevertheless, quantum friction [40, 41], a concept that refers to excitations above the energy of some equilibrium state with respect to a given environment, on the basis that, sooner or later the system will get in contact with the environment and the additional excitations will be dissipated into it. Thus, finite rate transformations of microscopic systems lead to quantum friction, unless a suitable STA is used, in which case undesired excitations are avoided. STA transformations of isolated quantum systems seem to be a situations in which no dissipation takes place, and one could be tempted to think that they are a way to implement a perpetual motion machine of the third kind, i.e., a machine that operates reversibly even at a non-vanishing rate because it eliminates any dissipative forces [61]. In other words, the frictionless regime attained by STA seemingly allows to increase the power output of a thermal device without diminishing its efficiency.

The solution to this thermodynamical impossibility lays in a key question for any fair thermodynamics analysis: where does the energy come from and where does it go? Or more suitably expressed for our problem: Is the energy that generates the evolution of the system contained within it, or is it drawn from the exterior? Crucially, all the STA operations studied in this Thesis are externally driven processes in which the transformation of the system is governed by an external force that results from the configuration of an external body [62]. This should clarify why the implementation of STA in thermal devices does not result in a perpetual motion machine. Their operation requires some exterior input and the generation of that input most certainly incurs in some form of dissipation. We have proven that to be the case in the models studies in [54, 55]. Also, we claim that any sensible thermodynamics accounting of an externally driven process should take the energy required to generate the control force into consideration, which, in the case of the quantum engine studied in [56], leads to vanishing efficiency.

In fact, beyond the specific context of STA, our results emphasize that externally driven strokes go against the fundamental idea of an engine, a machine devised to convert another form of energy into useful work. External driving amounts to attaching the piston of the engine to a second device responsible of driving it through the optimal path. It renders the piston useless, removed from its original role of converting the energy

delivered by the working substance into useful work. Externally driven quantum engines may nevertheless be useful, as, for example, they may induce motion into otherwise inaccessible degrees of freedom. However, even if we refer to them as engines, it is important to bear in mind that their operation differs fundamentally from that of an engine and, if we are going to borrow the performance criteria of engines to evaluate them, we must acknowledge that they operate at zero efficiency.

In contrast with externally driven processes, the proposal made in the early stages of finite time thermodynamics of optimizing the motion of the piston [34, 35] was based on an autonomous approach: installing a mechanism to attach the piston to the crankshaft that, once set up, involves no further consumption (other than increased friction that may result from the new mechanism). In essence, the idea of translating the optimal path into a passive element could be extended to STA, and used to speed up autonomous quantum engines. For example, a recent experimental realization of a single ion heat engine uses a tapered geometry in the confining electrodes to transform the radial excitation of the particle into axial movement [38]. Notice that no external actuation other than the interactions with the thermal baths is needed to drive this autonomous engine. Inspired by Mozurkewich's and Berry's suggestion, STA may be implemented in the mentioned heat engine by adapting the geometry of the electrodes to the design of the shortcut, in such a way that as the thermal energy forces the ion up and down the tapered trap, the modified form of the electrodes yields the desired evolution of the potential.

3.4 Results on the design of basic operations

3.4.1 Fast atom transport and launching in a nonrigid trap

The expansion of a harmonic oscillator was the original model in the dawn of shortcuts to adiabaticity [15]. Shuttling that same model, i.e., moving the minimum point of the harmonic potential, was also among the first proposed STA [16]. In [57] we present a shortcut for combined transport and expansion based in the Lewis-Leach Hamiltonian-invariant pair. First we study the shuttling of a single atom in time-dependent harmonic traps and then we extend the treatment to generic traps. Many applications could benefit from the simultaneous operation, for example, the working medium of a quantum

engine could be moved between thermal baths as it undergoes the power strokes. Also, the dynamical normal modes in certain transformations of interacting ions involve simultaneous shuttling and frequency change [26].

In principle, STA transport and expansion yield unexcited final states in arbitrarily short times, thus, a sequential approach to the combined process may be, also, arbitrarily fast. It is often the case, however, that velocity implies bigger expenditure of resources. In STA shuttling, for example, fast operations require to control the particle well beyond the region between the starting and finishing points, so more control segments of the trap have to be involved in the operation, with the consequent energetic cost. Also, as operation times get smaller, we may need to create deeper potentials to avoid unharmonicities, or the design of the STA may even imply transitory repulsive potentials that could spoil our control over the system. We compare the simultaneous and the sequential transport and expansion of a harmonic oscillator subject to two conditions: the ion should never leave the region between its initial position and the final destination, and the harmonic potential should never become repulsive. We find out that the sequential operation is faster.

The freedom to set the boundary conditions of the inverse engineered evolution allows us to design launching operations. When subject to the limitations just mentioned, we see that the simultaneous approach is more than two times faster than the sequential one. Moreover, the dual task offers more control options in the context of launching, for example, it enables the control of the free fly dispersion of the launched wave-packet. Additionally, we extend the design to generic potentials and, in particular, we show that different motional states of a single system could be launched separately if a double well potential is considered.

3.4.2 Fast state and trap rotation of a particle in an anisotropic potential

In [58] we address the paradigmatic problem for the application of invariant based inverse engineering beyond the domain of systems and operations described by independent dynamical normal modes. We consider the rotation of a single particle in an anisotropic 2D trap (the isotropic case is separable). The operation could be used to drive particles around corners in ion based scalable quantum processors [63]. There

are some straightforward recipes to decouple the dynamical modes, for example, implementing an angular momentum term that compensates the inertial effect that couples the modes [64], but such term could be difficult to implement in many physical platforms. Our design avoids adding extra terms to the Hamiltonian and, moreover, assumes constant rotation velocity, resulting in an easier to implement protocol.

At constant rotation rate, we are able to find the normal modes after a series of canonical transformations. Notice that the STA envisioned here is unconventional, in the sense that there are no controllable parameters in the Hamiltonian whose time-dependence we ought to design. Nevertheless, for a given potential configuration, we find specific values for the operation time and the constant rotation rate that yield a rotated version of the initial state at final time with no motional excitation. We consider several initial states, pure states, entangled states and coherent states, obtaining satisfactory results for all of them.

3.4.3 Invariant-based inverse engineering of time-dependent, coupled harmonic oscillators

In [60] we explore the use of a new set of 2D dynamical invariants [65, 66] to inverse engineer the evolution of quantum systems. This is the first step to go beyond Lewis-Leach invariants. We consider a generic Hamiltonian model formed by two coupled harmonic oscillators that could describe operations in various platforms such as trapped ions [23], superconducting qubits [67] and optomechanical systems [22]. We assume that the frequencies of the individual oscillators are independently controllable, as well as the interaction strength. The problem of interacting oscillators with common frequency is trivially described through independent dynamical modes.

We find out that, due to degeneracy, the role of commutativity between the invariant and the Hamiltonian does not guarantee one-to-one mapping between eigenstates of the total Hamiltonian at initial and final Times. Instead, the invariant based operations designed in [60] guarantee the conservation of some form of energy. As a working example, we design and simulate the deflection of a particle along a rotating wave guide like potential with entire control over the output average velocity of the wave-packet. The relation between the momentum of the manipulated particle and the ingoing momentum the particle had at the initial time is determined by the boundary values of

the auxiliary parameters that define the invariant. Thus, by choosing those values the particle could maintain its velocity or get slowed down or accelerated at will.

Finally, we develop a protocol that induces energy exchange between oscillators. Processes that exchange the state, or some property of it, between coupled systems are highly relevant for the development of quantum technologies [68, 69]. The particular case of coupled harmonic oscillators has also been thoroughly explored [70]. Our protocol exploits the fact that the invariant may turn into one of the individual oscillator Hamiltonians (or at least become proportional to it) if we allow it to have complex values. The auxiliary parameters in the invariant satisfy the classical equations of motion of coupled harmonic oscillators, which admit purely real and purely imaginary solutions combined into complex solutions. Thus, by finding the appropriate boundary conditions we were able to design a fast motional state transfer between the uncoupled harmonic oscillators.

3.4.4 Time-dependent harmonic potentials for momentum or position scaling

In [59] we adapt the invariant used in [60] to a one dimensional problem. It constitutes the last contribution of this Thesis to extend the range of systems amenable to invariant-based inverse engineering. We consider a single time dependent harmonic oscillator, and exploit the virtues of the novel invariant to design a protocol to scale the kinetic energy of a particle. We provide analytic expressions for the wave function of the system expanded in the basis of the eigenfunctions of the invariant, and for the first and second order moments for the position and the momentum of the driven wave-packet.

Slowing a particle down is a particularly relevant success of our protocol. It is an interesting operation for many applications, as illustrated by the various techniques developed to that end [71–73]. However, the protocol could be designed to speed up the particle, or even to reverse the motion and produce a “momentum mirror”. It could also be used to scale the position spread of the particle and design either focusing or scattering operations. Remarkably, our protocol yields satisfactory results irrespective of the initial conditions of the wave-packet, in contrast with earlier slowing methods whose good results usually rely strongly on having the proper initial conditions.

3.5 Discussion of the results on the design of basic operations

Invariant based inverse engineering has been a fruitful method to speed up many operations in various physical platforms. Each case may have its peculiarities, but there are some elements common to all inversely engineered transformations. First of all, the Hamiltonian-invariant pair. Essentially, we need the operator (or function in the classical domain) that dictates how the system at hand will evolve, and an element of the system that remains constant during that evolution. Additionally, the Hamiltonian must contain some time-dependent parameters, usually referred to as control parameters, and so does the invariant, commonly known as auxiliary parameters. Lastly, we need some kind of relation between the Hamiltonian and the invariant in the form of equations that relate the control and the auxiliary parameters. With these ingredients, we may chose a property of the system to remain constant by designing the auxiliary parameters that define the invariant element, and solve the connecting equations for the control parameters leading to the evolution that does not change the intended property of the system.

This Thesis tries to extend this simple but powerful idea to circumstances not addressed to date. For example, the Hamiltonian and the invariant may imply complicated connecting equations resulting in technically demanding inverse engineering problems. This has been the case in the simultaneous transport and expansion designed in [57]. Two equations connect the Lewis-Leach invariant to its corresponding Hamiltonian, typically known as Newton and Ermakov equations. They relate the two control and two auxiliary parameters, but, while the center of the trap depends only on one auxiliary parameter, the evolution of the frequency depends on both. In a similar line, the Hamiltonian in [60] contains three control parameters but the invariant has only two auxiliary parameters, leading to two connecting equations coupled among them by one of the controls. Solving these particular problems sets useful examples and could guide to further uses of invariant-based inverse engineering.

Another interesting path to extend the applicability of inverse engineered STA is the search of new invariant-Hamiltonian pairs. As fruitful as the Lewis-Leach invariant has been, it is only suited for systems influenced by a specific form of potential and there are

many setups and operations that do not fit into that structure. Moreover, the invariant has been used, almost exclusively, to drive systems to the state that would result from an adiabatic evolution. Other invariants may provide new perspectives and ideas to carry out different tasks. The quantity that remains constant may not be the expectation value of the operator for states driven by the corresponding Hamiltonian, it could be any other relevant property of the system, like, for example, a (hypothetical) invariant that keeps the correlations between subsystems intact during a given transformation. The invariant used in [59, 60] is an example of that. It renders full control over some form of energy, allowing also to interchange the value of different energy terms. We have presented some examples, but, surely, many other interesting tasks could exploit this property.

Most of the leading physical platforms to develop quantum technologies rely on some sort of cooling. In some cases, maintaining the system in a cold environment is key not to destroy the quantum properties of the system, like in superconducting qubits. In others, the need for cooling is even more fundamental, for example, ultracold atoms need to be maintained close to the absolute zero. The temperature of a macroscopic body is a reflection of the kinetic energy of its microscopic constituents. Hence, at the single particle level, slowing down means cooling down, which is useful for many applications. There are many techniques and devices devoted to that end, Zeeman [71] or Stark slowers [72], delta-kick cooling (DKC) [73] and the “inverse coil gun” [74] to name a few. The opposite operation, launching, is also interesting for implementation or deposition of ions with specific speeds [75]. The protocols devised in [57, 59] contribute to the goal of reducing/increasing wave-packet momenta, and constitute robust alternatives to the mentioned techniques.

Finally, as new invariant based STA unfold, it may be interesting to compare them and search for fundamental relations, similar to the connection between invariant based inverse engineering and counterdiabatic driving for single oscillators [76]. In particular, there are recent proposals for shortcut to adiabatic transformations of interacting harmonic oscillators based in counterdiabatic driving [77, 78] that could be compared to our proposal in [60]. It will also be interesting to compare the momentum scaling protocol designed in [59] with the widely used technique of Delta Kick Cooling [73], since they operate under the same principle of squeezing and rotating the Wigner function.

3.6 Prospects for future research

The inventive nature of research work hinders to comply with original goals. At times a new idea comes up in the head of the researcher in the middle of a project and compels him or her to decide between postponing the development of the new idea in favor of the realization of the ongoing work or following this new path and setting aside the current project. During the last four years, with the undoubted help of my advisors, I have chosen some research paths at the expense of some others. In the end, a finite amount of time only allows for a finite amount of results. Luckily, in most of the cases I have been able to go back and work on once postponed ideas, but there are still a couple of projects underway at the moment of writing this Thesis that, being not fully developed yet, have been left out of this work. Nevertheless I consider it appealing for the reader of this Thesis to say a few words about them.

The first one adds to the effort of extending invariant based STA to new systems and operations and it is deeply inspired by [79]. Based on independent dynamical normal modes, Sägger et. al. have designed robust and fast cooling of a trapped ion by controlling the width of a double well potential that contains another pre-cooled ion. The problem is separable if equal ions are considered. For ions of different species, however, the dynamical normal modes remain coupled. They deal with the inseparable problem by introducing a controllable linear term in the double well potential that breaks the symmetry and allows them to manipulate the equilibrium positions to decouple the normal modes. It would be interesting to apply this clever trick to the paradigmatic problem of rotation, in order to be able to generalize it for any 2D Hamiltonian.

The other proposal is a mechanism to reduce the total energy consumed in externally driven processes. We aim to get rid of one of the leading consumption terms, the cost of creating the inertia of the control system, by adding an element that will cause a consumption free movement and a geometric element to translate the uncontrolled evolution of the control into the desired evolution of the system. In this way it is enough if an external source provides energy to overcome the dissipation due to friction and the back-action that the movement of the system creates in the control to keep the thing going, somewhat similar to what happens in a grandfather clock.

4. Conclusions

Shortcuts to adiabaticity set the common ground where all the research presented in this Thesis lays. More than ten years have gone by since the first appearance of the term in a scientific journal [15]. Since then, STA have come to constitute its own research field with an ever growing community, as evidenced by the recent publication of a Review of Modern Physics [80] that synthesizes the vast amount of work done to develop and extend STA to various operations and physical setups. The relevance gained by STA responds to both fundamental and practical appealingings. On one side, STA contribute to a better understanding of basic concepts that lay in the boarder of scientific knowledge, such as decoherence, controllability, energy and work, entropy, environment effects, information or connection between classical and quantum systems. On the practical side, adiabatic invariance is one of the main routes towards precise control over quantum systems, and therefore a cornerstone element in the development of quantum technologies.

This Thesis tackles two of the open questions highlighted in the outlook of [80]. We have taken a significant step towards the clarification of the energetic cost of STA protocols by assessing the energy consumed by sped up operations in different contexts. We have demonstrated that, while the energy difference between two states connected by a STA protocol is the adiabatic difference regardless of the duration of the process, the acceleration implied by the use of a shortcut increases the energy needed to generate inertia on the body whose state dictates the force that drives the system and enhances dissipation on the control elements. Stated in terms of the concepts introduced in [56], we have proven that implementing a STA does not change the microscopic work required or provided by the system, but it definitely increases the total work on the system. This observation agrees with the common intuition, spread by the study of finite time thermodynamics, that doing things faster implies a higher energy consumption.

We have also applied invariant-based inverse engineering protocols to problems where a point transformation does not provide independent dynamical normal modes. We have made a first attempt to speed up the paradigmatic problem of 2D anisotropic rotation without motional excitation at final time considering realistic control over the system. Besides, we have used further Hamiltonian-invariant pairs beyond the Lewis-Leach family, and proven that they can be used to implement shortcuts-to-adiabatic manipulations of coupled 2D systems.

The 1D version of the new family of invariants has been used to design a protocol that uses a transient harmonic potential to manipulate at will the momentum of a particle regardless of its initial conditions. Statistical thermodynamics showed us that temperature is a reflection of kinetic energy, the result of the motion of the microscopic particles that compose the system. In a quantum mechanical context slowing down a particle and cooling it become almost synonyms, so the momentum scaling shortcut may be used to reach pikoKelvin temperatures, providing a robust alternative to procedures like Delta Kick Cooling that rely heavily in the initial state of the system.

During my Thesis I have had the opportunity to collaborate with great researchers. Among them, the partnership with the group of Ronnie Kosloff has been particularly meaningful. We addressed the extension of shortcuts to open quantum systems, an effort that resulted in two publications that are not explicitly included in this Thesis [81, 82]. We developed a protocol based on inverse engineering the non-adiabatic Markovian master equation [83] and dubbed it Shortcut to Equilibration, a non-unitary control task aimed at rapidly changing the entropy of the system. The protocol was originally created to accelerate the return to equilibrium of a manipulated open quantum harmonic oscillator and then extended for a driven two level system in contact with a thermal bath.

Overall, I think that it is fair to say that we have met the goals established for this Thesis. In a more personal note, I feel that the time elapsed since I started doing my research, first for the master Thesis and then for the PhD, has signified, not only a huge learning experience, but also, and even more importantly, a period of incredible personal growth. I have found that the challenge that means having to face problems for which no solution is yet known makes it hard to get bored of the research work. I hope to continue facing, and to the extent possible solving, this kind of problems.

Bibliography

- [1] T. Young, “*II. The Bakerian Lecture. On the theory of light and colours*”, Philosophical Transactions of the Royal Society of London **92**, 12-48 (1802).
- [2] C. J. Davisson and L. H. Germer, “*Reflection of Electrons by a Crystal of Nickel*”, Proceedings of the National Academy of Sciences **14**, 317–322 (1928).
- [3] O. Donati, G. P. Missiroli, and G. Pozzi, “*An Experiment on Electron Interference*”, American Journal of Physics **41**, 639-644 (1973).
- [4] J. P. Dowling and G. J. Milburn, “*Quantum technology: the second quantum revolution*”, Philosophical Transactions of the Royal Society of London. Series A: Mathematical, Physical and Engineering Sciences **361**, 1655-1674 (2003).
- [5] V. Giovannetti, S. Lloyd, and L. Maccone, “*Advances in quantum metrology*”, Nature Photonics **5**, 222-229 (2011).
- [6] N. Gisin and R. Thew, “*Quantum communication*”, Nature Photonics **1**, 165-171 (2007).
- [7] H. J. Kimble, Y. Levin, A. B. Matsko, K. S. Thorne, and S. P. Vyatchanin, “*Conversion of conventional gravitational-wave interferometers into quantum nondemolition interferometers by modifying their input and/or output optics*”, Phys. Rev. D **65**, 022002 (2001).
- [8] F. Arute, K. Arya, R. Babbush, D. Bacon, J. C. Bardin, R. Barends, R. Biswas, S. Boixo, F. G. Brandao, D. A. Buell, *et al.*, “*Quantum supremacy using a programmable superconducting processor*”, Nature **574**, 505–510 (2019).
- [9] H.-S. Zhong, H. Wang, Y.-H. Deng, M.-C. Chen, L.-C. Peng, Y.-H. Luo, J. Qin, D. Wu, X. Ding, Y. Hu, P. Hu, X.-Y. Yang, W.-J. Zhang, H. Li, Y. Li, X. Jiang,

- L. Gan, G. Yang, L. You, Z. Wang, L. Li, N.-L. Liu, C.-Y. Lu, and J.-W. Pan, “*Quantum computational advantage using photons*”, *Science* **370**, 1460–1463 (2020).
- [10] D. P. DiVincenzo, “*The physical implementation of quantum computation*”, *Fortschritte der Physik: Progress of Physics* **48**, 771–783 (2000).
- [11] M. Born and V. Fock, “*Beweis des Adiabatensatzes*”, *Zeitschrift für Physik* **51**, 165-180 (1928).
- [12] D. Kielpinski, C. Monroe, and D. J. Wineland, “*Architecture for a large-scale ion-trap quantum computer.*”, *Nature* **417**, 709–11 (2002).
- [13] H. E. D. Scovil and E. O. Schulz-DuBois, “*Three-Level Masers as Heat Engines*”, *Phys. Rev. Lett.* **2**, 262–263 (1959).
- [14] X. Chen, I. Lizuain, A. Ruschhaupt, D. Guéry-Odelin, and J. G. Muga, “*Shortcut to Adiabatic Passage in Two- and Three-Level Atoms*”, *Phys. Rev. Lett.* **105**, 123003 (2010).
- [15] X. Chen, A. Ruschhaupt, S. Schmidt, A. del Campo, D. Guéry-Odelin, and J. G. Muga, “*Fast Optimal Frictionless Atom Cooling in Harmonic Traps: Shortcut to Adiabaticity*”, *Physical Review Letters* **104**, 063002 (2010).
- [16] E. Torrontegui, S. Ibáñez, X. Chen, A. Ruschhaupt, D. Guéry-Odelin, and J. G. Muga, “*Fast atomic transport without vibrational heating*”, *Physical Review A* **83**, 013415 (2011).
- [17] H. R. Lewis and W. B. Riesenfeld, “*An Exact Quantum Theory of the Time-Dependent Harmonic Oscillator and of a Charged Particle in a Time-Dependent Electromagnetic Field*”, *Journal of Mathematical Physics* **10**, 1458 (1969).
- [18] H. R. Lewis and P. G. L. Leach, “*A direct approach to finding exact invariants for one-dimensional time-dependent classical Hamiltonians*”, *Journal of Mathematical Physics* **23**, 2371 (1982).
- [19] A. K. Dhara and S. V. Lawande, “*Feynman propagator for time-dependent Lagrangians possessing an invariant quadratic in momentum*”, *Journal of Physics A: Mathematical and General* **17**, 2423–2431 (1984).

- [20] A. Ruschhaupt, X. Chen, D. Alonso, and J. G. Muga, “*Optimally robust shortcuts to population inversion in two-level quantum systems*”, *New Journal of Physics* **14**, 093040 (2012).
- [21] H. Walther, B. T. H. Varcoe, B.-G. Englert, and T. Becker, “*Cavity quantum electrodynamics*”, *Reports on Progress in Physics* **69**, 1325–1382 (2006).
- [22] M. Aspelmeyer, T. J. Kippenberg, and F. Marquardt, “*Cavity optomechanics*”, *Rev. Mod. Phys.* **86**, 1391–1452 (2014).
- [23] M. Harlander, R. Lechner, M. Brownnutt, R. Blatt, and W. Hnsel, “*Trapped-ion antennae for the transmission of quantum information*”, *Nature* **471**, 200-203 (2011).
- [24] M. Palmero, E. Torrontegui, D. Guéry-Odelin, and J. G. Muga, “*Fast transport of two ions in an anharmonic trap*”, *Physical Review A* **88**, 053423 (2013).
- [25] M. Palmero, R. Bowler, J. P. Gaebler, D. Leibfried, and J. G. Muga, “*Fast transport of mixed-species ion chains within a Paul trap*”, *Physical Review A* **90**, 053408 (2014).
- [26] M. Palmero, S. Martínez-Garaot, U. G. Poschinger, A. Ruschhaupt, and J. G. Muga, “*Fast separation of two trapped ions*”, *New Journal of Physics* **17**, 093031 (2015).
- [27] M. Palmero, S. Martínez-Garaot, J. Alonso, J. P. Home, and J. G. Muga, “*Fast expansions and compressions of trapped-ion chains*”, *Physical Review A* **91**, 053411 (2015).
- [28] I. Lizuain, M. Palmero, and J. G. Muga, “*Dynamical normal modes for time-dependent Hamiltonians in two dimensions*”, *Phys. Rev. A* **95**, 022130 (2017).
- [29] M. Planck, “*On the law of distribution of energy in the normal spectrum*”, *Annalen der physik* **4**, 1 (1901).
- [30] A. Einstein, “*Über einen die Erzeugung und Verwandlung des Lichtes betreffenden heuristischen Gesichtspunkt*”, *Annalen der Physik* **322**, 132-148 (1905).

- [31] R. Berry, P. Salamon, and B. Andresen, “*How It All Began*”, *Entropy* **22**, 908 (2020).
- [32] F. L. Curzon and B. Ahlborn, “*Efficiency of a Carnot engine at maximum power output*”, *American Journal of Physics* **43**, 22-24 (1975).
- [33] B. Andresen, R. S. Berry, A. Nitzan, and P. Salamon, “*Thermodynamics in finite time. I. The step-Carnot cycle*”, *Phys. Rev. A* **15**, 2086–2093 (1977).
- [34] M. Mozurkewich and R. S. Berry, “*Finite-time thermodynamics: Engine performance improved by optimized piston motion*”, *Proceedings of the National Academy of Sciences* **78**, 1986-88 (1981).
- [35] M. Mozurkewich and R. S. Berry, “*Optimal paths for thermodynamic systems: The ideal Otto cycle*”, *Journal of Applied Physics* **53**, 34-42 (1982).
- [36] R. Kosloff, “*Quantum Thermodynamics: A Dynamical Viewpoint*”, *Entropy* **15**, 21002128 (2013).
- [37] F. Binder, L. A. Correa, C. Gogolin, J. Anders, and G. Adesso, “*Thermodynamics in the quantum regime*”, *Fundamental Theories of Physics* **195**, (2018).
- [38] J. Roßnagel, S. T. Dawkins, K. N. Tolazzi, O. Abah, E. Lutz, F. Schmidt-Kaler, and K. Singer, “*A single-atom heat engine*”, *Science* **352**, 325–329 (2016).
- [39] R. Kosloff and Y. Rezek, “*The Quantum Harmonic Otto Cycle*”, *Entropy* **19**, (2017).
- [40] R. Kosloff and T. Feldmann, “*Discrete four-stroke quantum heat engine exploring the origin of friction*”, *Phys. Rev. E* **65**, 055102 (2002).
- [41] F. Plastina, A. Alecce, T. J. G. Apollaro, G. Falcone, G. Francica, F. Galve, N. Lo Gullo, and R. Zambrini, “*Irreversible Work and Inner Friction in Quantum Thermodynamic Processes*”, *Phys. Rev. Lett.* **113**, 260601 (2014).
- [42] A. Levy, L. Diósi, and R. Kosloff, “*Quantum flywheel*”, *Phys. Rev. A* **93**, 052119 (2016).
- [43] J. Deng, Q.-h. Wang, Z. Liu, P. Hänggi, and J. Gong, “*Boosting work characteristics and overall heat-engine performance via shortcuts to adiabaticity: Quantum and classical systems*”, *Physical Review E* **88**, 062122 (2013).

- [44] A. Del Campo, J. Goold, and M. Paternostro, “*More bang for your buck: Towards super-adiabatic quantum engines*”, Scientific Reports **4**, 6208 (2014).
- [45] Y. Zheng, S. Campbell, G. De Chiara, and D. Poletti, “*Cost of counterdiabatic driving and work output*”, Phys. Rev. A **94**, 042132 (2016).
- [46] K. Funo, J.-N. Zhang, C. Chatou, K. Kim, M. Ueda, and A. del Campo, “*Universal Work Fluctuations During Shortcuts to Adiabaticity by Counterdiabatic Driving*”, Phys. Rev. Lett. **118**, 100602 (2017).
- [47] O. Abah and E. Lutz, “*Energy efficient quantum machines*”, EPL (Europhysics Letters) **118**, 40005 (2017).
- [48] A. Bravetti and D. Tapias, “*Thermodynamic Cost for Classical Counterdiabatic Driving*”, preprint arXiv:1706.07443 (2017).
- [49] E. Calzetta, “*Not-quite-free shortcuts to adiabaticity*”, Phys. Rev. A **98**, 032107 (2018).
- [50] P. Talkner, E. Lutz, and P. Hänggi, “*Fluctuation theorems: Work is not an observable*”, Phys. Rev. E **75**, 050102 (2007).
- [51] P. Talkner and P. Hänggi, “*Aspects of quantum work*”, Phys. Rev. E **93**, 022131 (2016).
- [52] M. Campisi, P. Hänggi, and P. Talkner, “*Colloquium: Quantum fluctuation relations: Foundations and applications*”, Rev. Mod. Phys. **83**, 771–791 (2011).
- [53] J. M. G. Vilar and J. M. Rubi, “*Failure of the Work-Hamiltonian Connection for Free-Energy Calculations*”, Phys. Rev. Lett. **100**, 020601 (2008).
- [54] E. Torrontegui, I. Lizuain, S. González-Resines, A. Tobalina, A. Ruschhaupt, R. Kosloff, and J. G. Muga, “*Energy consumption for shortcuts to adiabaticity*”, Phys. Rev. A **96**, 022133 (2017).
- [55] A. Tobalina, J. Alonso, and J. G. Muga, “*Energy consumption for ion-transport in a segmented Paul trap*”, New Journal of Physics **20**, 065002 (2018).
- [56] A. Tobalina, I. Lizuain, and J. G. Muga, “*Vanishing efficiency of a speeded-up ion-in-Paul-trap Otto engine*”, EPL (Europhysics Letters) **127**, 20005 (2019).

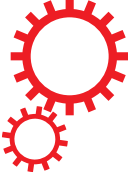
- [57] A. Tobalina, M. Palmero, S. Martínez-Garaot, and J. G. Muga, “*Fast atom transport and launching in a nonrigid trap*”, *Scientific Reports* **7**, 5753 (2017).
- [58] I. Lizuain, A. Tobalina, A. Rodriguez-Prieto, and J. G. Muga, “*Fast state and trap rotation of a particle in an anisotropic potential*”, *Journal of Physics A: Mathematical and Theoretical* **52**, 465301 (2019).
- [59] J. G. Muga, S. Martínez-Garaot, M. Pons, M. Palmero, and A. Tobalina, “*Time-dependent harmonic potentials for momentum or position scaling*”, *Phys. Rev. Research* **2**, 043162 (2020).
- [60] A. Tobalina, E. Torrontegui, I. Lizuain, M. Palmero, and J. G. Muga, “*Invariant-based inverse engineering of time-dependent, coupled harmonic oscillators*”, *Phys. Rev. A* **102**, 063112 (2020).
- [61] P. Salamon, B. Andresen, K. H. Hoffmann, J. D. Nulton, A. M. Segall, and F. L. Rohwer, “*Free Energies of Staging a Scenario and Perpetual Motion Machines of the Third Kind*”, *Proceedings of the 240 Conference* 43-56 (2014).
- [62] J. W. Gibbs, *Elementary Principles in Statistical Mechanics*. Cambridge University Press, 1902.
- [63] J. M. Amini, H. Uys, J. H. Wesenberg, S. Seidelin, J. Britton, J. J. Bollinger, D. Leibfried, C. Ospelkaus, A. P. VanDevender, and D. J. Wineland, “*Toward scalable ion traps for quantum information processing*”, *New Journal of Physics* **12**, 033031 (2010).
- [64] S. Masuda and S. A. Rice, “*Rotation of the Orientation of the Wave Function Distribution of a Charged Particle and its Utilization*”, .
- [65] K.-E. Thylwe and H. J. Korsch, “*The Ermakov - Lewis invariants for coupled linear oscillators*”, *Journal of Physics A: Mathematical and General* **31**, L279–L285 (1998).
- [66] A. R. Urzúa, I. Ramos-Prieto, M. Fernández-Guasti, and H. M. Moya-Cessa, “*Solution to the Time-Dependent Coupled Harmonic Oscillators Hamiltonian with Arbitrary Interactions*”, *Quantum Reports* **1**, 82–90 (2019).
- [67] R. Barends, J. Kelly, A. Megrant, D. Sank, E. Jeffrey, Y. Chen, Y. Yin, B. Chiaro, J. Mutus, C. Neill, P. O’Malley, P. Roushan, J. Wenner, T. C. White,

- A. N. Cleland, and J. M. Martinis, “*Coherent Josephson Qubit Suitable for Scalable Quantum Integrated Circuits*”, Phys. Rev. Lett. **111**, 080502 (2013).
- [68] D. N. Matsukevich and A. Kuzmich, “*Quantum State Transfer Between Matter and Light*”, Science **306**, 663–666 (2004).
- [69] P. Kurpiers, P. Magnard, T. Walter, B. Royer, M. Pechal, J. Heinsoo, Y. Salathé, A. Akin, S. Storz, J. Besse, S. Gasparinetti, A. Blais, and A. Wallraff, “*Deterministic quantum state transfer and remote entanglement using microwave photons*”, Nature **558**, 264–267 (2018).
- [70] A. S. M. de Castro, V. V. Dodonov, and S. S. Mizrahi, “*Quantum state exchange between coupled modes*”, Journal of Optics B: Quantum and Semiclassical Optics **4**, S191–S199 (2002).
- [71] W. D. Phillips, “*Nobel Lecture: Laser cooling and trapping of neutral atoms*”, Reviews of Modern Physics **70**, 721–741 (1998).
- [72] H. L. Bethlem, G. Berden, and G. Meijer, “*Decelerating Neutral Dipolar Molecules*”, Phys. Rev. Lett. **83**, 1558–1561 (1999).
- [73] S. Chu, J. E. Bjorkholm, A. Ashkin, J. P. Gordon, and L. W. Hollberg, “*Proposal for optically cooling atoms to temperatures of the order of 10^{-6} K*”, Opt. Lett. **11**, 73–75 (1986).
- [74] E. Narevicius, A. Libson, C. G. Parthey, I. Chavez, J. Narevicius, U. Even, and M. G. Raizen, “*Stopping Supersonic Beams with a Series of Pulsed Electromagnetic Coils: An Atomic Coilgun*”, Physical Review Letters **100**, 093003 (2008).
- [75] G. Jacob, K. Groot-Berning, S. Wolf, S. Ulm, L. Couturier, S. T. Dawkins, U. G. Poschinger, F. Schmidt-Kaler, and K. Singer, “*Transmission Microscopy with Nanometer Resolution Using a Deterministic Single Ion Source*”, Phys. Rev. Lett. **117**, 043001 (2016).
- [76] X. Chen, E. Torrontegui, and J. G. Muga, “*Lewis-Riesenfeld invariants and transitionless quantum driving*”, Phys. Rev. A **83**, 062116 (2011).

- [77] C. W. Duncan and A. del Campo, “*Shortcuts to adiabaticity assisted by counterdiabatic Born–Oppenheimer dynamics*”, *New Journal of Physics* **20**, 085003 (2018).
- [78] T. Villazon, A. Polkovnikov, and A. Chandran, “*Swift heat transfer by fast-forward driving in open quantum systems*”, *Phys. Rev. A* **100**, 012126 (2019).
- [79] T. Sgesser, R. Matt, R. Oswald, and J. P. Home, “*Robust dynamical exchange cooling with trapped ions*”, *New Journal of Physics* **22**, 073069 (2020).
- [80] D. Guéry-Odelin, A. Ruschhaupt, A. Kiely, E. Torrontegui, S. Martínez-Garaot, and J. G. Muga, “*Shortcuts to adiabaticity: Concepts, methods, and applications*”, *Rev. Mod. Phys.* **91**, 045001 (2019).
- [81] R. Dann, A. Tobalina, and R. Kosloff, “*Shortcut to Equilibration of an Open Quantum System*”, *Phys. Rev. Lett.* **122**, 250402 (2019).
- [82] R. Dann, A. Tobalina, and R. Kosloff, “*Fast route to equilibration*”, *Phys. Rev. A* **101**, 052102 (2020).
- [83] R. Dann, A. Levy, and R. Kosloff, “*Time-dependent Markovian quantum master equation*”, *Phys. Rev. A* **98**, 052129 (2018).

ORIGINAL PUBLICATIONS

SCIENTIFIC REPORTS



OPEN

Fast atom transport and launching in a nonrigid trap

A. Tobalina, M. Palmero, S. Martínez-Garaot & J. G. Muga

We study the shuttling of an atom in a trap with controllable position and frequency. Using invariant-based inverse engineering, protocols in which the trap is simultaneously displaced and expanded are proposed to speed up transport between stationary trap locations as well as launching processes with narrow final-velocity distributions. Depending on the physical constraints imposed, either simultaneous or sequential approaches may be faster. We consider first a perfectly harmonic trap, and then extend the treatment to generic traps. Finally, we apply this general framework to a double-well potential to separate different motional states with different launching velocities.

An important goal of modern atomic physics is to control atomic motion for fundamental studies or to develop quantum-based technologies. Technological advances allow for driving individual atoms (ions^{1,2} or neutral atoms³) along microscopic or mesoscopic predetermined space-time paths. This control will enable us to use the rich structure and interactions of ions and neutral atoms in circuits and devices where quantum phenomena play a significant role. Many operations require moving the atoms fast to keep quantum coherence, leaving them unexcited at their destination. Slow adiabatic shuttling may avoid excitation in principle, but the long times required make the processes prone to decoherence. Shortcuts to adiabaticity (STA)^{4,5} are protocols for the control parameters that produce final states of an adiabatic process in much shorter times, typically via diabatic transitions at intermediate times. In this paper, we find STA to drive a single atom by a moving and nonrigid potential with time-dependent frequency as schematically shown in Fig. 1. We shall focus first on harmonic traps, and then a theory for more general potentials is also put forward. Two types of basic processes addressed are: (i) transport where the wave packet center and trap start and end at rest, and also (ii) launching or stopping processes, where the wave-packet center and trap start (resp. end) at rest, and ends (resp. start) with a nonzero velocity. Invariant-based inverse engineering has been applied to designing STA for rigid transport (with a constant potential in the moving frame)^{6–8}, and trap expansions or compressions^{4,9–12}. While shuttling and expansion or compression could be performed sequentially, doing both operations simultaneously, as proposed here, may save time and offers broader control possibilities. “Dual-task” operations must thus be compared to sequential operations. In principle, STA for rigid transport and expansions can be done in arbitrarily short times, but only if infinite resources and energies are available, which is never the case in practice. Often, the control parameters cannot go beyond certain values. For example, a very fast trap expansion without final excitation needs transient imaginary frequencies of the external trap (a concave-down potential), which are not easy to implement in all trap types. In optical traps, for example, the passage through the atomic resonance of the laser frequency to go from a trap to an antitrap may produce undesired excitation. A different, common constraint is the limitation on the spatial domain allowed for the trap center. We shall show that, depending on the constraints imposed, either sequential or dual-task protocols may be faster.

There are different fields or applications where simultaneous transport and expansion or compression between initial and final states at rest is of relevance. In quantum heat engines and refrigerators^{13–22} for example, the (thermodynamically) adiabatic expansion or compression strokes of the cycle could be realized simultaneously transporting the quantum working medium between baths at different locations. Also, when expanding or separating ion chains, which are basic processes to develop a scalable quantum-information architecture²³, the effective dynamics of the normal modes involves simultaneous transport and frequency change^{24,25}. One more scenario where transport and frequency change occur simultaneously is the bias inversion of an asymmetric double-well potential²⁶.

Launching and stopping protocols are as well useful for many applications. An example of a stopping device is the “inverse coil gun” implemented by Mark Raizen and coworkers²⁷. It uses pulsed magnetic fields to slow down a supersonic beam (e.g. from 500 to 50 m/s²⁷) so as to leave the atoms ready for spectroscopic studies, controlled collisions, or further cooling techniques. One advantage of stopping techniques by magnetic (for paramagnetic

Departamento de Química Física, UPV/EHU, B. Sarriena s/n, 48940, Leioa, Bizkaia, Spain. Correspondence and requests for materials should be addressed to A.T. (email: ander.tobalina@ehu.eus)

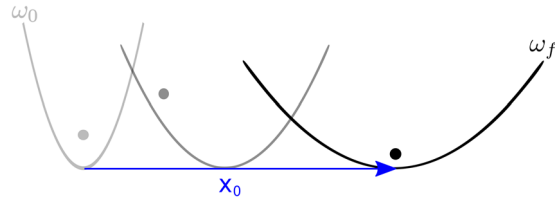


Figure 1. Scheme of the transport protocol with a change in the frequency of the trap.

species) or electric fields (for ions), is their broad range of applicability, beyond the very restricted class of atoms with a cycling transition that can be treated by standard laser cooling approaches. The opposite process, launching, is also of much current interest: launching ions with a specific speed is used in particular for their implantation or deposition²⁸. Accurately controlled launching can contribute to different quantum technologies such as ion microscopy, those using a controlled “soft landing” of slow ions on a surface, and those controlling the location of defects (NV centers) that have been proposed for sensors and also as the basis of a possible architectures for quantum information processing. Deterministic sources of single cold ions have been proposed and demonstrated^{28, 29} that limit the position-momentum uncertainty only due to the Heisenberg principle. Our goal here is to control the velocity, and its dispersion. This is facilitated by the possibility to change the trap frequency along the shuttling. Differential launching of different motional states is also possible as we shall demonstrate with a double well.

While the mathematical framework of this work is equally applicable to neutral atoms or trapped ions, the numerical examples make use of parameters adapted to trapped ions^{1, 2}.

Invariant-based inverse engineering. Lewis and Riesenfeld³⁰ noted that the solutions of the Schrödinger equation for a time-dependent Hamiltonian can be written as superpositions of eigenstates of its dynamical invariants. Dhara and Lawande³¹ and Lewis and Leach³² worked out the details for a particle of mass m that evolves according to Hamiltonians of the form

$$H = \frac{p^2}{2m} - F(t)x + \frac{m}{2}\omega^2(t)x^2 + \frac{1}{\rho^2(t)}U\left[\frac{x - \alpha(t)}{\rho(t)}\right], \tag{1}$$

where $F(t)$ is a homogeneous force, $\omega(t)/(2\pi)$ the frequency of a harmonic term, U an arbitrary function, and $\alpha(t)$ and $\rho(t)$ are auxiliary functions. x and p represent conjugate position and momentum operators of the particle.

The Hamiltonian in Eq. (1) has the quadratic-in-momentum invariant

$$I = \frac{1}{2m}[\rho(p - m\dot{\alpha}) - m\dot{\rho}(x - \alpha)]^2 + \frac{1}{2}m\omega_0^2\left(\frac{x - \alpha}{\rho}\right)^2 + U\left(\frac{x - \alpha}{\rho}\right), \tag{2}$$

where the dot means time derivative. I satisfies indeed the invariance equation

$$\frac{dI}{dt} \equiv \frac{\partial I(t)}{\partial t} + \frac{1}{i\hbar}[I(t), H(t)] = 0, \tag{3}$$

provided the scaling factor ρ and α satisfy the Ermakov and Newton equations,

$$\ddot{\rho} + \omega^2(t)\rho = \frac{\omega_0^2}{\rho^3}, \tag{4}$$

$$\ddot{\alpha} + \omega^2(t)\alpha = \frac{F(t)}{m}, \tag{5}$$

where ω_0 is a constant. For simplicity we choose $\omega_0 = \omega(0)$.

Any wavefunction $\psi(t)$ driven by the Hamiltonian (1) may be written in terms of eigenvectors ψ_n of the invariant (2),

$$\psi(x, t) = \sum_n c_n e^{i\theta_n} \psi_n(x, t), \quad I(t)\psi_n(x, t) = \lambda_n \psi_n(x, t), \tag{6}$$

where c_n are constant coefficients, the λ_n are the eigenvalues, and θ_n are Lewis-Riesenfeld phases that can be calculated from H and ψ_n ³⁰, $\theta_n(t) = \frac{1}{\hbar} \int_0^t dt' \langle \psi_n(t') | i\hbar \frac{\partial}{\partial t} - H(t') | \psi_n(t') \rangle$. The ψ_n have the form³¹

$$\psi_n(x, t) = e^{\frac{im}{\hbar}[\dot{\rho}x^2/2\rho + (\dot{\alpha}\rho - \alpha\dot{\rho})x/\rho]} \frac{1}{\rho^{1/2}} \phi_n\left(\frac{x - \alpha}{\rho}\right), \tag{7}$$

where the $\phi_n(\sigma)$ (normalized in $\sigma = \frac{x - \alpha}{\rho}$ space) are the solutions of the auxiliary, stationary Schrödinger equation

$$\left[-\frac{\hbar^2}{2m} \frac{\partial^2}{\partial \sigma^2} + \frac{1}{2} m \omega_0^2 \sigma^2 + U(\sigma) \right] \phi_n(\sigma) = \lambda_n \phi_n(\sigma). \quad (8)$$

The physical meaning of α is made evident in Eq. (7) as a centroid for the dynamical wavefunctions that satisfies the Newton equation (5). α is also the center of the potential term $\rho^{-2} U[(x - \alpha)/\rho]$ when U does not vanish.

To inverse engineer the interaction between the initial time, $t = 0$, and a final time t_f , we first set the initial and final Hamiltonians. For transport between stationary traps, commutativity is imposed between the Hamiltonian and the invariant at boundary times so that they share eigenstates. Thus the dynamics maps eigenstates of $H(0)$ onto eigenstates of $H(t_f)$ via the corresponding invariant eigenstates, even though at intermediate times diabatic transitions may occur. The commutation of H and I at boundary times implies boundary conditions for α , ρ , and their derivatives. We design these functions to satisfy the necessary boundary conditions, and then, from the auxiliary Eqs (4) and (5) the control parameters $\omega(t)$ and $F(t)$ are found. For launching/stopping processes the invariant and Hamiltonian do not commute at final time in the laboratory frame, but the states may be chosen as eigenstates of the Hamiltonian in the comoving and coexpanding frame.

Results

Dual-task transport in a nonrigid harmonic trap. Let us assume first that the external trap is purely harmonic, i.e., we take $U = 0$ and $F = m\omega^2(t)x_0(t)$, where $x_0(t)$ is the position of the trap center. Then, the Hamiltonian in Eq. (1) becomes, adding a purely time-dependent term that does not affect the physics to complete the square,

$$H = \frac{p^2}{2m} + \frac{1}{2} m \omega^2(t) [x - x_0(t)]^2. \quad (9)$$

The average energy for this system in the n th state (7) is given by

$$E = \langle H \rangle = \frac{(2n + 1)\hbar}{4\omega_0} \left[\rho^2 + \omega^2(t)\rho^2 + \frac{\omega_0^2}{\rho^2} \right] + \frac{1}{2} m \dot{\alpha} + \frac{1}{2} m \omega^2(t) [\alpha - x_0(t)]^2. \quad (10)$$

For rigid transport⁶, ω is constant and Eq. (4) is trivially satisfied for $\rho(t) = 1$. Here, the goal is to transport a particle a distance d , and additionally change the angular frequency of the trap from the initial value ω_0 to the final value $\omega_f \equiv \omega(t_f) = \omega_0/\gamma^2$, without final excitation. The control parameters are the frequency $\omega(t)$ and the position of the center of the trap $x_0(t)$. Figure 1 shows schematically this process. The auxiliary functions $\alpha(t)$ and $\rho(t)$ have to satisfy the boundary conditions

$$\begin{aligned} \alpha(0) &= 0, & \alpha(t_f) &= d, \\ \rho(0) &= 1, & \rho(t_f) &= \gamma. \end{aligned} \quad (11)$$

We also find, by imposing commutativity between Hamiltonian and invariant at boundary times, the boundary conditions

$$\begin{aligned} \dot{\alpha}(0) &= \dot{\alpha}(t_f) = 0, \\ \dot{\rho}(0) &= \dot{\rho}(t_f) = 0. \end{aligned} \quad (12)$$

Additionally, to satisfy the invariant condition in Eq. (3) we need to impose

$$\begin{aligned} \ddot{\alpha}(0) &= \ddot{\alpha}(t_f) = 0, \\ \ddot{\rho}(0) &= \ddot{\rho}(t_f) = 0. \end{aligned} \quad (13)$$

Now, we may propose ansatzes that satisfy all boundary conditions in Eqs (11), (12) and (13). A simple choice is $\rho(t) = \sum_{i=0}^5 \rho_i s^i$ and $\alpha(t) = \sum_{i=0}^5 \alpha_i s^i$, where $s = t/t_f$. Fixing the coefficients ρ_i and α_i to satisfy the boundary conditions, the auxiliary functions become

$$\rho(t) = 1 + 10(\gamma - 1)s^3 - 15(\gamma - 1)s^4 + 6(\gamma - 1)s^5, \quad \alpha(t) = 10ds^3 - 15ds^4 + 6ds^5. \quad (14)$$

Substituting ρ in Eq. (4), the time dependent frequency in (9) takes the form

$$\omega(t) = \sqrt{\frac{\omega_0^2}{\rho^4} - \frac{\ddot{\rho}}{\rho}}, \quad (15)$$

whereas, from Eq. (5), the transport function (position of the trap center) is

$$x_0(t) = \frac{\ddot{\alpha}}{\omega^2} + \alpha, \quad (16)$$

	$\omega > 0$	trap in $[0, d]$	Both conditions
Sequential	0.443 μs	0.2 μs	0.643 μs
Dual	0.443 μs	0.91 μs	0.91 μs

Table 1. Minimal times for the transport + expansion process when the trap frequency or/and center are limited, see text. Parameters: $d = 370 \mu\text{m}$, $\gamma = \sqrt{10}$, and $\omega_0/(2\pi) = 2 \text{ MHz}$.

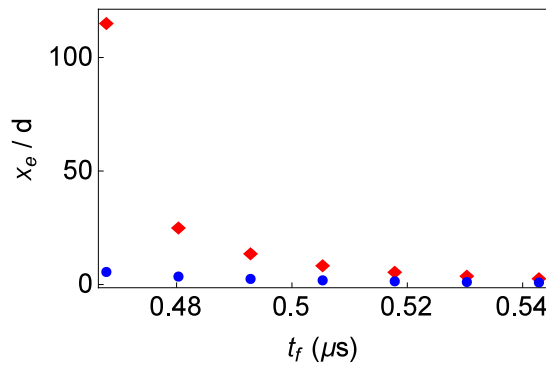


Figure 2. Ratio of the exceeded distance x_e and the transport distance d for the dual (blue circles) and sequential (red diamonds) non-rigid harmonic transport protocols, for final times that do not require imaginary frequencies. Parameters used are $d = 370 \mu\text{m}$, $\gamma = \sqrt{10}$, and $\omega_0/(2\pi) = 2 \text{ MHz}$.

that can be now calculated with Eqs (14) and (15). The form of the polynomial for ρ in Eq. (14) is not affected by the transport, so the function for the frequency in Eq. (15) is the same as the one used for pure expansions⁴. Similarly, the form of $\alpha(t)$ is not affected by the expansion, but the trap position $x_0(t)$ is different from the one in rigid transport⁶ due to the time dependence of the frequency. The dual task protocol is thus not just a simultaneous superposition of recipes for pure expansions and rigid transport but a genuinely different process.

We performed a number of tests to compare the times required by the sequential or dual protocols. In principle, both the sequential and the dual drivings can be done arbitrarily fast, if no limitations are imposed. However, subjected to technical limitations the minimal times may be different. One of the bounds will be to keep the frequency always real, $\omega^2(t) > 0$, since a repulsive parabola may be difficult to implement in some trapping methods. Other natural constraint is to limit the trap position bounded within the “box” $[0, d]$.

We carry out the comparisons for a ${}^9\text{Be}^+$ ion, shuttled over a distance $d = 370 \mu\text{m}$ in a trap with initial frequency $\omega_0/(2\pi) = 2 \text{ MHz}$ expanded by a factor of 10, $\gamma^2 = 10$. For these parameters and polynomial ansatzes, the simple expansion has a minimal final time $t_{f_{exp}}^{(min)} = 0.443 \mu\text{s}$, below which imaginary frequencies appear. Note that this will also be the limit time before getting imaginary frequencies in the dual process, as Eq. (15) gives exactly the same evolution for ω in a simple expansion or a dual process. For rigid transport, carried out before the expansion at the highest trap frequency, the limit time is $t_{f_{tra}}^{(min)} = 0.2 \mu\text{s}$ before exceeding the box. Thus, the total minimal time for the sequential protocol is $t_{f_{seq}} = 0.643 \mu\text{s}$. For the dual protocol, the minimal final time before exceeding the box is $t_{f_{dual}} = 0.91 \mu\text{s}$. Under the stated restrictions (real frequencies and the trap bounded by the predetermined box $[0, d]$), the dual protocol is slower than the sequential one, if performing the transport first and then the expansion. All final times are summarized in Table 1.

If the only restriction is to keep real frequencies, dropping the limitation on the domain of the trap position, the minimal final time is in principle $t_f^{(min)} = 0.443 \mu\text{s}$ for both the sequential and dual protocols, but in the sequential protocol this is a really challenging limit since the transport should be done in zero time. In both protocols the transport function exceeds the box $[0, d]$. In Fig. 2 we compare the ratio between the exceeded distance beyond $[0, d]$ and d for the sequential and the dual drivings, with respect to the total process time. The exceeded distance is defined in terms of the maximum ($x_{0_{max}}$) and the minimum ($x_{0_{min}}$) values of the trajectory as $x_e = x_{0_{max}} - x_{0_{min}} - d$. The figure shows that the dual protocol is much more robust. As the minimal possible time is approached, the ratio in the sequential protocol increases dramatically. In contrast, the ratio in the dual protocol is very stable, making potentially easier to perform the dual protocol for short times.

Dual-task launching in a harmonic trap. We study now launching processes where the frequency of the trap is time dependent (stopping processes may be designed by inverting the launching protocols). If the ion is to be launched adiabatically with a very precise velocity, the trap should have a small final frequency to minimize the uncertainty. STA protocols will achieve the same goal in a shorter time.

The order of the sequence plays a relevant role to compare sequential or dual launching protocols. In the previous subsection, when the final state is at rest, the sequential protocol may be faster than the dual one when transport is done first, then the expansion. For the launching process, the only meaningful sequential process implies to expand first, and then to transport, but a small trap frequency does not enable us to implement a fast

	$\omega > 0$	trap in $[0, d]$	Both conditions
Sequential	0.443 μs	2.295 μs	2.734 μs
Dual	0.443 μs	1.216 μs	1.216 μs

Table 2. Minimal final times for the launching + expansion process with limited frequency or/and trap center, see text. Parameters: $d = 370 \mu\text{m}$, $\gamma = \sqrt{10}$, $v_f = 10 \text{ m/s}$, and $\omega_0/(2\pi) = 2 \text{ MHz}$.

launching. It is therefore useful to combine the time dependences of frequency and displacement of the trap in a dual protocol.

The boundary conditions to be imposed for this launching protocol are the same as in Eqs (11), (12) and (13), except that the first derivative of α at final time, is now the final launching velocity v_f ,

$$\dot{\alpha}(t_f) = v_f. \tag{17}$$

Additionally, boundary conditions are imposed on the third derivative of α ,

$$\alpha^{(3)}(0) = \alpha^{(3)}(t_f) = 0, \tag{18}$$

where $^{(n)}$ means n th derivative, so that, according to Eq. (16), the velocity of the trap \dot{x}_0 and the velocity of the wave packet $\dot{\alpha}$ are the same at the boundary times. In order to satisfy the additional boundary conditions, we consider a higher-order polynomial ansatz for α , $\alpha = \sum_{i=0}^7 \alpha_i s^i$, which upon fixing parameters to satisfy all boundary conditions gives

$$\alpha(t) = 5(7d - 3t_f v_f) s^4 - 3(28d - 13t_f v_f) s^5 + 2(35d - 17t_f v_f) s^6 - 10(2d - t_f v_f) s^7. \tag{19}$$

Boundary conditions for ρ are the same as in the previous subsection, so the same ansatz used in Eq. (14) is valid here. Thus, the evolution of the frequency is given in Eq. (15), while the evolution of the trap position is found substituting Eqs (15) and (19) into Eq. (16).

We evaluated the sequential and dual launching protocols limiting the frequencies to real values and the domain of the trap center to $[0, d]$. For the same parameters used in the previous subsection, and for a final velocity $v_f = 10 \text{ m/s}$, the minimal expansion time is the one given in the previous subsection, $t_{f,exp}^{(min)} = 0.443 \mu\text{s}$, as the expansion does not change for the new boundary conditions. The rigid transport, however, performed with the final trap frequency, can be done in a minimal time $t_{f,tra}^{(min)} = 2.295 \mu\text{s}$ without exceeding the box. Thus, the minimal sequential time is $t_{f,tot}^{(min)} = 2.734 \mu\text{s}$. For the dual protocol, the minimal time not exceeding the box is $t_{f,dual} = 1.216 \mu\text{s}$. The times are summarized in Table 2. Here the dual protocol clearly outperforms the sequential one.

A control possibility we have for the dual process, which does not exist for the sequential one, is to design the launching with a given constant expanding velocity, i.e., we impose $\dot{\alpha}(t_f) = v_f$ as before and also

$$\dot{\rho}(t_f) = \varepsilon. \tag{20}$$

Additionally, boundary conditions may be imposed on the third derivative,

$$\rho^{(3)}(0) = \rho^{(3)}(t_f) = 0, \tag{21}$$

so that, from Eq. (4), $\dot{\omega}(0) = 0$ and $\dot{\omega}(t_f) = -2\varepsilon\omega_0/\gamma^3$, which guarantees that the expansion velocity of the dynamical state matches that of the instantaneous eigenstates of the trap, consistently with the time derivative of $\rho(t_f) = \sqrt{\frac{\omega_0}{\omega_f}}$.

For the polynomial ansatz $\rho = \sum_{i=0}^7 \rho_i s^i$ the coefficients are fixed to satisfy the boundary conditions,

$$\rho(t) = 1 + 5(-7 + 7\gamma - 3\varepsilon t_f) s^4 - 3(-28 + 28\gamma - 13\varepsilon t_f) s^5 + 2(-35 + 35\gamma - 17\varepsilon t_f) s^6 - 10(-2 + 2\gamma - \varepsilon t_f) s^7. \tag{22}$$

With the evolutions considered in this section, either for the expanding or the nonexpanding launching, a state which is initially an eigenstate of $H(0)$ will not become an eigenstate of the Hamiltonian $H(t_f)$. Instead, the state of the system at the end of the process is, see Eq. (7), $\psi_n(x, t_f) = e^{\frac{im}{\hbar}[\varepsilon x^2/2\gamma + (v_f \gamma - d\varepsilon)x/\gamma]} \frac{1}{\sqrt{2}^{1/2}} \varphi_n\left(\frac{x-d}{\gamma}\right)$, which can be shown to correspond to the Hamiltonian eigenstate in the moving and expanding reference system of the trap (see Methods).

The expectation value of the velocity for $\psi_n(x, t_f)$ is v_f and its dispersion is

$$\Delta v = \sqrt{\frac{\hbar(2n + 1)}{2m\omega_0} \left(\gamma^2 \varepsilon^2 + \frac{\omega_0^2}{\gamma^4} \right)}, \tag{23}$$

minimal with respect to ε for $\varepsilon = 0$. It can be lowered further by decreasing the final trap frequency (increasing γ). This result may be compared with the process where the initial trap is turned off and a constant electric field is

applied. Then the dispersion does not change, $\Delta v = \sqrt{[\hbar(2n + 1)\omega_0]/(2m)}$. Much smaller spreads can be achieved by the dual protocol, but γ cannot be made arbitrarily small in a fixed process time. In particular, the requirement of keeping the frequency real implies the bound^{9,14} $t_f > \sqrt{\gamma^2 - 1}/\omega_0$. A constant electric field has its own, different limitations, in particular, with constant acceleration the time is fixed as $t_f = 2d/v_f$ to reach a given final velocity v_f in a distance d .

Dual-task shortcuts in an arbitrary trap. Now, we extend the analysis to move and expand or compress an arbitrary confining potential from $U(x)$ to $\frac{1}{\rho(t_f)^2} U\left[\frac{x - \alpha(t_f)}{\rho(t_f)}\right]$. To stay within the family of processes described by Eq. (1), so that invariants are known, we must impose that the harmonic and linear terms depending on ω^2 and F vanish at the boundary times. We thus set $\omega_0 = 0$ hereafter. If initial and final potentials are at rest, by imposing commutativity between the Hamiltonian (1) and the invariant (2) and continuity at the boundary times, we get the same boundary conditions as in Eqs (12) and (13). We must also impose the boundary conditions in Eq. (11) for the system to be displaced and expanded or compressed, noting that now the constant γ is not related to ω_0 . With these boundary conditions, using the auxiliary Eqs (4) and (5), $F(0) = F(t_f) = \omega(0) = \omega(t_f) = 0$. That is, the only non vanishing term of the potential at the boundary times $t_b = 0$, t_f is $V(t_b) = \frac{1}{\rho(t_b)^2} U\left[\frac{x - \alpha(t_b)}{\rho(t_b)}\right]$. We design the functions $\alpha(t)$ and $\rho(t)$ polynomially as before, so that they satisfy all boundary conditions, and introduce them in the auxiliary equations to inversely obtain the control parameters. The auxiliary functions can be the same as in Eq. (14). Substituting ρ in Eq. (4),

$$\omega^2(t) = -\frac{\ddot{\rho}}{\rho}, \tag{24}$$

and substituting this result and α in Eq. (5) we get

$$F(t) = m\ddot{\alpha} + m\omega^2\alpha. \tag{25}$$

In other words, the protocol requires auxiliary time-dependent linear and quadratic potential terms apart from the scaled potential $\frac{1}{\rho^2(t)} U\left[\frac{x - \alpha(t)}{\rho}\right]$. This protocol is of course technically more demanding than the one designed for the simple harmonic trap, because of the need to implement and control all terms (linear, quadratic, and U -term) of the Hamiltonian (1).

The results can be extended to a launching scenario. To be specific, we shall consider the double well, a paradigmatic quantum model that has been used, for example, to study and control some of the most fundamental quantum effects, like interference or tunneling. With the advent of ultracold-atom-based technology, it also finds applications in metrology, sensors, and the implementation of basic operations for quantum information processing, like separation or recombination of ions²⁴, as well as Fock state creation³³, and multiplexing/demultiplexing vibrational modes^{34,35}. Here, we explore the possibility of using it for differential launching of vibrational modes.

We set U (in σ : $= \frac{x - \alpha}{\rho}$ space) as

$$U(\sigma) = \beta\sigma^4 + \lambda\sigma^2 + \mu\sigma, \tag{26}$$

where β , λ and μ are constant parameters. β , is positive and λ negative so that we have indeed a double well. The linear term produces a bias between the wells. The condition²⁶ $|\mu| \ll \frac{4\sqrt{2}}{3} \sqrt{-\frac{\lambda^3}{\beta}}$ enables us to approximate $U(\sigma)$ as the sum of two harmonic potentials with minima at²⁶

$$\sigma_{\pm}(t) = \pm \frac{1}{\sqrt{2}} \sqrt{-\frac{\lambda}{\beta}} + \frac{\mu}{4\lambda} \tag{27}$$

in σ -space, and effective angular frequency

$$\Omega = 2\sqrt{-\frac{\lambda}{m}}. \tag{28}$$

Limiting the linear coefficient as $|\mu| < \hbar(2\beta/m)^{1/2}$, the first excited and ground states lie in different wells³⁴. We want to implement a protocol with a nonzero final expansion velocity, such that the effective launching velocities for ground and first excited states are different so that they separate further. We choose the boundary conditions for the auxiliary functions in Eqs (11) and (13) and for the first derivatives

$$\begin{aligned} \dot{\alpha}(0) &= 0, \quad \dot{\alpha}(t_f) = v_0, \\ \dot{\rho}(0) &= 0, \quad \dot{\rho}(t_f) = \varepsilon. \end{aligned} \tag{29}$$

Here the boundary conditions for the third derivatives [Eqs (18) and (21)] are not necessary. With these conditions, using fifth-order polynomial ansatzes, the auxiliary functions are finally given by

$$\alpha(t) = 2(5d - 2t_f v_0)s^3 + (-15d + 7t_f v_0)s^4 + 3(2d - t_f v_0)s^5, \tag{30}$$

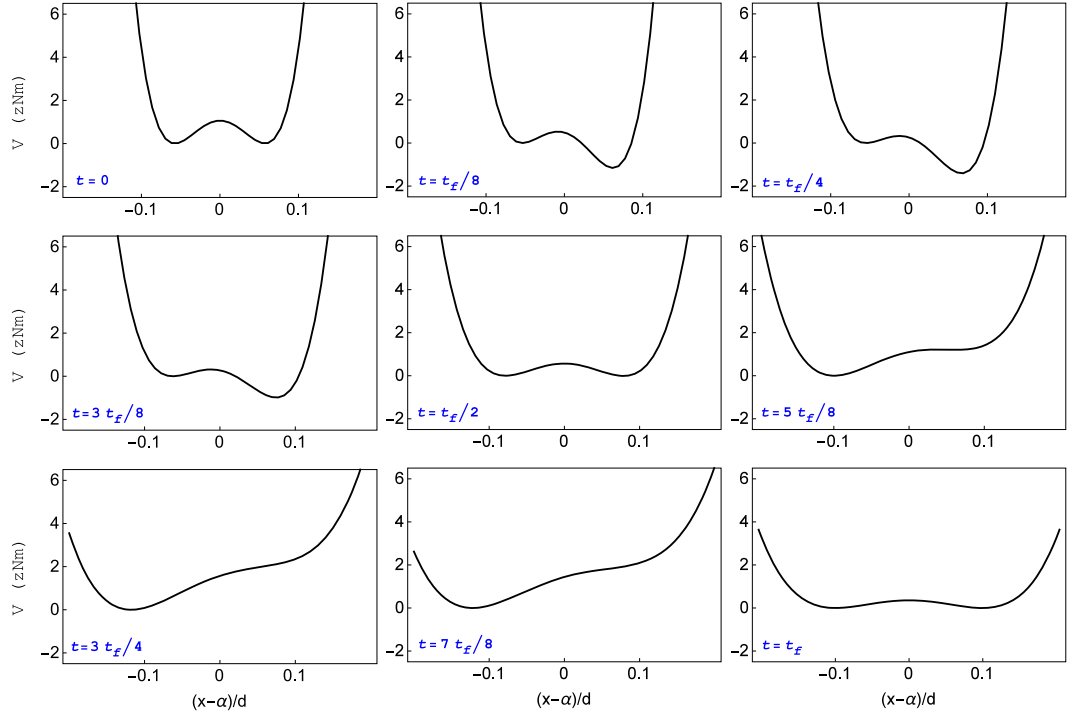


Figure 3. Time evolution of the shape of the launching double-well potential with velocities $v_f = 10$ m/s and $\varepsilon=2/s$. Each snapshot has been vertically displaced, without affecting the dynamics of the system, so that the minimum of the left well always lies at zero potential. The parameters used are $\lambda = -4.7$ pN/m, $\beta = 5.2$ mN/m³, $\mu = 86.4$ zN, $d = 370$ μ m, $\gamma = \sqrt{3}$ and $t_f = 1$ μ s. Even though not appreciated by the naked eye in the

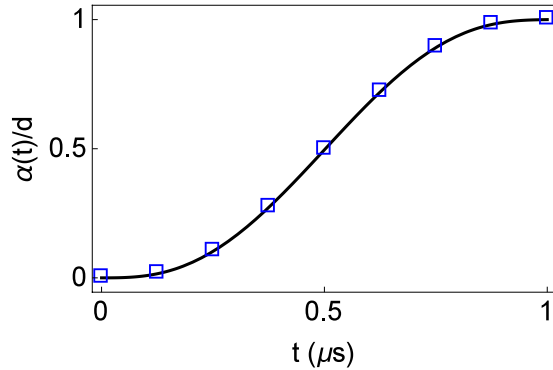


Figure 4. Scaled trajectory α , Eq. (30), of the center of the trap in a double well launching protocol with parameters $\lambda = -4.7$ pN/m, $\beta = 5.2$ mN/m³, $\mu = 86.4$ zN, $d = 370$ μ m, $\gamma = \sqrt{3}$ and $t_f=1$ μ s, and velocities $v_f=10$ m/s and $\varepsilon=2/s$. Blue rectangles mark the points of the trajectory in which a snapshot of the potential is depicted in Fig. 3.

$$\rho(t)=1 + 2(-5 + 5\gamma - 2t_f\varepsilon)s^3 + (15 - 15\gamma + 7t_f\varepsilon)s^4 + 3(-2 + 2\gamma - t_f\varepsilon)s^5. \tag{31}$$

These parameters directly give us the evolution of the potential term $\rho^{-2}U[(x - \alpha)/\rho]$. The auxiliary harmonic and linear terms in the total Hamiltonian (1) are found by substituting α and ρ in Eqs (24) and (25), respectively. The resulting potential (the sum of the three potential terms in Eq. (1)) is depicted in Fig. 3 as a function of $(x - \alpha)/d$, with α depicted in Fig. 4.

For this evolution, we can calculate the average final velocity of the ground states in each well, and the final dispersion,

$$\langle v_{\pm} \rangle = v_0 + \varepsilon \left(\frac{\mu}{4\lambda} \pm \frac{1}{\sqrt{2}} \sqrt{\frac{-\lambda}{\beta}} \right), \quad \Delta v = \sqrt{\frac{\hbar}{4\sqrt{-m\lambda}} \left(\varepsilon^2 - \frac{4\lambda}{m\gamma^2} \right)}, \tag{32}$$

which is the same in both wells, as the effective frequency is also equal. Details of these calculations are displayed in Methods. Choosing the parameters so that $\langle v_+ \rangle - \langle v_- \rangle > 2\Delta v$, guarantees that the wave packets of each well will never overlap.

Discussion

In this paper, we have used the invariant-based inverse-engineering method to design shortcuts to adiabaticity for nonrigid driven transport and launching. Shortcuts for a harmonic trap are designed first, and then the analysis is extended to an arbitrary trapping potential. Compared to rigid transport⁶, nonrigid transport requires a more demanding manipulation, but it also provides a wider range of control opportunities, for example to achieve narrow final velocity distributions in a launching process, suitable for accurate ion implantation or low-energy scattering experiments. A further example is the possibility to launch the ground states of each well in a double well with different velocities. In a previous work³⁴ processes to separate the ground and the first-excited states of a harmonic trap into different wells of a biased double well using STA were described. The processes discussed here can be applied to different systems such as neutral atoms in optical traps, or classical mechanical oscillators, for which, *mutatis mutandis*, most of the results apply.

Methods

Unitary displacement and dilatation transformations. First, we prove that given an arbitrary unitary transformation U , the transformed invariant $I' = UIU^\dagger$ is an invariant of the effective Hamiltonian $H' = UHU^\dagger + i\hbar\frac{\partial U}{\partial t}U^\dagger$. Their commutator is given by

$$[I', H'] = [UHU^\dagger + i\hbar\frac{\partial U}{\partial t}U^\dagger, UIU^\dagger] = U[H, I]U^\dagger + i\hbar\frac{\partial U}{\partial t}IU^\dagger - i\hbar UIU^\dagger\frac{\partial U}{\partial t}U^\dagger, \tag{33}$$

and the invariance condition [see Eq. (3)] for the transformed operators is satisfied,

$$i\hbar\frac{\partial I'}{\partial t} - [I', H'] = U\left(i\hbar\frac{\partial I}{\partial t} - [H, I]\right)U^\dagger = 0. \tag{34}$$

Now we introduce the specific unitary time-dependent operator $U = U_{d_2}U_{d_1}U_pU_x$. Operators U_{d_1} and U_{d_2} perform a time-dependent dilatation, and U_x and U_p a time-dependent translation in space and momentum, and are given by³⁶

$$\begin{aligned} U_{d_1} &= e^{-\frac{im\rho}{2\hbar\rho}x^2}; & U_{d_2} &= e^{\frac{im\rho}{2\hbar}(px+xp)}, \\ U_p &= e^{-\frac{im\dot{\alpha}}{\hbar}x}; & U_x &= e^{\frac{i\alpha}{\hbar}x}. \end{aligned} \tag{35}$$

In the comoving and coexpanding frame defined by this transformation, the new invariant

$$I' = UIU^\dagger = U_{d_2}U_{d_1}U_pU_xIU_x^\dagger U_p^\dagger U_{d_1}^\dagger U_{d_2}^\dagger = \frac{1}{2m}p^2 + \frac{1}{2}m\omega_0x^2 + U(x), \tag{36}$$

becomes time independent³⁷. Note that I' has the same form of the Hamiltonian in Eq. (8) and therefore, the eigenstates of I' are given by $\phi_n(x)$. The inverse transformation acting on ϕ_n provides the time dependent eigenvectors of $I(t)$ in Eq. (7),

$$\psi_n(x, t) = U^\dagger\phi_n(x) = U_x^\dagger U_p^\dagger U_{d_1}^\dagger U_{d_2}^\dagger \phi_n(x) = e^{\frac{im}{\hbar}[\rho x^2/2\rho + (\alpha\rho - \alpha\rho)x/\rho]} \frac{1}{\sqrt{\rho}} \phi_n\left(\frac{x - \alpha}{\rho}\right). \tag{37}$$

The Hamiltonian in the comoving and coexpanding frame is

$$H' = UHU^\dagger + i\hbar\frac{\partial U}{\partial t}U^\dagger = \frac{1}{\rho^2}\left(\frac{1}{2m}p^2 + \frac{1}{2}m\omega_0x^2 + U(x)\right) + \frac{m}{2}\left(\frac{\dot{\rho}\alpha^2}{\rho} - \dot{\alpha}^2\right) - m\ddot{\alpha}\alpha, \tag{38}$$

which, up to global terms that depend only on time, is proportional to the transformed invariant (36), so they commute at all times and thereby, share eigenstates at all times.

Note that the noninertial frame considered is comoving with α , which is the center of the term $\rho^{-2}U[(x - \alpha)/\rho]$, but not necessarily the center of the harmonic potential $\frac{m}{2}\omega^2(x - x_0)^2$ in Eq. (9) when $U = 0$. However, the boundary conditions are set, see Eq. (18), so that indeed the frames moving with α and x_0 coincide at boundary times $t_b = 0, t_f$, as $\alpha(t_b) = x_0(t_b)$, and $\dot{\alpha}(t_b) = \dot{x}_0(t_b)$. Similarly Eq. (21) implies that the coexpanding frame depending on ρ agrees with the one defined by the scaling factor $\rho_{trap} = \sqrt{\omega_0/\omega_f}$ associated with the expansion of the trap, $\rho(t_b) = \rho_{trap}(t_b)$, and $\dot{\rho}(t_b) = \dot{\rho}_{trap}(t_b)$.

Average velocity and dispersion in a double well. Here, we consider the Hamiltonian in Eq. (1) with $U(\sigma)$ given by a double well, Eq. (26), where ground and first-excited states lie in different wells and may be approximated by ground states of corresponding harmonic oscillators centered in σ_\pm [see Eq. (27)], and effective angular frequency Ω [see Eq. (28)]. If the initial state is either the ground or first-excited state, the dynamical state of the system is in either case

$$\psi^\pm(x, t) = e^{\frac{im}{\hbar}[\rho x^2/2\rho + (\dot{\alpha}\rho - \alpha\dot{\rho})x/\rho]} \frac{1}{\rho^{1/2}} \varphi_0^\pm, \quad (39)$$

$$\text{where } \varphi_0^\pm = \left(\frac{m\Omega}{\pi\hbar}\right)^{1/4} e^{-\frac{m\Omega}{2\hbar}\left(\frac{x-\alpha}{\rho} - \sigma_\pm\right)^2} H_0\left[\sqrt{\frac{m\Omega}{\hbar}}\left(\frac{x-\alpha}{\rho} - \sigma_\pm\right)\right].$$

Using standard properties of Hermite polynomials the average of the velocity and its square are found to be

$$\langle v_\pm \rangle = -\frac{i\hbar}{m} \int (\psi^\pm)^* \partial_x \psi^\pm dx = \dot{\alpha} + \rho \sigma_\pm, \quad (40)$$

$$\langle v_\pm^2 \rangle = -\frac{\hbar^2}{m^2} \int (\psi^\pm)^* \partial_x^2 \psi^\pm dx = (\dot{\alpha} + \rho \sigma_\pm)^2 + \frac{\hbar}{2m\Omega} \left(\dot{\rho}^2 + \frac{\Omega^2}{\rho^2} \right). \quad (41)$$

Finally, the dispersion, common to both wells, is given by

$$\Delta v = \Delta v_\pm = \sqrt{\langle v_\pm^2 \rangle - \langle v_\pm \rangle^2} = \sqrt{\frac{\hbar}{2m\Omega} \left(\dot{\rho}^2 + \frac{\Omega^2}{\rho^2} \right)}. \quad (42)$$

Equation (32) follows by substituting in Eqs (40) and (42) the expressions for σ_\pm and Ω , Eqs (27) and (28), and the final values of the auxiliary functions and their derivatives in Eqs (11) and (29).

References

- Bowler, R. *et al.* Coherent Diabatic Ion Transport and Separation in a Multizone Trap Array. *Phys. Rev. Lett.* **109**, 080502, doi:10.1103/PhysRevLett.109.080502 (2012).
- Walther, A. *et al.* Controlling Fast Transport of Cold Trapped Ions. *Phys. Rev. Lett.* **109**, 080501, doi:10.1103/PhysRevLett.109.080501 (2012).
- Steffen, A. *et al.* A digital atom interferometer with single particle control on a discretized spacetime geometry. *PNAS* **109**, 9770, doi:10.1073/pnas.1204285109 (2012).
- Chen, X. *et al.* Fast Optimal Frictionless Atom Cooling in Harmonic Traps: Shortcut to Adiabaticity. *Phys. Rev. Lett.* **104**, 063002, doi:10.1103/PhysRevLett.104.063002 (2010).
- Torrontegui, E. *et al.* Shortcuts to Adiabaticity, *Adv. At. Mol. Opt. Phys.* **62** (Elsevier, 2013). doi:10.1016/B978-0-12-408090-4.00002-5
- Torrontegui, E. *et al.* Fast atomic transport without vibrational heating. *Phys. Rev. A* **83**, 013415, doi:10.1103/PhysRevA.83.013415 (2011).
- Chen, X., Torrontegui, E., Stefanatos, D., Li, J.-S. & Muga, J. G. Optimal trajectories for efficient atomic transport without final excitation. *Phys. Rev. A* **84**, 043415, doi:10.1103/PhysRevA.84.043415 (2011).
- Fürst, H. A. *et al.* Controlling the transport of an ion: classical and quantum mechanical solutions. *New J. Phys* **16**, 075007, doi:10.1088/1367-2630/16/7/075007 (2014).
- Chen, X. & Muga, J. G. Transient energy excitation in shortcuts to adiabaticity for the time-dependent harmonic oscillator. *Phys. Rev. A* **82**, 053403, doi:10.1103/PhysRevA.82.053403 (2010).
- Stefanatos, D., Ruths, J. & Li, J.-S. Frictionless atom cooling in harmonic traps: A time-optimal approach. *Phys. Rev. A* **82**, 063422, doi:10.1103/PhysRevA.82.063422 (2010).
- Torrontegui, E. *et al.* Fast transitionless expansion of cold atoms in optical Gaussian-beam traps. *Phys. Rev. A* **85**, 033605, doi:10.1103/PhysRevA.85.033605 (2012).
- Cui, Y.-Y., Chen, X. & Muga, J. G. Transient particle energies in shortcuts to adiabatic expansions of harmonic traps. *J. Chem. Phys.* **120**, 2962–2969, doi:10.1021/acs.jpca.5b06090 (2016).
- Rezek, Y. & Kosloff, R. Irreversible performance of a quantum harmonic heat engine. *New J. Phys* **8**, 83, doi:10.1088/1367-2630/8/5/083 (2006).
- Salamon, P., Hoffmann, K. H., Rezek, Y. & Kosloff, R. Maximum work in minimum time from a conservative quantum system. *Phys. Chem. Chem. Phys.* **11**, 1027–1032, doi:10.1039/B816102J (2009).
- Hoffmann, K., Salamon, P., Rezek, Y. & Kosloff, R. Time-optimal controls for frictionless cooling in harmonic traps. *EPL* **96**, 60015, doi:10.1209/0295-5075/96/60015 (2011).
- Abah, O. *et al.* Single-ion heat engine at maximum power. *Phys. Rev. Lett.* **109**, 203006, doi:10.1103/PhysRevLett.109.203006 (2012).
- Deng, J., Wang, Q.-H., Liu, Z., Hänggi, P. & Gong, J. Boosting work characteristics and overall heat-engine performance via shortcuts to adiabaticity: Quantum and classical systems. *Phys. Rev. E* **88**, 062122, doi:10.1103/PhysRevE.88.062122 (2013).
- Jarzynski, C. Generating shortcuts to adiabaticity in quantum and classical dynamics. *Phys. Rev. A* **88**, 040101, doi:10.1103/PhysRevA.88.040101 (2013).
- Stefanatos, D. Optimal efficiency of a noisy quantum heat engine. *Phys. Rev. E* **90**, 012119, doi:10.1103/PhysRevE.90.012119 (2014).
- Del Campo, A., Goold, J. & Paternostro, M. More bang for your buck: Towards super-adiabatic quantum engines. *Sci. Rep* **4**, 6208, doi:10.1038/srep06208 (2014).
- Beau, M., Jaramillo, J. & del Campo, A. Scaling-up quantum heat engines efficiently via shortcuts to adiabaticity. *Entropy* **18**, 168, doi:10.3390/e18050168 (2016).
- Rofnagel, J. *et al.* A single-atom heat engine. *Science* **352**, 325–329, doi:10.1126/science.aad6320 (2016).
- Wineland, D. J. *et al.* Experimental issues in coherent quantum-state manipulation of trapped atomic ions. *J. Res. Natl. Inst. Stand. Technol.* **103** doi:10.6028/jres.103.019 (1998).
- Palmero, M., Martínez-Garaot, S., Poschinger, U. G., Ruschhaupt, A. & Muga, J. G. Fast separation of two trapped ions. *New J. Phys* **17**, 093031, doi:10.1088/1367-2630/17/9/093031 (2015).
- Palmero, M., Martínez-Garaot, S., Alonso, J., Home, J. P. & Muga, J. G. Fast expansions and compressions of trapped-ion chains. *Phys. Rev. A* **91**, 053411, doi:10.1103/PhysRevA.91.053411 (2015).
- Martínez-Garaot, S., Palmero, M., Guéry-Odelin, D. & Muga, J. G. Fast bias inversion of a double well without residual particle excitation. *Phys. Rev. A* **92**, 053406, doi:10.1103/PhysRevA.92.053406 (2015).
- Narevicius, E. *et al.* Stopping supersonic beams with a series of pulsed electromagnetic coils: An atomic coilgun. *Phys. Rev. Lett.* **100**, 093003, doi:10.1103/PhysRevLett.100.093003 (2008).
- Jacob, G. *et al.* Transmission microscopy with nanometer resolution using a deterministic single ion source. *Phys. Rev. Lett.* **117**, 043001, doi:10.1103/PhysRevLett.117.043001 (2016).

29. Meijer, J. *et al.* Concept of deterministic single ion doping with sub-nm spatial resolution. *Appl. Phys. A* **83**, 321–327, doi:10.1007/s00339-006-3497-0 (2006).
30. Lewis, H. R. & Riesenfeld, W. B. An Exact Quantum Theory of the Time-Dependent Harmonic Oscillator and of a Charged Particle in a Time-Dependent Electromagnetic Field. *J. Math. Phys.* **10**, 1458, doi:10.1063/1.1664991 (1969).
31. Dhara, A. K. & Lawande, S. V. Feynman propagator for time-dependent Lagrangians possessing an invariant quadratic in momentum. *J. Phys. A* **17**, 2423–2431, doi:10.1088/0305-4470/17/12/014 (1984).
32. Lewis, H. R. & Leach, P. G. L. A direct approach to finding exact invariants for one-dimensional time-dependent classical Hamiltonians. *J. Math. Phys.* **23**, 2371, doi:10.1063/1.525329 (1982).
33. Martínez-Garaot, S., Palmero, M., Muga, J. G. & Guéry-Odelin, D. Fast driving between arbitrary states of a quantum particle by trap deformation. *Phys. Rev. A* **94**, 063418, doi:10.1103/PhysRevA.94.063418 (2016).
34. Martínez-Garaot, S. *et al.* Vibrational mode multiplexing of ultracold atoms. *Phys. Rev. Lett.* **111**, 213001, doi:10.1103/PhysRevLett.111.213001 (2013).
35. Martínez-Garaot, S. Shortcuts to adiabaticity in the double well. *Ph.D. thesis* UPV/EHU (2016).
36. Lohe, M. Exact time dependence of solutions to the time-dependent Schrödinger equation. *J. Phys. A* **42**, 035307, doi:10.1088/1751-8113/42/3/035307 (2009).
37. Pedrosa, I. A., Serra, G. P. & Guedes, I. Wave functions of a time-dependent harmonic oscillator with and without a singular perturbation. *Phys. Rev. A* **56**, 4300–4303, doi:10.1103/PhysRevA.56.4300 (1997).

Acknowledgements

We thank G.C. Hegerfeldt for discussions. This work was partially supported by the Basque Government (Grant IT986-16), and Grant FIS2015-67161-P (MINECO/FEDER,UE). M.P. and S.M.-G. acknowledge fellowships by UPV/EHU.

Author Contributions

A.T., M.P., S.M.-G. and J.G.M. conceived the work, discussed the results, and reviewed the manuscript, A.T. lead the calculations.

Additional Information

Competing Interests: The authors declare that they have no competing interests.

Publisher's note: Springer Nature remains neutral with regard to jurisdictional claims in published maps and institutional affiliations.



Open Access This article is licensed under a Creative Commons Attribution 4.0 International License, which permits use, sharing, adaptation, distribution and reproduction in any medium or format, as long as you give appropriate credit to the original author(s) and the source, provide a link to the Creative Commons license, and indicate if changes were made. The images or other third party material in this article are included in the article's Creative Commons license, unless indicated otherwise in a credit line to the material. If material is not included in the article's Creative Commons license and your intended use is not permitted by statutory regulation or exceeds the permitted use, you will need to obtain permission directly from the copyright holder. To view a copy of this license, visit <http://creativecommons.org/licenses/by/4.0/>.

© The Author(s) 2017

Energy consumption for shortcuts to adiabaticityE. Torrontegui,^{1,2,*} I. Lizuain,³ S. González-Resines,⁴ A. Tobalina,⁴ A. Ruschhaupt,⁵ R. Kosloff,² and J. G. Muga^{4,†}¹*Instituto de Física Fundamental IFF-CSIC, Calle Serrano 113b, 28006 Madrid, Spain*²*Institute of Chemistry and The Fritz Haber Research Center, The Hebrew University, Jerusalem 91904, Israel*³*Department of Applied Mathematics, University of the Basque Country UPV/EHU, Plaza Europa 1, 20018 Donostia-San Sebastian, Spain*⁴*Departamento de Química Física, Universidad del País Vasco-Euskal Herriko Unibertsitatea, Apartado 644, Bilbao, Spain*⁵*Department of Physics, University College Cork, Cork, Ireland*

(Received 26 April 2017; published 25 August 2017)

Shortcuts to adiabaticity let a system reach the results of a slow adiabatic process in a shorter time. We propose to quantify the “energy cost” of the shortcut by the energy consumption of the system enlarged by including the control device. A mechanical model where the dynamics of the system and control device can be explicitly described illustrates that a broad range of possible values for the consumption is possible, including zero (above the adiabatic energy increment) when friction is negligible and the energy given away as negative power is stored and reused by perfect regenerative braking.

DOI: [10.1103/PhysRevA.96.022133](https://doi.org/10.1103/PhysRevA.96.022133)**I. INTRODUCTION**

Shortcuts to adiabaticity (STAs) [1,2] are protocols for the time dependence of the control parameters of a system (hereafter primary system, PS) so that it reaches the same final conditions (energy, populations, or state) of a slow adiabatic process in a shorter time. STAs have found widespread applications in atomic, molecular, and optical physics and beyond, e.g., for classical systems [3–5], as a generic tool to combat decoherence and design robust, fast processes or devices. Some STAs use the structure of the Hamiltonian describing the slow process for the PS, as in invariant-based methods [1], and others add new control terms, as in counterdiabatic approaches [6], but this distinction does not affect the following discussion.

The total mechanical work done on the PS in a given STA is, by definition, equal to the work done in the adiabatic process, i.e., the adiabatic energy increment between initial and final states. It was soon clear that this quantity could not represent all relevant energy flows, which led to the consideration of alternative measures [7]. Several disparate definitions of energy cost have been proposed in the context of quantum thermodynamics to characterize quantum engines and refrigerators [8–18]. These definitions have been systematically formulated in terms of the cycling system (PS) alone. Even if the existing proposals have their own merits and applications, the point of view put forward in this article is that a broader perspective is necessary for the definition to be useful and practically relevant, addressing not only the PS but also the control system (CS) that drives the time-dependent parameters. In other words, we advocate redefining and expanding the “system” in the model to include the PS and the CS in an enlarged system. It might appear that this simply shifts the system-defining border so that the same problem is translated towards the new border. The important point is to find a meaningful divide, for which the energy changes with the outer world are modeled by forces that can be easily translated into fuel or electric power consumption by an active device.

Such a shift is crucial to make the energy “cost” a significant quantity that indeed has something to do with the feasibility of the processes, minimal times allowed, or economic costs. Some examples help to clarify this: If a train (CS) transports cargo (PS) horizontally between two stations, the total energy increment of the cargo is zero. Surely what interests us more as a relevant cost is the energy consumption by the active force that the engines should do, translated into fuel consumption. We thus need to evaluate this force by expanding the physical model to include the train itself, taking into account friction and the braking mechanism and paying attention to the maximum power deliverable by the engine, which will put limits on the minimal transport times. Similar examples can be drawn from studies by nutritionists or biomechanicists concerned with the kilocalories the body consumes or the oxygen intake to perform a given task or exercise [19]. For a weightlifter (CS) pushing a weight (PS) up, the energy expenditure depends not only on the work done on the weight but also on CS-dependent factors such as the lifter’s skill and weight and muscular mass.

This paper is based on a simple model for which enlightening, explicit expressions for the dynamics, power, and energy consumption are worked out. In Sec. II we present our model, a mechanical crane, and the main results. The model is described by equations similar to the ones used for the transport of neutral atoms or ions in microscopic traps. In Sec. III we find the optimal protocol with respect to energy consumption, and the paper ends with a discussion in which we surmise the implications that we expect to be broadly applicable.

II. MODEL AND RESULTS

The model is an overhead crane, as depicted in Fig. 1, composed of a trolley of mass M (CS) moving along a horizontal bridge and a load of mass m (PS) pending by a constant-length rope [20]. We neglect the stiffness and mass of the rope and air resistance. The load can be regarded, in the small-oscillation regime characteristic of these devices, as a harmonic oscillator with a moving center. The generalized coordinates are the position of the trolley $x(t)$ and the swing angle $\theta(t)$. The process we consider is a transport of the load by moving the trolley from $x = 0$ to $x = d$ in a time t_f . If

*eriktm@iff.csic.es

†jg.muga@ehu.es

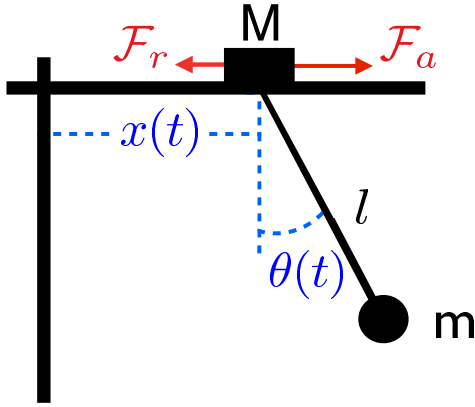


FIG. 1. Overhead crane composed of a load of mass m and a trolley of mass M connected through a rope of constant length l . The red solid arrows represent the active force \mathcal{F}_a and the friction force \mathcal{F}_r acting on a rightward-moving trolley.

done adiabatically, the initial and final energies of the load should be equal. Shortcuts for quantum systems subjected to a moving harmonic (or otherwise) trap have been extensively studied (see, e.g., [21–23]).

The external forces depicted in Fig. 1 are the actuating force \mathcal{F}_a (e.g., due to an engine or to a braking mechanism if it opposes the direction of motion of the trolley) and the friction, modeled here as $\mathcal{F}_r = -\gamma\dot{x}$, $\gamma \geq 0$. The Lagrangian, without friction, is $\mathcal{L} = \mathcal{L}_1 + \mathcal{L}_2$,

$$\begin{aligned}\mathcal{L}_1 &= \frac{m}{2}[\dot{x}^2 + l^2\dot{\theta}^2 + 2l\dot{x}\dot{\theta}\cos\theta] + mgl\cos\theta, \\ \mathcal{L}_2 &= \frac{M}{2}\dot{x}^2 + \mathcal{F}_a x,\end{aligned}\quad (1)$$

where the dots represent time derivatives, l is the rope length, and g is the gravitational acceleration. With friction, the equations of motion are derived from the Euler-Lagrange equations, with the equation on the trolley position modified to include a friction term, $\frac{d}{dt}(\frac{\partial\mathcal{L}}{\partial\dot{x}}) - \frac{\partial\mathcal{L}}{\partial x} + \frac{\partial\mathcal{F}}{\partial\dot{x}} = 0$, where $\mathcal{F} = \gamma\dot{x}^2/2$ is Rayleigh's dissipation function [24],

$$0 = l\ddot{\theta} + \ddot{x}\cos\theta + g\sin\theta, \quad (2)$$

$$\mathcal{F}_a + \mathcal{F}_r = M\ddot{x} + m(\ddot{x} + l\ddot{\theta}\cos\theta - l\dot{\theta}^2\sin\theta). \quad (3)$$

Equation (2) defines the kinematics of the load in terms of only $x(t)$; that is, it is formally independent of characteristics of the trolley such as mass or friction for a given $x(t)$. This allows the formal treatment of the load as an open system subject to an external time-dependent control, but $x(t)$ depends on these characteristics and on the angle and the pulling force via Eq. (3). We may compute the frictionless Hamiltonian of the total system through the Lagrangian $\mathcal{L} = \mathcal{L}_1 + \mathcal{L}_2$ given by Eq. (1), $\mathcal{H} = \dot{x}p_x + \dot{\theta}p_\theta - \mathcal{L}$, where $p_x = \partial\mathcal{L}/\partial\dot{x}$ and $p_\theta = \partial\mathcal{L}/\partial\dot{\theta}$. To account for friction, one of Hamilton's equations changes to [25,26] $\dot{p}_x = -\frac{\partial\mathcal{H}}{\partial x} - \frac{\partial\mathcal{F}}{\partial\dot{x}}$. The power produced by the force \mathcal{F}_a can be expressed as the rate of change of $\mathcal{H}_0 = \mathcal{H} + \mathcal{F}_a x$ (the last term cancels the external interaction $-\mathcal{F}_a x$ in \mathcal{H} , leaving the bare mechanical energy) plus the energy loss

rate due to friction,

$$\mathcal{P} = \frac{d\mathcal{H}_0}{dt} + \gamma\dot{x}^2 = \mathcal{F}_a\dot{x}. \quad (4)$$

The total derivative is computed along the trajectory making use of Hamilton's equations for \mathcal{H} modified by the friction term. Here a meaningful divide is established, with the relevant connection to the outer world being a force \mathcal{F}_a produced by an external engine that, for positive power, consumes fuel to increase the internal mechanical energy and fight against friction. The total energy consumption could be defined as the integral of the power [20], but this would ignore the peculiarities of braking phases where \mathcal{F}_a and \dot{x} have different signs. We propose instead a more realistic expression parameterized by $-1 \leq \eta \leq 1$, which depends on the braking mechanism,

$$\mathcal{E} = \int_0^{t_f} dt\mathcal{P}_+ + \eta \int_0^{t_f} dt\mathcal{P}_- = \mathcal{E}_+ + \eta\mathcal{E}_-, \quad (5)$$

where $\mathcal{P}_\pm = \Theta(\pm\mathcal{P})\mathcal{P}$ are the positive and negative parts of \mathcal{P} for accelerating or braking phases of the trolley motion and Θ is the Heaviside function. \mathcal{E}_\pm are the positive and negative parts of the integral. While more sophisticated descriptions are possible, with η depending on several variables, our aim here is to set a crude model that captures the essence of the energy trade during braking and provides limiting scenarios: $\eta = 1$ corresponds to a mechanism able to fully accumulate the braking energy \mathcal{E}_- and give it back on demand, i.e., perfect regenerative braking; $\eta = -1$ corresponds to using the engine in both phases of the motion, whereas $\eta = 0$ is the limit in which braking fully dissipates the energy loss of the system with negligible energy consumption.

To find STAs we use the horizontal deviation of the load from the trolley position, $q(t) = l\sin\theta(t)$, and assume the small-oscillation regime. Equation (2) becomes

$$\ddot{q} + \omega^2 q = -\ddot{x}, \quad (6)$$

where $\omega^2 = g/l$. The dynamics of the load (PS) is described in a moving frame by a forced harmonic oscillator, which can be derived from the Hamiltonian

$$H = \frac{p^2}{2m} + \frac{1}{2}m\omega^2 q^2 + m\ddot{x}q, \quad (7)$$

where $p = m\dot{q}$ is the canonical momentum of q . Associated with H is an invariant of motion [27]

$$I = \frac{1}{2m}(p - m\dot{\alpha})^2 + \frac{m}{2}\omega^2(q - \alpha)^2, \quad (8)$$

where $\alpha(t)$ is an auxiliary trajectory that must follow the dynamics of a forced harmonic oscillator [27],

$$\ddot{\alpha} + \omega^2\alpha = -\ddot{x}. \quad (9)$$

We choose $\alpha(t)$ functions that satisfy the boundary conditions (BCs) $\alpha(t_b) = \dot{\alpha}(t_b) = \ddot{\alpha}(t_b) = 0$ for $t_b = 0, t_f$. In this way $\ddot{x}(t_b) = 0$ and, from Eqs. (7) and (8), $H(0) = I(0) = E_0$ for any arbitrary trajectory $q(t)$ satisfying Eq. (6) with initial energy E_0 (for the auxiliary trajectory α , $E_0 = 0$). As I is invariant, $I(t_f) = E_0$. Moreover, the final energy is $H(t_f) = I(t_f) = E_f$. In summary, imposing the appropriate BCs on α , $E_f = E_0$ for any trajectory, as for an adiabatic, slow process, but in a finite time.

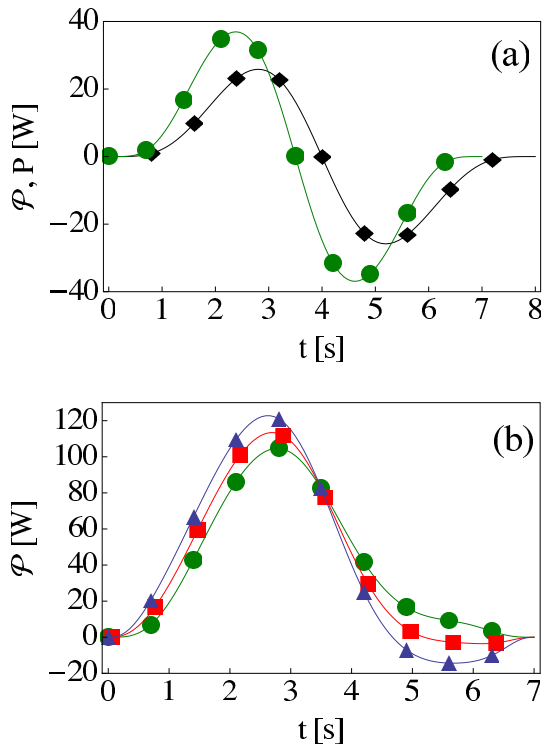


FIG. 2. The total power \mathcal{P} to control $x(t)$ for different M and friction coefficients and load power P . Symbols represent \mathcal{P} using the small-oscillation approximation, Eq. (10), and lines represent using the exact Eq. (4). (a) Power P of the load (symbols) and total power \mathcal{P} (lines) in the $M = \gamma = 0$ limit for $t_f = 7$ s (green line and circles) and $t_f = 8$ s (black line and diamonds). (b) Total power \mathcal{P} with friction, $\gamma = 15$ kg/s, $t_f = 7$ s, for different values of the trolley mass: $M = 0$ kg (green solid line and circles), $M = 10$ kg (red solid line and squares), and $M = 20$ kg (blue solid line and triangles). $m = 10$ kg, $l = 5$ m, $d = 10$ m, $q(0) = 0$ m, $\dot{q}(0) = 0$ m/s, and $g = 9.8$ m/s².

We interpolate $\alpha(t)$ with a polynomial, $\alpha(t) = \sum_{i=0}^7 a_i t^i$, where the first six coefficients (a_0 – a_5) are derived from the six BCs for α . The trajectory $x(t)$ of the trolley is deduced from Eq. (9), $x(t) = -\int_0^t dt' \int_0^{t'} dt'' [\ddot{\alpha}(t'') + \omega^2 \alpha(t'')]$ and satisfies $\ddot{x}(t_b) = \dot{x}(0) = x(0) = 0$. The coefficients a_6 and a_7 are set by demanding $\dot{x}(t_f) = 0$ and $x(t_f) = d$. Due to the freedom to design α , optimal-control theory could be used to find trolley trajectories that optimize a chosen variable given some physical constraints [21]. For small oscillations, the total power in Eq. (4) takes the form

$$\mathcal{P} = (M\ddot{x} - m\omega^2 + \gamma\dot{x})\dot{x}, \quad (10)$$

plotted in Fig. 2 for $q(t) = \alpha(t)$. The terms in parentheses represent the force to move a free trolley (with no load or friction) minus the force that the load exerts on the trolley (a “pull or drag” back-action whose sign depends on their relative positions) minus the friction force (which always gives a positive contribution to the power). Let us compare this quantity to the power on the load, $P = \frac{dE(t)}{dt}$, where $E(t)$ is the mechanical energy of the load, $E(t) = m(\dot{x} + \dot{q})^2/2 + m\omega^2 q^2/2$. [For arbitrary t , this is different from $H(t)$ since

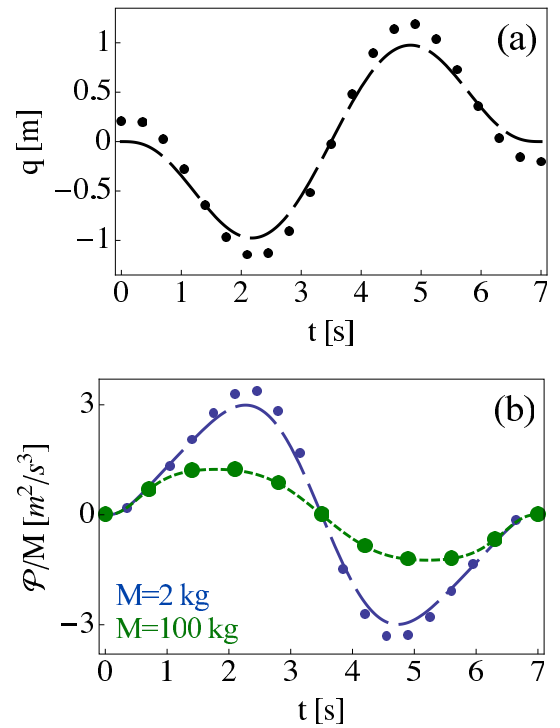


FIG. 3. Effect of the trajectory $q(t)$ on the total power \mathcal{P} for different trolley masses. $q(0) = \dot{q}(0) = 0$ (dashed lines), $q(0) = 0.2$ m, and $\dot{q}(0) = 0.1$ m/s (circles). (a) $q(t)$ for different initial conditions. (b) Corresponding power consumed for different m/M ratios: $M = 2$ kg (blue long-dashed line and small circles) and $M = 100$ kg (green short-dashed line and big circles). $m = 1$ kg, $l = 5$ m, $d = 10$ m, $t_f = 7$ s, $\gamma = 0$ kg/s, and $g = 9.8$ m/s².

H is defined in a moving frame, but they coincide at the boundary times.] Using Eq. (6), $P = -mq\omega^2\dot{x}$, which is the rate of energy change in the PS, but for a given $x(t)$, it ignores other features of the trolley. In contrast, \mathcal{P} and \mathcal{E} generally depend [see Eq. (10)] on the characteristics of the CS (M, γ), on its dynamics (\dot{x}, \ddot{x}), and on the deviation of the load $q(t)$. If $M = \gamma = 0$, $\mathcal{P}_{M=\gamma=0} = -mq\omega^2\dot{x} = P$ (see Fig. 2). A practical advantage of the limit $M \gg m$ is that \mathcal{P} can be made essentially independent of $q(t)$, i.e., of the initial conditions $\{q(0), \dot{q}(0)\}$ (see Fig. 3), where the $\alpha(t)$ chosen implies that $\ddot{x} = 0$ at the boundary times and at the middle time. This stabilization comes with a price, namely, higher-power peaks due to a larger M .

The integral of \mathcal{P} , without friction, $\gamma = 0$, is zero by construction of the STAs (the final adiabatic energy of the load must be equal to the initial one, and the trolley starts and ends at rest), so the total energy consumption would be zero for $\eta = 1$. The other parameters may be arbitrary, even t_f , within small oscillations. Friction and realistic braking mechanisms ($\eta \neq 1$) imply $|\eta\mathcal{E}_-| < \mathcal{E}_+$ and therefore dependences of $\mathcal{E} > 0$ on γ, M , or t_f . Note that \mathcal{E} depends linearly on η with minimum $\mathcal{E}_+ + \mathcal{E}_-$ at $\eta = 1$ and maximum $\mathcal{E}_+ - \mathcal{E}_-$ at $\eta = -1$. Since the time integral of the frictionless part of Eq. (10) is zero, we get, using the Euler-Lagrange equation, the lower bound

$$\mathcal{E} \geq \gamma d^2/t_f, \quad (11)$$

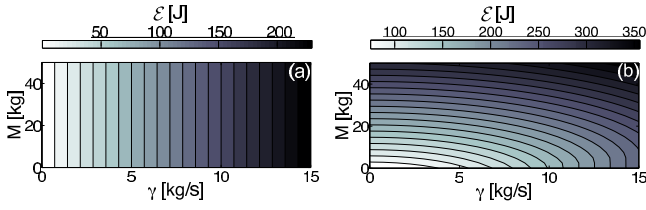


FIG. 4. Contour surface of the energy consumption \mathcal{E} as a function of the CS variables M and γ for different values of the η parameter: (a) $\eta = 1$ and (b) $\eta = -1$. $m = 10$ kg, $l = 5$ m, $d = 10$ m, $t_f = 9$ s, $q(0) = 0$ m, $\dot{q}(0) = 0$ m/s, and $g = 9.8$ m/s².

which is valid for all η . This agrees with Landauer's expectation for energy costs of processes not involving information losses [28]. However, a different, tighter bound is found in Sec. III from the optimal protocol.

Some trends are seen in Figs. 2 and 4: Friction enhances \mathcal{E}_+ and diminishes or even suppresses \mathcal{E}_- . A larger M generally increases the power peaks and also hinders the suppression of \mathcal{E}_- by friction; longer process times decrease power peaks and, typically, \mathcal{E} too, with the mentioned exception of an ideal setting, $\gamma = 0$, $\eta = 1$, for which $\mathcal{E} = 0$ for any time t_f . The contour plots of \mathcal{E} for $\eta = \pm 1$ are quite different (see Fig. 4), with \mathcal{E} independent of M if $\eta = 1$ and nearly independent of γ for weak friction if $\eta = -1$.

The feasibility of a given STA will depend not only on the additive energy consumption \mathcal{E} but also on the possibility to deliver the instantaneous power peaks, which increase with diminishing process times. STAs can be designed to lower the peak in \mathcal{P} , as done for P in [29]. The mean-value theorem provides bounds for the peak of \mathcal{P} in different regimes dominated by one of the terms in Eq. (10): $\mathcal{P} \geq Md^2/t_f^3$ for a regime dominated by the trolley frictionless dynamics (M term), whereas $\mathcal{P} \geq \gamma d^2/t_f^2$ for a friction-dominated one. Finally, peak bounds for $M = \gamma = 0$ scale as md^2/t_f^3 at long process times and as $4md^2/(\omega^2 t_f^5)$ at short times. (The bounds at short times are meaningful only for a pure harmonic oscillator since the pendulum will abandon the small-oscillation regime, and we have assumed $\sqrt{2E_0/m/\omega} \ll d$.) Minimal times for a given maximal power can be read directly from the bounds.

III. PROTOCOL FOR MINIMAL ENERGY CONSUMPTION

We use the degeneracy of the STAs to design a protocol that minimizes energy consumption, combining inverse-engineering STAs with optimal-control theory [21,30]. In this section we assume that the harmonic model holds.

It is convenient to use the horizontal position of the load in the laboratory frame, $X \equiv q + x$, which obeys the Newton equation

$$\ddot{X} + \omega^2(X - x) = 0. \quad (12)$$

Like we did for the difference between a general q and a particular trajectory α in the previous section, we distinguish a particular trajectory ξ that satisfies Eq. (12) and the boundary conditions $\xi(0) = 0, \xi(t_f) = d$ and $\dot{\xi}(t_b) = \dot{\xi}(t_b) = 0$, with $t_b = 0, t_f$. To follow the usual conventions in optimal-control

theory, we use a new notation,

$$y_1 = \xi, \quad y_2 = \dot{\xi}, \quad u(t) = x, \quad (13)$$

where y_1, y_2 are the components of a "state vector" \mathbf{y} and the trolley position $u(t)$ is considered the (scalar) control function. With this notation Eq. (12) for ξ becomes

$$\dot{y}_1 = y_2, \quad (14)$$

$$\dot{y}_2 = -\omega^2(y_1 - u). \quad (15)$$

The optimal-control problem is to find $|u(t)| \leq \delta$ for some fixed bound δ , with $u(0) = 0$ and $u(t_f) = d$, such that the system starts at $\{y_1(0) = 0, y_2(0) = 0\}$, ends up at $\{y_1(t_f) = d, y_2(t_f) = 0\}$, and minimizes a cost function J .

In order to match the boundary conditions at the initial and final times, the optimal control obtained may be complemented by appropriate jumps. We use Pontryagin's maximum principle, which provides necessary conditions for optimality [31]. Generally, to minimize the cost function

$$J(u) = \int_0^{t_f} g(\mathbf{y}(t), u) dt, \quad (16)$$

the maximum principle states that for the dynamical system $\dot{\mathbf{y}} = \mathbf{f}(\mathbf{y}(t), u)$, the coordinates of the extremal vector $\mathbf{y}(t)$ and of the corresponding adjoint state $\mathbf{k}(t)$ formed by Lagrange multipliers k_1, k_2 fulfill the Hamilton's equations for a control Hamiltonian H_c ,

$$\dot{\mathbf{y}} = \frac{\partial H_c}{\partial \mathbf{k}}, \quad (17)$$

$$\dot{\mathbf{k}} = -\frac{\partial H_c}{\partial \mathbf{y}}, \quad (18)$$

where H_c is defined as

$$H_c(\mathbf{k}(t), \mathbf{y}(t), u) = k_0 g(\mathbf{y}(t), u) + \mathbf{k}^T \cdot \mathbf{f}(\mathbf{y}(t), u). \quad (19)$$

The superscript T used here denotes the transpose of a vector, and $k_0 < 0$ can be chosen for convenience since it amounts to multiplying the cost function by a constant. The (augmented) vector with components (k_0, k_1, k_2) is nonzero and continuous. Note that the Lagrange multiplier k_0 is a constant; however, k_1 and k_2 are time dependent since the equations of motion (14) and (15) must be satisfied at all times. For almost all $0 \leq t \leq t_f$ the function $H_c(\mathbf{k}(t), \mathbf{y}(t), u^*)$ attains its maximum at $u = u^*$, and $H_c(\mathbf{k}(t), \mathbf{y}(t), u^*) = c$, where c is constant. Assuming that the integrals of two of the terms of the total power (10) depending on M and m vanish (this is explicitly confirmed later), we shall consider only the term $\gamma \dot{x}^2$, so the cost function is

$$J_{\mathcal{P}} = \int_0^{t_f} \dot{x}^2 dt = \int_0^{t_f} \dot{u}^2 dt \quad (20)$$

for an "unbounded problem" (i.e., without restrictions on the possible values of the control) and an ideal ($\eta = 1$) type of process with perfect regenerative braking. The control Hamiltonian is

$$H_c(k_1, k_2, y_1, y_2, u) = k_0 \dot{u}^2 + k_1 y_2 - k_2 \omega^2 (y_1 - u), \quad (21)$$

which sets the costate equations

$$\dot{k}_1 = \omega^2 k_2, \quad \dot{k}_2 = -k_1. \quad (22)$$

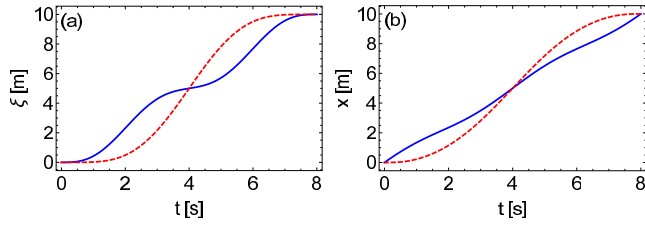


FIG. 5. (a) Designed function $\xi = \alpha + x$ as a function of time. Polynomial interpolation used in Sec. II (red dashed line) and optimal solution to minimize the energy consumption (blue solid line). (b) Trolley displacement x as a function of time. Parameter values: $t_f = 8$ s, $l = 5$ m, $d = 10$ m, $g = 9.8$ m/s², and $k_0 = -1$.

The solution to this set of equations is

$$\begin{aligned} k_1(t) &= c_1 \cos(\omega t) + \omega c_2 \sin(\omega t), \\ k_2(t) &= c_2 \cos(\omega t) - \frac{c_1}{\omega} \sin(\omega t), \end{aligned} \quad (23)$$

where c_1 and c_2 are arbitrary constants. According to Pontryagin's maximum principle, the time-optimal control $u(t)$ maximizes the control Hamiltonian H_c . Using the Euler-Lagrange equation, this is done when u satisfies $k_2\omega^2 = 2k_0\ddot{u}$. Using Eq. (23), we find

$$u(t) = x(t) = c_3 + tc_4 - \frac{c_2}{2k_0} \cos(\omega t) + \frac{c_1}{2k_0\omega} \sin(\omega t), \quad (24)$$

with c_3 and c_4 also being arbitrary constants. Finally, solving the differential equation (12), the optimal $\xi(t)$ is found. The constants are fixed by imposing the boundary conditions on ξ . In Fig. 5(a) we plot the optimal function ξ and the one deduced from Sec. II with a polynomial α . The optimal trolley displacement $x_{\text{op}}(t)$ [Fig. 5(b)] satisfies $x_{\text{op}}(0) = 0$ and $x_{\text{op}}(t_f) = d$,

$$x_{\text{op}}(t) = [d\{-2 + \omega^2 t_f t + 2 \cos(\omega t) - 2 \cos[\omega(t - t_f)] + 2\bar{c} + \omega t \bar{s}\}] / [-4 + t_f^2 \omega^2 + 4\bar{c} + \omega t_f \bar{s}], \quad (25)$$

with $\bar{c} = \cos(\omega t_f)$ and $\bar{s} = \sin(\omega t_f)$. However, $\dot{x}_{\text{op}}(0^+) = \dot{x}_{\text{op}}(t_f^-) \neq 0$, $\dot{x}_{\text{op}}(0^+) = -\dot{x}_{\text{op}}(t_f^-) \neq 0$, and instantaneous jumps are required to satisfy the boundary conditions $\dot{x}(0^-) = \dot{x}(t_f^+) = \ddot{x}(0^-) = \ddot{x}(t_f^+) = 0$, where the plus (minus) represents an approach from the right (left). The trajectory (25) must be limited to the domain $0 < t < t_f$ and must be complemented by $x_{\text{op}} = 0$ for $t < 0$ and $x_{\text{op}} = d$ for $t > t_f$. \dot{x} is discontinuous at $t = 0$ jumping from zero to $x_{\text{op}}(0^+)$. Similarly, at t_f , \dot{x} jumps from $\dot{x}(t_f^-)$ to zero. The acceleration thus includes Dirac δ impulses [29,32],

$$\ddot{x}_{\text{op}} = \begin{cases} 0, & t \leq 0^-, \\ \dot{x}_{\text{op}}(0^+) \delta(t), & 0^- < t < 0^+, \\ \ddot{x}_{\text{op}}(t), & 0^+ \leq t \leq t_f^-, \\ -\dot{x}_{\text{op}}(t_f^-) \delta(t - t_f), & t_f^- < t < t_f^+, \\ 0, & t_f^+ \leq t, \end{cases} \quad (26)$$

where \dot{x}_{op} and \ddot{x}_{op} represent the first and second time derivatives of Eq. (25). This implies that q , X , and \dot{X} are continuous at the edges. The protocol, including the jumps, is indeed a shortcut, as the mechanical energy of the load,

$E(t) = m(\dot{x} + \dot{q})^2/2 + m\omega^2 q^2/2$, is equal at initial (0^-) and final (t_f^+) times. This can be seen from the vanishing of the integral

$$\int_{0^-}^{t_f^+} q \dot{x}_{\text{op}} dt = 0, \quad (27)$$

which does not get any contribution at the edges, $E(0^-) = E(0^+) = E(t_f^-) = E(t_f^+)$. Comparing explicitly load mechanical energies immediately before and after the boundary times, this is consistent with the following jumps in \dot{q} :

$$\dot{q}(0^+) = \dot{q}(0^-) - \dot{x}(0^+), \quad (28)$$

$$\dot{q}(t_f^+) = \dot{q}(t_f^-) + \dot{x}(0^-). \quad (29)$$

The total mechanical energy,

$$E_{\text{tot}}(t) = E(t) + \frac{1}{2} M \dot{x}^2, \quad (30)$$

is also equal at initial and final times since the trolley begins and ends at rest,

$$\int_{0^-}^{t_f^+} \ddot{x}_{\text{op}} \dot{x}_{\text{op}} dt = 0. \quad (31)$$

In more detail, the integral vanishes in the interior domain, from 0^+ to t_f^- , since $\dot{x}_{\text{op}}(0^+) = \dot{x}_{\text{op}}(t_f^-)$, and the jumps due to initial and final δ impulses compensate, $\int_{0^-}^{0^+} M \ddot{x}_{\text{op}} \dot{x}_{\text{op}} dt = M \dot{x}_{\text{op}}^2(0^+)/2$ and $\int_{t_f^-}^{t_f^+} M \ddot{x}_{\text{op}} \dot{x}_{\text{op}} dt = -M \dot{x}_{\text{op}}^2(t_f^-)/2$. Moreover, since the singularity of \dot{x}_{op} at the boundaries corresponds to a finite jump,

$$\int_{0^-}^{0^+} \dot{x}_{\text{op}}^2 dt = 0, \quad \int_{t_f^-}^{t_f^+} \dot{x}_{\text{op}}^2 dt = 0, \quad (32)$$

the Dirac impulses do not contribute to the energy dissipated by friction. Using expression (25) for the optimal trajectory, we find the explicit expression for the minimal energy consumption. This sets a bound for any other process,

$$\mathcal{E} \geq \frac{\gamma d^2}{t_f + \frac{4[-1 + \cos(\omega t_f)]}{\omega[\omega t_f + \sin(\omega t_f)]}}, \quad (33)$$

tighter than Eq. (11), $\mathcal{E} \geq \gamma d^2/t_f$. At large times, compared to the oscillation period, they coincide. Indeed, $\gamma d^2/t_f$ agrees with Landauer's prediction on the energy dissipation proportional to the "velocity of the process" when there is no information loss [28]. However, whereas he emphasized that the dissipation can be made arbitrarily small for sufficiently long times, STAs are, by construction, intended as fast processes where the dissipation due to friction does not vanish. A second difference with Landauer's discussion is that at short times, the dependence in Eq. (33) changes to

$$\mathcal{E} \gtrsim \frac{720 d^2}{\omega^4 t_f^5}, \quad (34)$$

with the caveat that this result indeed requires harmonic oscillator dynamics.

Note that the discontinuities in the derivatives of $x_{\text{op}}(t)$ imply infinite-power peaks, but the energy consumed by the

engine controlling the motion of the trolley, which is equal to the dissipated energy since the initial and final mechanical energies are equal, is finite. The ability to approach this ideal scenario of infinite-power peaks will depend on the characteristics of the engine, but in any case, the bound (33) sets the minimum energy required to produce a STA protocol for a given transport time t_f .

IV. DISCUSSION

We have worked out an explicit model to analyze the energy consumption in shortcuts to adiabaticity. The model helps to point out a number of fundamental aspects, such as the importance of considering the control system together with the primary system. In our model the power for the primary system and the total power agree only in a rather unrealistic scenario, namely, a control system with zero mass and no friction. The small mass limit of the control system is not only unrealistic but also undesirable, as it would make the total power and the external actuating control force depend on the specific dynamics (i.e., the initial boundary conditions) of the primary system. This is against the spirit of useful shortcuts, intended to take systems from initial to final Hamiltonian configurations without final excitation, irrespective of the initial conditions. Control systems for microscopic primary systems will typically involve macroscopic masses, currents, or classical fields, so the need to consider the control system to examine energy costs will be prevalent.

The model also provides an ideal test bed to realize that different types of braking affect the results dramatically. It illustrates that the stability of a given control protocol with respect to the primary system dynamics implies an energy cost and higher-power peaks, and it underlines the importance of both integrated and local-in-time quantities to determine the feasibility of shortcuts.

The current analysis may be extended to further classical, quantum, or hybrid systems. In particular a quantum load represented by a particle in a harmonic trap could be driven by exactly the same STA protocols devised here since I and H have the same form as in our model. Close to the current model is the transport of ions or neutral atoms for which different experiments have been performed or are planned [33–35]. For the transport of ultracold atoms in [33], the trap was formed by optical tweezers, moved by displacing a lens mounted on a motorized translation stage. This setting realizes the stabilizing $M > m$ limit, a typical scenario with microscopic loads. Similarly, Zenesini *et al.* moved an optical lattice by displacing the mirror mounted on piezoelectric actuators [36]. For ion transport in linear, multielectrode Paul traps, the cost will involve assessing the energy consumed by the microchip controlling the effective moving trap by means of time-varying electrode potentials. The stabilization of the total power will depend on the macroscopic charges in the electrodes to change the voltages being much larger than the ion charge.

While the results so far have been for a harmonic potential, deviations from the harmonic approximation could be taken into account following [37]. We may also consider initial angles of the load θ_i beyond the small-oscillation regime and redesign the protocol for the trolley motion $x(t)$ to minimize the difference between initial and final mechanical energies

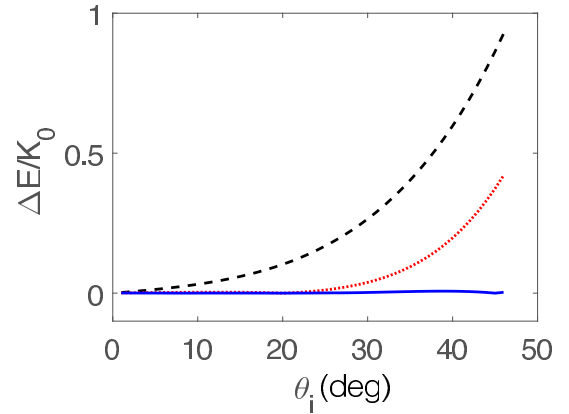


FIG. 6. Energy excitation of the load versus initial angle (with load initially at rest) in an inversely engineered transport process with $d = 10$ m, $t_f = 10$ s, $l = 5$ m, and $m = 10$ kg, using additional free parameters in the ansatz for $\alpha(t)$. The scaling factor is the kinetic energy for a constant-velocity process, $K_0 = md^2/(2t_f^2)$. Black dashed line: process without additional parameters; red dotted line: one parameter added to minimize excitation in $\theta_i = 20^\circ$ ($b_8 = -3513.3$); solid blue line: minimization for the excitation in $\theta_i = 20^\circ$ and $\theta_i = 45^\circ$ using two free parameters ($b_8 = -13862$ and $b_9 = 2941.5$).

of the load ($\Delta E = |E_f - E_0|$). This requires a higher-order polynomial functions $\alpha(t) = \sum_{j=0}^{7+n} b_j t^j$ to minimize the energy difference for one or more (n) initial angles θ_i with the extra parameters. The number of free parameters n is set by the number of initial angles used to minimize the excitation, and the rest of the coefficients in $\alpha(t)$ are fixed by the boundary conditions as in Sec. II. In Fig. 6 we plot the excitation energy for processes with one and two free parameters and for the process in Sec. II ($n = 0$). Figure 6 demonstrates clearly that STAs beyond the small-oscillation regime are indeed possible. This implies zero or negligible energy consumption under ideal conditions (no friction, $\gamma = 0$, and regenerative braking, $\eta = 1$).

For a general system, beyond transport systems, regardless of the specific dynamics involved, friction, the combination of positive and negative power domains, and the independence of the external forces with respect to the primary system dynamics will be ubiquitous in STA implementations and thus essential elements to evaluate actual energy consumptions. Whereas for slow processes the energy dissipated by friction can be made negligible (a standard assumption for infinite-time processes), even if the friction coefficient is not zero, STAs are, by definition, fast processes, so to neglect energy dissipation in STAs the stronger assumption of zero-friction coefficients is necessary. Again, the fast nature of STA protocols implies large positive and negative powers, which enhances the importance of braking. Braking mechanisms determine the cost of the energy integrated in negative power segments and if this energy can indeed be reused. In typical scenarios this is not the case, i.e., $\eta \neq 1$, so negative power segments consume energy (the extreme case is $\eta = -1$), or if they do not consume energy ($\eta = 0$), they do not compensate for the consumption in positive segments. For the realistic expectation that $\gamma \neq 0$

and $\eta \neq 1$, shorter process times imply higher-power peaks and an increased energy consumption. Note that even in the highly idealized limit $\gamma = 0$, $\eta = 1$, with zero global cost (with respect to final adiabatic energy minus initial energy), shortening the time also implies higher-power peaks, which become a limiting factor that cannot be ignored when determining the feasibility of a shortcut.

ACKNOWLEDGMENTS

We thank D. Guéry-Odelin and A. Levy for discussions. We acknowledge funding from the Basque government (Grant No. IT986-16), MINECO/FEDER, UE (Grants No. FIS2015-67161-P and No. FIS2015-70856-P), and QUITEMAD+CM S2013-ICE2801.

-
- [1] X. Chen, A. Ruschhaupt, S. Schmidt, A. del Campo, D. Guéry-Odelin, and J. G. Muga, *Phys. Rev. Lett.* **104**, 063002 (2010).
- [2] E. Torrontegui, S. Ibáñez, S. Martínez-Garaot, M. Modugno, A. del Campo, D. Guéry-Odelin, A. Ruschhaupt, X. Chen, and J. G. Muga, *Adv. At. Mol. Opt. Phys.* **62**, 117 (2013).
- [3] C. Jarzynski, *Phys. Rev. A* **88**, 040101(R) (2013).
- [4] M. Okuyama and K. Takahashi, *J. Phys. Soc. Jpn.* **86**, 043002 (2017).
- [5] C. Jarzynski, S. Deffner, A. Patra, and Y. Subaşı, *Phys. Rev. E* **95**, 032122 (2017).
- [6] M. Demirplak and S. Rice, *J. Chem. Phys.* **129**, 154111 (2008).
- [7] X. Chen and J. G. Muga, *Phys. Rev. A* **82**, 053403 (2010).
- [8] A. del Campo, J. Goold, and M. Paternostro, *Sci. Rep.* **4**, 6208 (2014).
- [9] A. C. Santos, R. D. Silva, and M. S. Sarandy, *Phys. Rev. A* **93**, 012311 (2016).
- [10] I. B. Coulamy, A. C. Santos, I. Hen, and M. S. Sarandy, *Front. ICT* **3**, 19 (2016).
- [11] Y. Zheng, S. Campbell, G. De Chiara, and D. Poletti, *Phys. Rev. A* **94**, 042132 (2016).
- [12] O. Abah and E. Lutz, *Europhys. Lett.* **118**, 40005 (2017).
- [13] K. Funo, J. N. Zhang, C. Chatou, K. Kim, M. Ueda, and A. del Campo, *Phys. Rev. Lett.* **118**, 100602 (2017).
- [14] R. Kosloff and Y. Rezek, *Entropy* **19**, 136 (2017).
- [15] M. Kieferová and N. Wiebe, *New J. Phys.* **16**, 123034 (2014).
- [16] S. Campbell and S. Deffner, *Phys. Rev. Lett.* **118**, 100601 (2017).
- [17] A. Bravetti and D. Tapias, [arXiv:1706.07443](https://arxiv.org/abs/1706.07443).
- [18] O. Abah and E. Lutz, [arXiv:1707.09963](https://arxiv.org/abs/1707.09963).
- [19] D. A. Winter, *Biomechanics and Motor Control of Human Movement* (Wiley, Hoboken, NJ, 2009).
- [20] Z. Wu and X. Xia, *IET Control Theory Appl.* **8**, 1833 (2014).
- [21] X. Chen, E. Torrontegui, D. Stefanatos, J.-S. Li, and J. G. Muga, *Phys. Rev. A* **84**, 043415 (2011).
- [22] S. Masuda and K. Nakamura, *Proc. R. Soc. A* **466**, 1135 (2010).
- [23] E. Torrontegui, S. Ibáñez, X. Chen, A. Ruschhaupt, D. Guéry-Odelin, and J. G. Muga, *Phys. Rev. A* **83**, 013415 (2011).
- [24] H. Goldstein, C. Poole, and J. Safko, *Classical Mechanics*, 3rd ed. (Adison-Wesley, Reading, MA, 2002).
- [25] L. Meirovitch, *Methods of Analytical Dynamics* (McGraw-Hill, New York, 1970).
- [26] S. Montgomery-Smith, *Electron. J. Differ. Equations* **2014**, 89 (2014).
- [27] H. R. Lewis and P. G. L. Leach, *J. Math. Phys.* **23**, 2371 (1982).
- [28] R. Landauer, *Appl. Phys. Lett.* **51**, 2056 (1987).
- [29] Y.-Y. Cui, X. Chen, and J. G. Muga, *J. Phys. Chem. A* **120**, 2962 (2015).
- [30] D. Stefanatos, J. Ruths, and J.-S. Li, *Phys. Rev. A* **82**, 063422 (2010).
- [31] L. S. Pontryagin, V. G. Boltyanskii, R. V. Gamkrelidze, and E. F. Mishchenko, *The Mathematical Theory of Optimal Processes* (Interscience, New York, 1962).
- [32] D. Stefanatos and J.-S. Li, *American Control Conf.* **85**, 5061 (2012).
- [33] A. Couvert, T. Kawalec, G. Reinaudi, and D. Guéry-Odelin, *Europhys. Lett.* **83**, 13001 (2008).
- [34] R. Bowler, J. Gaebler, Y. Lin, T. R. Tan, D. Hanneke, J. D. Jost, J. P. Home, D. Leibfried, and D. J. Wineland, *Phys. Rev. Lett.* **109**, 080502 (2012).
- [35] A. Walther, F. Ziesel, T. Ruster, S. T. Dawkins, K. Ott, M. Hettrich, K. Singer, F. Schmidt-Kaler, and U. Poschinger, *Phys. Rev. Lett.* **109**, 080501 (2012).
- [36] A. Zenesini, H. Lignier, D. Ciampini, O. Morsch, and E. Arimondo, *Phys. Rev. Lett.* **102**, 100403 (2009).
- [37] A. Ruschhaupt, X. Chen, D. Alonso, and J. G. Muga, *New J. Phys.* **14**, 093040 (2012).



PAPER

Energy consumption for ion-transport in a segmented Paul trap

A Tobalina¹, J Alonso² and J G Muga¹¹ Department of Physical Chemistry, University of the Basque Country UPV/EHU, Apdo 644, Bilbao, Spain² Institute for Quantum Electronics, ETH Zürich, Otto-Stern-Weg 1, 8093 Zürich, SwitzerlandE-mail: ander.tobalina@ehu.eus

Keywords: quantum control, quantum thermodynamics, shortcuts to adiabaticity

OPEN ACCESS

RECEIVED

23 February 2018

REVISED

25 April 2018

ACCEPTED FOR PUBLICATION

21 May 2018

PUBLISHED

12 June 2018

Original content from this work may be used under the terms of the [Creative Commons Attribution 3.0 licence](https://creativecommons.org/licenses/by/4.0/).

Any further distribution of this work must maintain attribution to the author(s) and the title of the work, journal citation and DOI.



Abstract

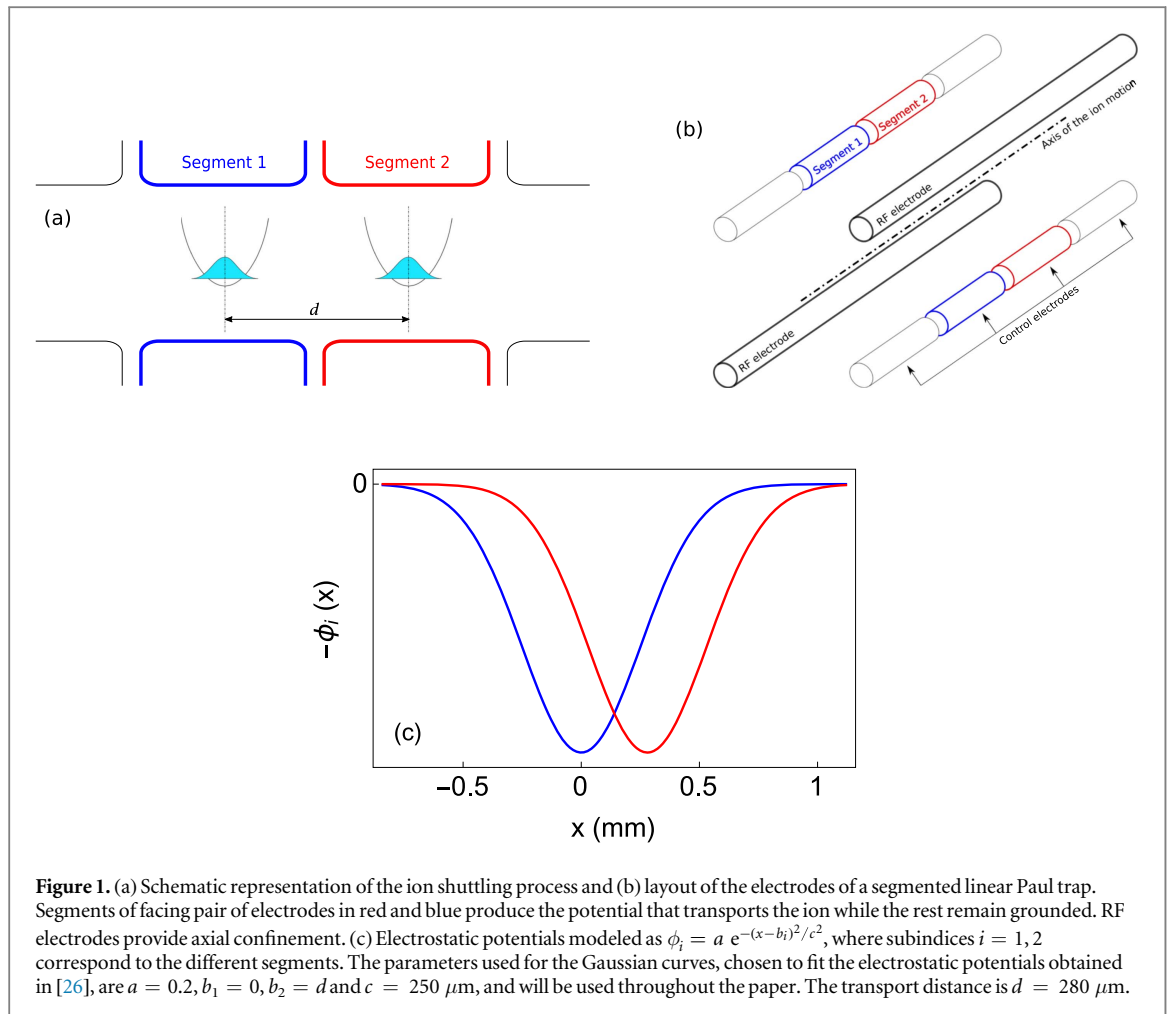
There is recent interest in determining energy costs of shortcuts to adiabaticity (STA), but different definitions of ‘cost’ have been used. We demonstrate the importance of taking into account the control system (CS) for a fair assessment of energy flows and consumptions. We model the energy consumption and power to transport an ion by a STA protocol in a multisegmented Paul trap. The ion is driven by an externally controlled, moving harmonic oscillator. Even if no net ion-energy is gained at destination, setting the time-dependent control parameters is a macroscopic operation that costs energy and results in energy dissipation for the short time scales implied by the intrinsically fast STA processes. The potential minimum is displaced by modulating the voltages on control (dc) electrodes. A secondary effect of the modulation, usually ignored as it does not affect the ion dynamics, is the time-dependent energy shift of the potential minimum. The non trivial part of the energy consumption is due to the electromotive forces to set the electrode voltages through the low-pass filters required to preserve the electronic noise from decohering the ion’s motion. The results for the macroscopic CS (the Paul trap) are compared to the microscopic power and energy of the ion alone. Similarities are found—and may be used quantitatively to minimize costs—only when the CS-dependent energy shift of the harmonic oscillator is included in the ion-energy.

1. Introduction

Several papers [1–12] have studied the ‘energy cost’ or ‘energy consumption’ of shortcuts to adiabaticity (STA) [13, 14], fast track routes to the results of slow adiabatic processes. Assessing the energy consumption of STA protocols is particularly relevant in quantum thermodynamics as they may appear to imply zero costs above the differential between initial and final energies, for example in expansion/compression strokes of a quantum heat engine or refrigerator. Often the primary system (PS), whose state is of interest for the application at hand, is microscopic while the control system (CS) is macroscopic, so that the PS is described as governed by a semiclassical Hamiltonian with (classical) external time-dependent control parameters. Different STA are commonly formulated by specifying the protocol, i.e., the time dependences of the parameters that induce fast state changes of the PS.

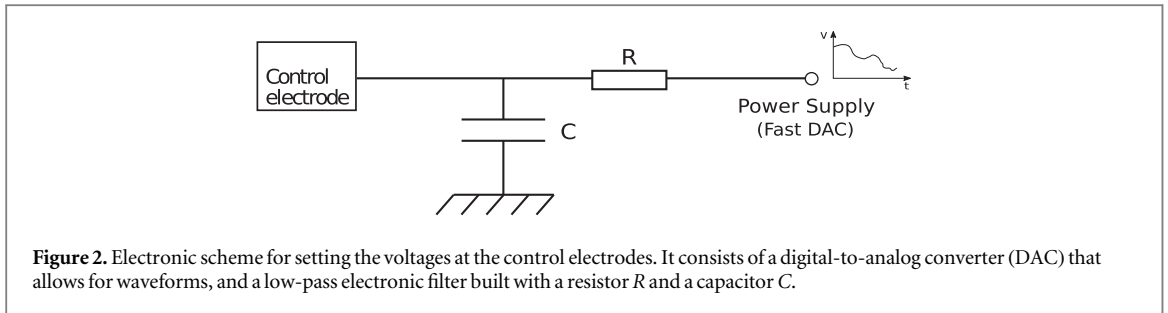
While the cited works ignore the energetic needs of control elements and focus on the energy of the PS, or even on parts of the Hamiltonian of the PS, in [15] a more general approach was suggested. There, the energy flow with the outer world is studied for an enlarged system that includes the PS and the CS required to change the time-dependent parameters that drive the PS. The divide between the enlarged system PS+CS and the outer world should be drawn such that the energy flow through that boundary can indeed be translated into actual fuel or electric power consumption. For recent, related discussions of the need to include a CS along with the PS, see e.g. [16], where the energy required to manipulate a mesoscopic quantum system in the presence of noise is examined, or [17], where fundamental limits of quantum refrigeration are discussed.

Torrontegui *et al* carried out their study for a mechanical system that could be thoroughly analyzed, the transport of a load (PS) suspended from a moving trolley (CS) in a mechanical crane [15]. This model is in fact quite close mathematically to experimental setups that shuttle ions or cold atoms by moving mirrors [18] or



lenses [19]. A number of conclusions that were conjectured to be broadly applicable were drawn in [15]. To test these conclusions and explore different models that may help to build general concepts and an embracing theory, it is worth investigating the energies involved in different transport experiments that do not rely on control elements subjected to mechanical displacements.

Here we shall study the energy consumption to transport via STA a single ion (PS), in its ground motional state at initial and final times, in a linear Paul trap made of parallel radiofrequency (rf) electrodes and segmented pairs of dc electrodes [20–22], see figures 1(a) and (b). Strong radial confinement is assumed, which is primarily due to ponderomotive forces caused by the rf field, whereas the potential along the longitudinal trap axis x is controlled by the voltage biases applied to the control electrode pairs of each segment [23]. The potential minimum is displaced along the trap axis by applying waveforms that change the voltages of the control electrodes in time. Adiabatic [20] and faster-than-adiabatic shuttling experiments of this type have been performed [24, 25]. In our simplified model, and without loss of generality, we consider the transport of an ion between two nearby segments with centers at $x = 0$ and $x = d$, as in [26]. The voltage in each segment of facing pairs of dc electrodes is controlled by a programmable waveform generator and a low-pass electronic filter as shown in figure 2. The latter is used in trapped-ion experimental setups to limit the heating and decohering action of electronic noise on the ion motion. Filters are preferably placed close to the trap electrodes, inside the vacuum chamber housing the trap. In this way, it is possible to suppress significantly the amplitude of noise generated at the voltage supplies or picked up along the wires connecting these to the trap electrodes [27]. The filters are commonly built with a resistor R and capacitor C (first-order RC filters), although higher order filters and active filters are also possible. In this work we will consider RC filters without incurring in loss of generality, since finite resistances and large capacitors are inherent to the control circuitry regardless of the filters used, whereas parasitic inductances produce negligible effects. We assume a constant power supply to generate the rf field, which makes this consumption trivial, unlike that due to the voltage waveforms applied at the control dc electrodes. In this model, the energy flow between the enlarged system implies a consumption of power due to energy dissipated by the resistances, and the energy required to charge and discharge the capacitors. In the mechanical analogy of [15] different limits were identified depending on whether time intervals with negative power of the control consume energy, save it, or become energetically neutral. In the current model for the ion-



transport process the capacitor charge and discharge have to be actively driven, and thus both imply consumption. This is analogous to the scenario in which both the accelerating and the braking phases of the control trolley use an engine to pull the trolley in different directions in the mechanical analogy.

The specific STA protocol we consider here to set the time-dependent location of the axial potential is based on the ‘compensating force approach’. This technique compensates with a homogeneous, time-dependent force the inertial forces due to the motion of a reference trap trajectory, so the ion wave function remains at rest in the frame moving with the reference trap [28–30]. It amounts to the trick that a waiter uses to carry the tray quickly, tilting it to avoid spilling the drinks [31]. In the harmonic approximation for the trap, the compensation displaces the minimum. Within the set of STA-transport protocols based solely on choosing a certain path for the harmonic trap, the compensating force approach is generic in the sense that any reference trajectory is allowed, subjected to certain boundary conditions. The compensating force approach may be also regarded as invariant-based inverse engineering of the transport protocol [28], as explained in the next section. Other STA-transport protocols may be based on counterdiabatic driving, which changes the structure of the Hamiltonian adding a momentum dependent interaction [28]. The counterdiabatic (CD) driving method and the compensating force approach are unitarily connected—they can be found from each other by a unitary transformation—[30, 32, 33], although the physical implementation involves different interactions and a different experimental setting. Actual transport—in the fixed laboratory frame—has not yet been implemented with CD driving although An *et al* [32] simulated CD transport experimentally in an interaction picture with respect to the harmonic oscillation. They also performed the compensating force approach as ‘unitarily equivalent transport’ in the interaction picture. The driving forces were induced optically rather than by varying voltages of control electrodes. Controllable momentum and spin dependent interactions for actual CD-driven transport in the lab frame may in principle be applied with synthetic spin–orbit coupling [34] but the spin dependence would be a strong limitation for many applications, e.g. to transport arbitrary qubits. The corresponding energetic analysis lays beyond the scope of this work.

In section 2 we review briefly the compensating force approach and find the voltages needed to implement the desired potentials. This will also set the time-dependent term in the PS Hamiltonian. In section 3 we define and compare the different energies and powers involved. Power peaks that limit how short the process times may be, asymptotic dependences, and an optimization of the consumption are also discussed. The values of the parameters used in the computations have been taken from [26]. The paper ends with a summary and outlook for future work.

2. Methods

2.1. Compensating force approach for a transport process

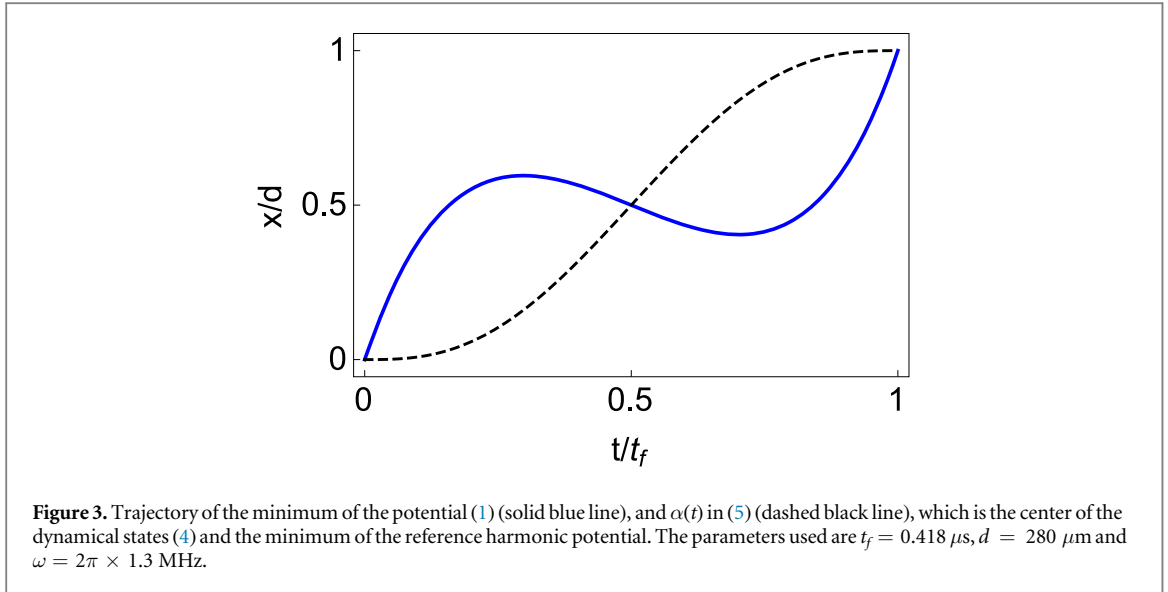
Let us consider an ion of mass m driven by a Hamiltonian of the form $H = \frac{p^2}{2m} + V(x, t)$, with

$$V(x, t) = -F(t)x + \frac{m}{2}\omega^2[x - \alpha(t)]^2 + f(t), \quad (1)$$

where

$$F(t) = m\ddot{\alpha}(t), \quad (2)$$

and dots represent derivatives with respect to time. $F(t)$ is a homogeneous force that compensates the inertial force generated by the acceleration of the reference harmonic potential with angular frequency ω given by the second, quadratic term in (1)[28]. $\alpha(t)$ may be in principle an arbitrary reference trajectory from $\alpha(0) = 0$ to $\alpha(t_f) = d$ in a given time t_f . Different trapping configurations, such as a non-rigid harmonic potential or a double well potential have been examined for more complex transport protocols, e.g. in [35], but these generalizations are not needed for our current purpose.



H supports an invariant of motion, $I = [p - m\dot{\alpha}(t)]^2/(2m) + \frac{m}{2}\omega^2[x - \alpha(t)]^2$, provided that the force $F(t)$ and $\alpha(t)$ satisfy (2) [13]. Any wave function $\Psi(x, t)$ that evolves with H may be expanded in terms of eigenvectors ψ_n of I ,

$$\Psi(x, t) = \sum_n c_n e^{i\theta_n} \psi_n(x, t), \quad I(t)\psi_n(x, t) = \lambda_n \psi_n(x, t), \quad (3)$$

where c_n are constant coefficients, λ_n the time-independent eigenvalues of the invariant, and θ_n are Lewis–Riesenfeld phases that can be calculated as [36] $\theta_n(t) = \frac{1}{\hbar} \int_0^t dt' \langle \psi_n(x, t') | i\hbar \frac{\partial}{\partial t} - H(t') | \psi_n(x, t') \rangle$. The eigenstates of the invariant can be written as [37]

$$\psi_n(x, t) = e^{\frac{im}{\hbar}\alpha(t)x} \Phi_n[x - \alpha(t)], \quad (4)$$

where Φ_n are the eigenfunctions of the harmonic oscillator centered at $\alpha(t)$, the ‘transport function’.

The purely time-dependent potential energy term $f(t)$ in (1) is frequently ignored since it ‘only adds’ a global phase to the wave function [38]. Nevertheless, this term is physically meaningful. In particular, it will determine the actual energy of the ion relative to a fixed zero of energy and the corresponding power.

The potential (1) drives the ion from an initial to a non-excited displaced state if we impose commutativity between the Hamiltonian and its invariant at boundary times and thus $H(t_b)$ and $I(t_b)$ share eigenstates ($t_b = 0, t_f$). A simple choice for the transport function is $\alpha(t) = \sum_{j=0}^5 \alpha_j (t/t_f)^j$. While other functional forms are also possible, the polynomial function is known to yield smooth and technically feasible results [28]. The parameters α_j are fixed so that $\alpha(t)$ satisfies $\alpha(0) = 0$, $\alpha(t_f) = d$, $\dot{\alpha}(t_b) = 0$ for commutativity, and also $\ddot{\alpha}(t_b) = 0$ to have a continuous force with $F = 0$ for $t \leq 0$ and $t \geq t_f$. These boundary conditions yield

$$\alpha(t) = d[10(t/t_f)^3 - 15(t/t_f)^4 + 6(t/t_f)^5]. \quad (5)$$

Unless stated otherwise, we shall use the transport function in (5) in the examples and computations. Later in section 3.5 we shall use a higher order polynomial with additional freedom to optimize consumptions. Note that $\alpha(t)$ represents the trajectory of the center of the dynamical states (4), which coincides with the minimum of the reference harmonic potential $\frac{m}{2}\omega^2[x - \alpha(t)]^2$, but not with the trajectory followed by the minimum of the total potential (1), displaced due to the compensating force to $\alpha(t) + \ddot{\alpha}(t)/\omega^2$, as shown in figure 3.

2.2. Evolution of segment voltages

We consider a simple setting to transport the ion between two (pairs of) electrodes centered at $x = 0$ and $x = d$. The time-dependent potential in (1) that shuttles the ion is in practice generated as a local approximation from

$$V(x, t) = q[U_1(t)\phi_1(x) + U_2(t)\phi_2(x)], \quad (6)$$

where U_i are segment voltages, ϕ_i are dimensionless electrostatic potentials, q is the electric charge of the ion, and subindices $i = 1, 2$ correspond to the different segments. We use a $^{40}\text{Ca}^+$ ion in the numerical calculations so q is the elementary charge.

Electrostatic potentials are usually computed through the boundary element method or finite element method solvers such as NIST BEM or COMSOL [22, 39], but the results can be well approximated by Gaussian

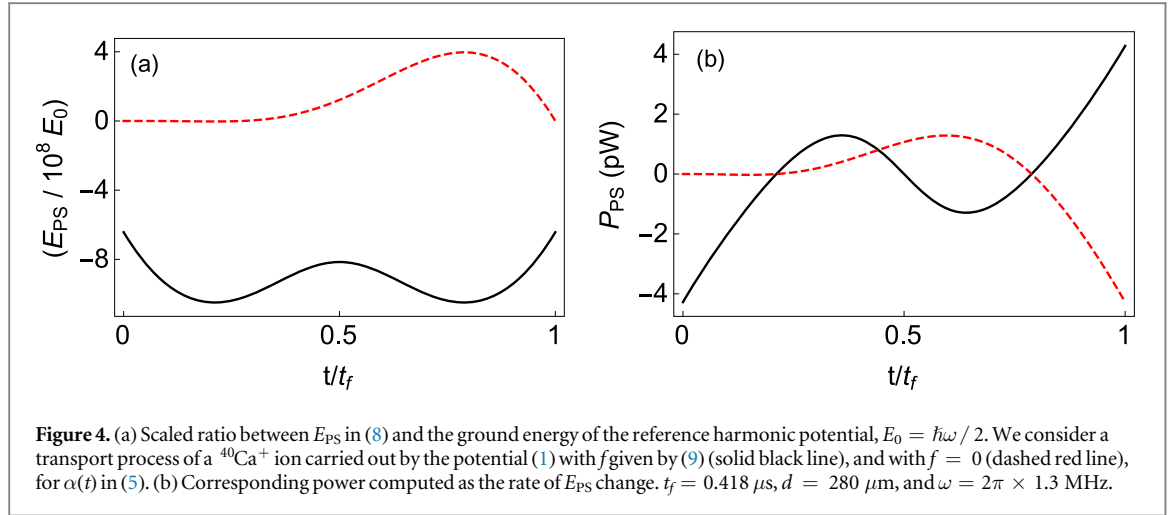


Figure 4. (a) Scaled ratio between E_{PS} in (8) and the ground energy of the reference harmonic potential, $E_0 = \hbar\omega/2$. We consider a transport process of a $^{40}\text{Ca}^+$ ion carried out by the potential (1) with f given by (9) (solid black line), and with $f = 0$ (dashed red line), for $\alpha(t)$ in (5). (b) Corresponding power computed as the rate of E_{PS} change. $t_f = 0.418 \mu\text{s}$, $d = 280 \mu\text{m}$, and $\omega = 2\pi \times 1.3 \text{ MHz}$.

functions $\phi_i = ae^{-(x-b_i)^2/2c^2}$, see figure 1(c). The approximation provides analytical results and more exact but numerical functions will not change quantitatively any of the conclusions drawn here.

By imposing that first and second derivatives of the potential (6) at α should be equal to $-F(t)$ and $m\omega^2$, respectively, we find

$$U_i = \frac{(-1)^i m\omega^2 \phi'_j[\alpha(t)] + (-1)^i m\ddot{\alpha}(t) \phi''_j[\alpha(t)]}{\{\phi''_2[\alpha(t)] \phi'_1[\alpha(t)] - \phi'_2[\alpha(t)] \phi''_1[\alpha(t)]\} q}, \quad i, j \in \{1, 2\}, \quad j \neq i, \quad (7)$$

where the primes represent spatial derivatives. The same result may also be found as in [26], by splitting U_i into two parts set to impose a harmonic potential term centered at α and a linear compensating term.

3. Results

3.1. Energy and instantaneous power of the PS

The time-dependent energy of the ground dynamical mode $\psi_0(x, t)$ driven by H is

$$E_{PS} = \frac{\hbar\omega}{2} + \frac{m}{2} \dot{\alpha}(t)^2 - m\ddot{\alpha}(t)\alpha(t) + f(t). \quad (8)$$

Expanding the potential (6) in Taylor series around $\alpha(t)$, the additional time-dependent term in (1) is given by

$$f(t) = m\alpha(t)\ddot{\alpha}(t) - \frac{c^2 m [c^2 \omega^2 + (d - 2\alpha(t))\ddot{\alpha}(t)]}{c^2 - d\alpha(t) + \alpha(t)^2}, \quad (9)$$

which depends on the chosen reference trajectory $\alpha(t)$ and its acceleration, on the width of the Gaussian electrostatic potentials c , and on the distance d between segment centers. Thus the power for the primary system, and any definition of energy consumption that depends on the energy of the PS, in fact depend on the control system through $f(t)$. Obviating the control system and thus leaving $f(t)$ indeterminate makes the energy of the PS undefined. Often $f(t)$ is taken as zero for simplicity, but this provides the wrong energy function $E_{PS}(t; f = 0)$, since it is not defined with respect to a fixed zero of energy so it cannot provide the true power.

Figure 4(a) depicts the completely different time evolution of the energy of the ion with the physical $f(t)$ in (9) and with $f = 0$, and figure 4(b) their corresponding instantaneous power, which for the physical $f(t)$ reads

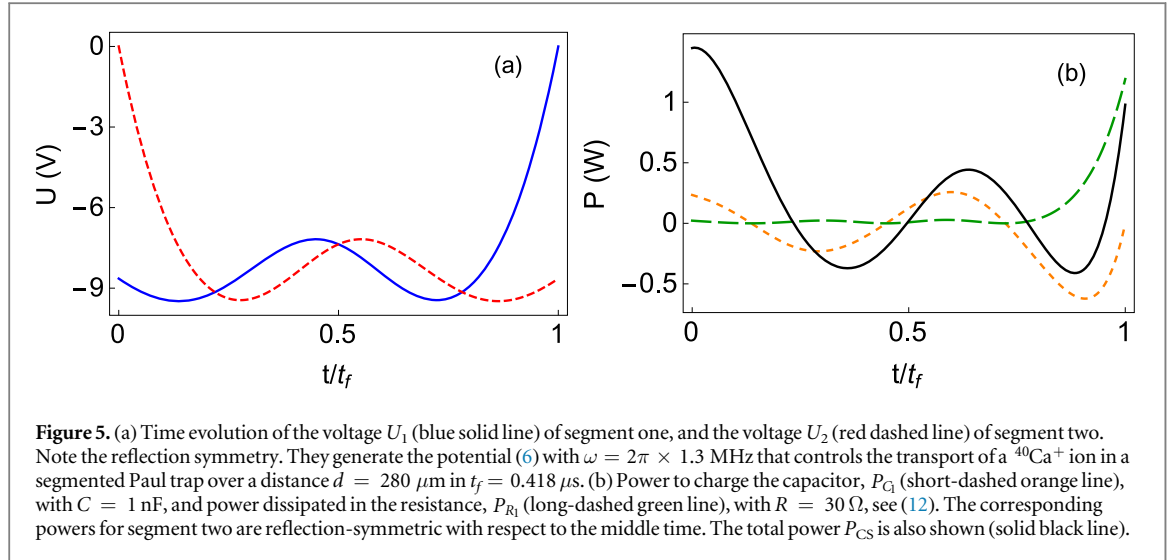
$$P_{PS} = \frac{dE_{PS}}{dt} = m(A + B\omega^2), \quad (10)$$

where A and B depend on the parameters of the trap c and d , and on the transport function α and its derivatives,

$$A = \dot{\alpha}(t)\ddot{\alpha}(t) - \frac{c^2 [d - 2\alpha(t)]^2 \dot{\alpha}(t)\ddot{\alpha}(t)}{[c^2 - d\alpha(t) + \alpha(t)^2]^2} - \frac{c^2 \{-2\dot{\alpha}(t)\ddot{\alpha}(t) + [d - 2\alpha(t)]\alpha^{(3)}(t)\}}{c^2 - d\alpha(t) + \alpha(t)^2},$$

$$B = \frac{c^4 [-d\dot{\alpha}(t) + 2\alpha(t)\dot{\alpha}(t)]}{[c^2 - d\alpha(t) + \alpha(t)^2]^2}. \quad (11)$$

Although not appreciable in the scale of the figure, at boundary times ($t_b = 0, t_f$) $E_{PS}(t_b; f = 0)$ is the ground state energy of the harmonic potential $E_0 = \hbar\omega/2$, while $E_{PS}(t_b) = E_0 - m\omega^2 c^2$, that is, initial and final energies have been displaced from the ground energy of the reference harmonic potential by $f(t_b)$. Both processes, with $f = 0$ or $f(t)$ given by (9), are formally valid shortcuts without final excitations on the transported state, and, seemingly,



with no energy cost as the power P_{PS} integrates to zero in both cases. This is a general property in STA processes with the same energy of the PS at boundary times, as in transport protocols. The instantaneous power does not integrate to zero in STA processes that imply a net energy change for the PS, such as expansions or compressions.

3.2. Power of the CS

Let us now consider the power we have to supply to the CS to implement the STA protocol. Transporting an ion requires moving the potential minimum by varying the segment voltages in time, as explained in methods. This is achieved by inducing currents that go through the RC low-pass filters and govern the voltages in the electrodes. The total power exerted by the electromotive force at the source of the electrode circuits includes the rate of change of the energy accumulated at the capacitor and the power dissipated in the resistance through the Joule effect, $P_{CS} = \sum_i (P_{C_i} + P_{R_i})$, respectively, given by

$$P_{C_i} = C U_i \partial_t U_i, \quad P_{R_i} = R C^2 (\partial_t U_i)^2, \quad (12)$$

where R and C are the resistance and the capacitance of each electrode circuit (assumed equal for both segments). See figure 5(b) for the evolution of these power terms in the first segment. Those for the second segment are symmetrical.

The power required by the CS is orders of magnitude larger than the one for the PS, as we are dealing with macroscopic charges instead of a single ion. In fact this disparity of scales is helpful in that the effect of the exact state of the PS has a negligible influence in the implementation of the protocol. This is one of the observations in the mechanical crane model in [15], where the stability of the STA protocol in the control system required a small mass of the load compared to the mass of the trolley. (Otherwise each initial condition of the PS would require a different control protocol.)

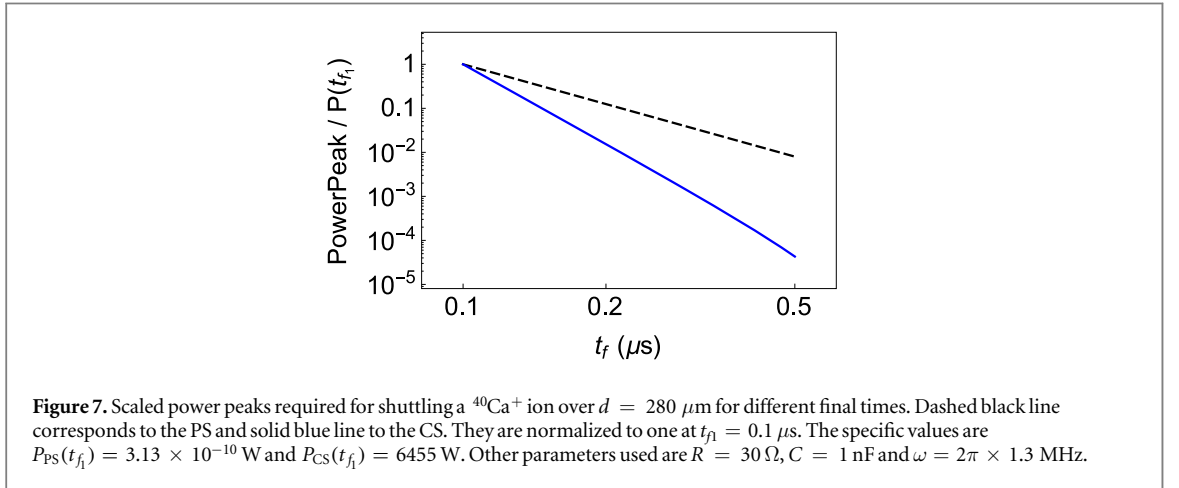
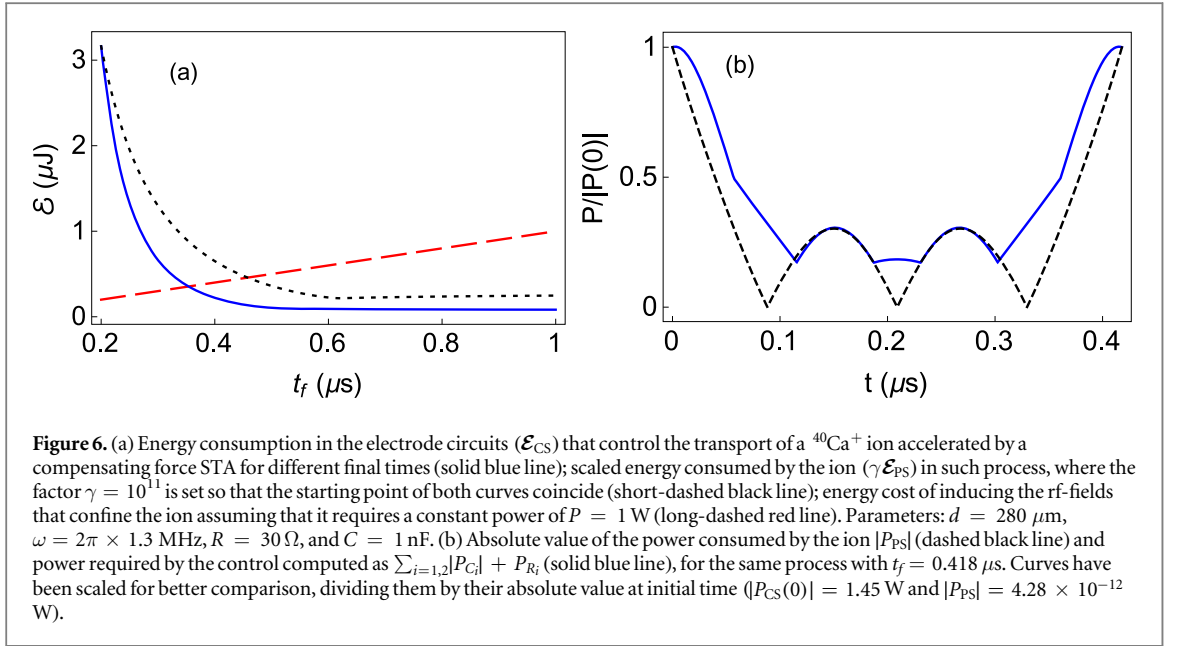
3.3. Comparison between the energy consumed by the PS and by the CS

In [15] it was emphasized that the way to implement a negative power has a decisive influence on the energy cost. Negative powers do not necessarily imply a reduction in the energy cost of the process. To implement such a reduction, the system has to store and reuse the energy given away, which is often not the case or only partially true. To calculate the energy consumption by integration of the power, Torrontegui *et al* proposed to include a parameter η in the negative power segments,

$$\mathcal{E} = \int_0^{t_f} P_+ dt + \eta \int_0^{t_f} P_- dt. \quad (13)$$

Here $P_{\pm} = \Theta(\pm P)P$ are positive/negative parts of the power of the system and $-1 \leq \eta \leq 1$ accounts for different possible scenarios. The limit $\eta = -1$ means that the negative power implies as much energy consumption as the positive one, while $\eta = 1$ means that the energy can be stored and reused (regenerative braking).

In our CS, the power dissipated in the resistance, P_{R_i} , is always positive but P_{C_i} becomes negative when the capacitor is discharging, see figure 5(b). However, the short time scales intrinsic to STA require to charge and discharge the capacitor much faster than the circuit's time constant, so we always need to actively drive it. This is achieved by changing the polarity of the power source, reversing the direction of the current whenever we need to change the energy flow in the capacitor. This makes impossible to retrieve the energy stored in the capacitor,



which translates as an $\eta = -1$ scenario in our analysis. The energy consumed by the control is in summary given by

$$\mathcal{E}_{CS} = \int_0^{t_f} \sum_{i=1}^2 (|P_{C_i}| + P_{R_i}) dt. \quad (14)$$

For the reference trajectory (5) and $t_f \rightarrow 0$ it scales as t_f^{-5} ($\sim t_f^{-4}$ for the time scale considered in figure 6(a)) while \mathcal{E}_{PS} , defined as

$$\mathcal{E}_{PS} = \int_0^{t_f} |P_{PS}| dt \quad (15)$$

by analogy with \mathcal{E}_{CS} , scales as t_f^{-2} (see figure 6(a)).

In figure 6(b) we compare $|P_{PS}|$ and $\sum_{i=1,2}|P_{C_i}| + P_{R_i}$ normalized by their initial value. Although they have a similar evolution, they are not just scaled with respect to each other. A consequence of their different orders of magnitude is that the actual energy consumption \mathcal{E} can be computed in terms of the CS alone with great accuracy, i.e., $\mathcal{E} = \mathcal{E}_{PS} + \mathcal{E}_{CS} \approx \mathcal{E}_{CS}$.

3.4. Power peaks

The power peaks of the protocol may limit the minimum time to implement a STA, as a generic power source is only able to reach a certain maximum value. Figure 7 depicts the value of the power peak of the PS and the CS for different final times in a transport process with (5). For the CS the power peak occurs at boundary times ($t_b = 0$, t_f) and it reads

Table 1. Energy consumptions for transport processes with reference trajectory given by $\alpha(t) = \sum_{j=0}^7 a_j (t/t_f)^j$. $\mathcal{E}_{\text{PS}(f=0)}$ is the energy consumed by the ion given in (15) with $f(t) = 0$, \mathcal{E}_{PS} is the same quantity with $f(t)$ given by (9) and \mathcal{E}_{CS} is the energy consumption in the control given in (14). Parameters $a_j, j < 6$, are fixed (as functions of a_6 and a_7) by the boundary conditions described in methods. The first titled column corresponds to the original non-optimized protocol with (5), while the others correspond to different criterions to find the free parameters, based on minimizing one of the mentioned energy consumptions. The values of the free parameters are $a_6 = -0.0195$ and $a_7 = -0.0049$ for the ‘optimized for $\mathcal{E}_{\text{PS}(f=0)}$ ’ column, $a_6 = -0.0093$ and $a_7 = 0.0027$ for the ‘Optimized for \mathcal{E}_{PS} ’ column and $a_6 = -0.0094$ and $a_7 = 0.0027$ for the ‘optimized for \mathcal{E}_{CS} ’ column.

	Non-optimized	Optimized for $\mathcal{E}_{\text{PS}(f=0)}$	Optimized for \mathcal{E}_{PS}	Optimized for \mathcal{E}_{CS}
$\mathcal{E}_{\text{PS}(f=0)}$	3.441×10^{-19} J	2.179×10^{-19} J	3.363×10^{-19} J	3.355×10^{-19} J
\mathcal{E}_{PS}	5.513×10^{-19} J	6.242×10^{-19} J	5.169×10^{-19} J	5.169×10^{-19} J
\mathcal{E}_{CS}	1.882×10^{-7} J	2.696×10^{-7} J	1.572×10^{-7} J	1.572×10^{-7} J

$$P_{\text{CS}}(t_b) = \frac{m^2}{q^2} \left(\frac{G}{t_f^6} + \frac{J\omega^2}{t_f^3} \right), \quad (16)$$

where

$$G = \frac{3600RC^2}{a^2} [(c^2 - d^2)^2 + c^4 e^{(d/c)^2}]; J = \frac{60Cc^2}{a^2} (c^2 - d^2). \quad (17)$$

For the PS and for the parameters used in the paper and final times shorter than 1 μs , the power peak is at initial and final times as well (see figure 6 where $t_f = 0.418 \mu\text{s}$) and it is given by

$$P_{\text{PS}}(t_b) = \frac{60d^2m}{t_f^3}. \quad (18)$$

Again, the difference between the PS and the CS power peaks is not just a matter of scaling, they show a different qualitative behavior. The power peak of the PS scales as t_f^{-3} while the one of the CS scales as t_f^{-6} .

3.5. Optimization

The freedom to choose different transport functions $\alpha(t)$ may be used to optimize physically relevant variables. For example this freedom was used in [40] to avoid deviations from the harmonic regime at intermediate times in the transport of a load by a mechanical crane. Here we use a 7th degree polynomial ansatz with two free parameters to minimize the energy consumption of the transport process. The optimization, i.e., the final form of the reference trajectory, must be based on minimizing the total energy consumption. However, it is interesting to compare the results with alternative optimization criteria. In particular, we shall also minimize the energy consumption of the primary system \mathcal{E}_{PS} with the physical, CS-based f function (9), and $\mathcal{E}_{\text{PS}(f=0)}$ with $f = 0$. Table 1 shows the energy consumption of the PS (with $f = 0$ and with the physical $f(t)$), and of the CS for each of the optimized protocols. Notice that the optimization of \mathcal{E}_{PS} with the physical f , yields essentially the same results than the optimization of \mathcal{E}_{CS} . Both protocols achieve a reduction in the consumption of 6% for the ion and 17% for the control. On the contrary, optimizing $\mathcal{E}_{\text{PS}(f=0)}$ turns out to be unsatisfactory, as it increases significantly the total energy consumption of the process: \mathcal{E}_{PS} increases by 13% and \mathcal{E}_{CS} by 43% with respect to the non-optimized trajectory that uses the fifth degree polynomial (5). These numerical results confirm the importance of including the CS-dependent term f in the PS-energy so as to mimic the evolution of the energy consumption and to use PS-energies for optimizing consumptions.

4. Discussion

As new quantum technologies unfold from laboratory prototypes to commercially available devices, energetic costs of processes may become more and more relevant. STA can play an important role in this transition by providing a toolbox of approaches to design control protocols that minimize process times and the effects of decoherence. Determining the energetic cost of a shortcut requires a global perspective that includes the primary system and the control system as well. The shortcuts are by definition fast processes so one cannot assume that the control system may change infinitely slowly to avoid dissipation, as in Landauer’s analysis of minimal costs of computation [41], or in ideal thermodynamical reversible processes. To be more precise, very slow processes are physically possible, but STA are never applied in the long-time domain.

The study case chosen in this paper is a microscopic ion transported with a STA protocol implemented by macroscopic operations to modulate the voltages of a segmented Paul trap. Features of the energy consumption

that were speculated to be broadly applicable after the analysis of a mechanical crane [15] have been found here too. For example, negative power time-segments may imply as much consumption as the positive power segments. In the model, as it will be typically the case in controlling microscopic systems, the consumption is dominated by far by the control system. This is in fact desirable, otherwise the control operations to implement a given STA would have to depend on the specific initial conditions of the PS. The power for the CS is due to dissipation in the resistances and to the charge or discharge of capacitors. This dual origin (dissipative and non-dissipative) is once again analogous to the mechanical crane model, where the power was employed to compensate dissipation (friction losses) and move (accelerate or brake) the control trolley.

The integrated energy consumption of the PS alone is not zero when evaluated with the absolute value of the power of the PS. This integral quantity, properly scaled, resembles the consumption of the CS, and in fact can be used to find optimal transport trajectories, but only when a purely time-dependent energy shift that depends on the CS is included in the PS Hamiltonian. In other applications this term is neglected or set as zero, but it is a crucial factor to determine energy flows.

We have paid attention to global energy consumptions rather than differential ones (relative to some reference process). A definition of energy consumption based on a differential power may have some uses, e.g., to compare different ways to achieve a shortcut for a given reference process. However, it depends on the reference process and it is inappropriate if we are interested in the actual energy consumption, the reason being that the reference process also consumes energy.

The main text has focused on the non trivial part of the energy consumption of the CS, associated with the dc electrodes, which grows strongly when diminishing process times, leaving aside the linear-in-time consumption of the rf electrodes. Combining the two contributions, minimal times for energy consumption can be identified.

Further examples of systems subjected to STA may be examined to build a general theory, e.g. analyzing energy consumptions in discrete systems [42]. After completion of this work, a relevant paper [43] was brought to our attention.

Acknowledgments

We thank Kihwan Kim for discussions. We acknowledge funding by the Basque Government (Grant No. IT986-16) and MINECO/FEDER,UE (Grant No. FIS2015-67161-P). The research is based upon work supported by the Office of the Director of National Intelligence (ODNI), Intelligence Advanced Research Projects Activity (IARPA), via the U.S. Army Research Office grant W911NF-16-1-0070. The views and conclusions contained herein are those of the authors and should not be interpreted as necessarily representing the official policies or endorsements, either expressed or implied, of the ODNI, IARPA, or the US Government. Any opinions, findings, and conclusions or recommendations expressed in this material are those of the author(s) and do not necessarily reflect the view of the US Army Research Office.

References

- [1] Campbell S and Deffner S 2017 Trade-off between speed and cost in shortcuts to adiabaticity *Phys. Rev. Lett.* **118** 100601
- [2] Zheng Y, Campbell S, De Chiara G and Poletti D 2016 Cost of counterdiabatic driving and work output *Phys. Rev. A* **94** 042132
- [3] Abah O and Lutz E 2017 Energy efficient quantum machines *Europhys. Lett.* **118** 40005
- [4] Funo K, Zhang J-N, Chatou C, Kim K, Ueda M and del Campo A 2017 Universal work fluctuations during shortcuts to adiabaticity by counterdiabatic driving *Phys. Rev. Lett.* **118** 100602
- [5] Chen X and Muga J G 2010 Transient energy excitation in shortcuts to adiabaticity for the time-dependent harmonic oscillator *Phys. Rev. A* **82** 053403
- [6] Del Campo A, Goold J and Paternostro M 2014 More bang for your buck: towards super-adiabatic quantum engines *Sci. Rep.* **4** 6208
- [7] Santos A C, Silva R D and Sarandy M S 2016 Shortcut to adiabatic gate teleportation *Phys. Rev. A* **93** 012311
- [8] Coulamy I B, Santos A C, Hen I and Sarandy M S 2016 Energetic cost of superadiabatic quantum computation *Frontiers ICT* **3** 19
- [9] Kosloff R and Rezek Y 2017 The quantum harmonic otto cycle *Entropy* **19** 136
- [10] Kieferová M and Wiebe N 2014 On the power of coherently controlled quantum adiabatic evolutions *New J. Phys.* **16** 123034
- [11] Bravetti A and Tapias D 2017 Thermodynamic cost for classical counterdiabatic driving *Phys. Rev. E* **96** 052107
- [12] Abah O and Lutz E 2017 Performance of shortcut-to-adiabaticity quantum engines arXiv:1707.09963
- [13] Torrontegui E, Ibáñez S, Martínez-Garaot S, Modugno M, del Campo A, Guéry-Odelin D, Ruschhaupt A, Chen X and Muga J G 2013 Shortcuts to adiabaticity *Advances in Atomic, Molecular, and Optical Physics* (vol 62) (Amsterdam: Elsevier) pp 117–69
- [14] Chen X, Ruschhaupt A, Schmidt S, del Campo A, Guéry-Odelin D and Muga J G 2010 Fast optimal frictionless atom cooling in harmonic traps: shortcut to adiabaticity *Phys. Rev. Lett.* **104** 063002
- [15] Torrontegui E, Lizuain I, González-Resines S, Tobalina A, Ruschhaupt A, Kosloff R and Muga J G 2017 Energy consumption for shortcuts to adiabaticity *Phys. Rev. A* **96** 022133
- [16] Horowitz J M and Jacobs K 2015 Energy cost of controlling mesoscopic quantum systems *Phys. Rev. Lett.* **115** 130501
- [17] Clivaz F, Silva R, Haack G, Brask J, Brunner N and Huber M 2017 Unifying paradigms of quantum refrigeration: resource-dependent limits arXiv:1710.11624
- [18] Zenesini A, Lignier H, Ciampini D, Morsch O and Arimondo E 2009 Coherent control of dressed matter waves *Phys. Rev. Lett.* **102** 100403

- [19] Couvert A, Kawalec T, Reinaudi G and Guéry-Odelin D 2008 Optimal transport of ultracold atoms in the non-adiabatic regime *Europhys. Lett.* **83** 13001
- [20] Rowe M A et al 2002 Transport of quantum states and separation of ions in a dual rf ion trap *Quantum Inf. Comput.* **2** 257–71 arXiv: [quant-ph/0205094](https://arxiv.org/abs/quant-ph/0205094)
- [21] Leibfried D, Blatt R, Monroe C and Wineland D 2003 Quantum dynamics of single trapped ions *Rev. Mod. Phys.* **75** 281–324
- [22] Singer K, Poschinger U, Murphy M, Ivanov P, Ziesel F, Calarco T and Schmidt-Kaler F 2010 Colloquium *Rev. Mod. Phys.* **82** 2609–32
- [23] Wineland D J, Monroe C, Itano W M, Leibfried D, King B E and Meekhof D M 1998 Experimental issues in coherent quantum-state manipulation of trapped atomic ions *J. Res. Natl. Inst. Stand. Technol.* **103** 259–328 arXiv: [9710025](https://arxiv.org/abs/9710025)
- [24] Bowler R, Gaebler J, Lin Y, Tan T R, Hanneke D, Jost J D, Home J P, Leibfried D and Wineland D J 2012 Coherent diabatic ion transport and separation in a multizone trap array *Phys. Rev. Lett.* **109** 080502
- [25] Walther A, Ziesel F, Ruster T, Dawkins S T, Ott K, Hettrich M, Singer K, Schmidt-Kaler F and Poschinger U 2012 Controlling fast transport of cold trapped ions *Phys. Rev. Lett.* **109** 080501
- [26] Fürst H A, Goerz M H, Poschinger U G, Murphy M, Montangero S, Calarco T, Schmidt-Kaler F, Singer K and Koch C P 2014 Controlling the transport of an ion: classical and quantum mechanical solutions *New J. Phys.* **16** 075007
- [27] Alonso J, Leupold F M, Keitch B C and Home J P 2013 Quantum control of the motional states of trapped ions through fast switching of trapping potentials *New J. Phys.* **15** 023001
- [28] Torrontegui E, Ibáñez S, Chen X, Ruschhaupt A, Guéry-Odelin D and Muga J G 2011 Fast atomic transport without vibrational heating *Phys. Rev. A* **83** 013415
- [29] Masuda S and Nakamura K 2010 Fast-forward of adiabatic dynamics in quantum mechanics *Proc. R. Soc. A* **466** 1135–54
- [30] Ibáñez S, Chen X, Torrontegui E, Muga J G and Ruschhaupt A 2012 Multiple Schrödinger pictures and dynamics in shortcuts to adiabaticity *Phys. Rev. Lett.* **109** 100403
- [31] Sels D and Polkovnikov A 2017 Minimizing irreversible losses in quantum systems by local counterdiabatic driving *Proc. Natl Acad. Sci.* **31** E3909–16
- [32] An S, Lv D, del Campo A and Kim K 2016 Shortcuts to adiabaticity by counterdiabatic driving for trapped-ion displacement in phase space *Nature* **7** 12999
- [33] Chen Y-H, Shi Z-C, Song J, Xia Y and Zheng S-B 2017 Optimal shortcut approach based on an easily obtained intermediate Hamiltonian *Phys. Rev. A* **95** 062319
- [34] Chen X, Jiang R-L, Li J, Ban Y and Sherman E Y 2018 Inverse engineering for fast transport and spin control of spin-orbit-coupled Bose-Einstein condensates in moving harmonic traps *Phys. Rev. A* **97** 013631
- [35] Tobalina A, Palmero M, Martínez-Garaot S and Muga J G 2017 Fast atom transport and launching in a nonrigid trap *Sci. Rep.* **7** 5753
- [36] Lewis H R and Riesenfeld W B 1969 An exact quantum theory of the time-dependent harmonic oscillator and of a charged particle in a time-dependent electromagnetic field *J. Math. Phys.* **10** 1458
- [37] Dhara A K and Lawande S V 1984 Feynman propagator for time-dependent Lagrangians possessing an invariant quadratic in momentum *J. Phys. A: Math. General* **17** 2423–31
- [38] Torrontegui E, Chen X, Modugno M, Schmidt S, Ruschhaupt A and Muga J G 2012 Fast transport of Bose-Einstein condensates *New J. Phys.* **14** 013031
- [39] de Clercq L E 2015 Transport quantum logic gates for trapped ions *PhD Thesis* ETH Zürich
- [40] González-Resines S, Guéry-Odelin D, Tobalina A, Lizuain I, Torrontegui E and Muga J G 2017 Invariant-based inverse engineering of crane control parameters *Phys. Rev. Appl.* **8** 054008
- [41] Landauer R 1961 Irreversibility and heat generation in the computing process *IBM J. Res. Dev.* **5** 183–91
- [42] Hu C-K, Cui J-M, Santos A C, Huang Y-F, Sarandy M S, Li C-F and Guo G-C 2018 Experimental implementation of generalized transitionless quantum driving arXiv: [1803.10410](https://arxiv.org/abs/1803.10410)
- [43] A C Barato and U Seifert 2017 Thermodynamic cost of external control *New J. Phys.* **19** 073021

Focus Article

Vanishing efficiency of a speeded-up ion-in-Paul-trap Otto engine^(a)

A. TOBALINA¹, I. LIZUAIN² and J. G. MUGA¹¹ Department of Physical Chemistry, University of the Basque Country UPV/EHU - Apdo 644, Bilbao, Spain² Department of Applied Mathematics, University of the Basque Country UPV/EHU - Plaza Europa 1, 20018 Donostia-San Sebastian, Spainreceived 5 July 2019; accepted in final form 13 August 2019
published online 28 August 2019PACS 07.20.Pe – Heat engines; heat pumps; heat pipes
PACS 37.10.Ty – Ion trapping

Abstract – We assess the energy cost of shortcuts to adiabatic expansions or compressions of a harmonic oscillator, the power strokes of a quantum Otto engine. Difficulties to identify the cost stem from the interplay between different parts of the total system (the primary system—the particle—and the control system) and definitions of work (exclusive and inclusive). While attention is usually paid to the inclusive work of the microscopic primary system, we identify the energy cost as the exclusive work of the total system, which, for a clear-cut scale disparity between a microscopic primary system and a macroscopic control system, coincides with the exclusive work for the control system alone. We redefine the “engine efficiency” taking into account this cost. Our working horse model is an engine based on an ion in a Paul trap with power strokes designed via shortcuts to adiabaticity. Opposite to the paradigm of slow-cycle reversible engines with vanishing power and maximal efficiency, this fast-cycle engine increases the microscopic power at the price of a vanishing efficiency. The Paul trap fixes the gauge for the primary system, resulting in a counterintuitive evolution of its inclusive power and internal energy. Conditions for which inclusive power of the primary system and exclusive power control system are proportional are found.

focus article

Copyright © EPLA, 2019

Introduction. – One of the challenges to realize quantum technologies and devices that outperform classical counterparts, is to achieve an exhaustive control over the state and dynamics of quantum systems. To this effect, shortcuts to adiabaticity (STA) [1,2] stand as a useful toolbox, mimicking the final result of a slow adiabatic evolution in shorter times, which avoids the drawbacks of long-time processes, such as decoherence. An open question is to determine their energy cost.

As devices based on quantum properties, such as quantum computers, engines and refrigerators are being proposed, it is important to understand their energy flows and costs. A useful model for an engine, exactly solvable but complex enough to represent friction and heat leaks [3], considers a quantum harmonic oscillator as the working medium of an Otto engine [4]. During the cycle,

the oscillator undergoes two power strokes between two frequencies and two thermalizations. Compared to the macroscopic Otto engine, the frequency plays the role of an inverse volume, and the harmonic potential the role of the piston [3]. This quantum engine could be implemented by an ion (primary system) in a Paul trap (control system), our model hereafter. Analyzing specific elementary operations is important to reach or test more general conclusions. In particular, expansions and compressions, apart from being strokes of the Otto engine, have been key to develop STA in theory [5] and experiments [6,7]. While the results of our calculations are model dependent, they also give hints on what to expect in a broad domain of systems as discussed in the last section.

In a standard analysis the (angular) frequency $\omega(t)$ is assumed to be classical, with definite values, whereas the particle is treated quantumly. This hybrid classical-quantum scenario is justified by the different scales involved and is a general feature, well discussed in

^(a)Contribution to the Focus Issue *The Physics of Quantum Engineering and Quantum Technologies* edited by Roberta Citro, J. Gonzalo Muga and Bart A. van Tiggelen.

foundational work on quantum mechanics [8], when driving microscopic systems. A related and widespread feature, again a consequence of different scales, is the negligible effect of the particle on the classical control, whereas the classical control determines the quantum dynamics. As a consequence, we can design useful STA protocols that are independent of the particle state and its dynamics.

The basic performance criteria of a thermal device are power output and efficiency. Any thermal device that operates in finite time incurs in rate-dependent losses that diminish efficiency, as opposite to a device operating reversibly with no power output [9]. At the microscopic level, increasing the rate of a given transformation usually increases quantum friction [10,11], *i.e.*, undesired excitations at final time which imply a waste of energy. STA, however, suppress quantum friction in the power strokes [12–14]. It may therefore seem that STA enhance the power output arbitrarily without affecting efficiency, enabling a “perpetual-motion machine of the third kind” [15]. While there is widespread agreement that some kind of “cost” inherent in the STA process precludes these machines, many different “costs” have been put forward [3,13,14,16–25], which are not necessarily in conflict if regarded as different aspects of the system energy or its interactions [2].

Here, we refine the viewpoint originally proposed in [26] with more accurate work definitions, perfecting as well the model in [27] which is applied to a new set of operations in Paul traps (in [27] we only considered transport and the Hamiltonian was not as detailed as here). We identify the cost with the exclusive work for the total system, which is essentially the energy consumption to set the driving protocol, *i.e.*, the classical parameters of the Hamiltonian for the primary system. Several examples dealing with STA demonstrate that this perspective is crucial to reach sensible conclusions [26,27]. Beyond STA see, *e.g.*, [15,28,29] as examples of the need to account for all the energy flows.

This work focuses on the compression/expansion strokes of the quantum harmonic Otto cycle, without explicitly modeling the heat baths nor their interaction with the working medium. A comprehensive review of the quantum harmonic Otto cycle may be found in [3], see, *e.g.*, [30,31] for some recent results.

Definitions of work. – We point out two factors that lead to different definitions for the work done or required by a transformation of a microscopic system. The first one corresponds to the definition of work in externally driven systems [32]. Suppose a simple setting described by the Hamiltonian $H(y, t) = H_0(y) + \lambda(t)y$ with externally driving potential $\lambda(t)y$ along some coordinate y . The exclusive work definition evaluates only the change of the internal energy defined by the “unperturbed” H_0 . It considers this difference as work injected to the unperturbed system by the action of $\lambda(t)$ [33] and corresponds to the standard expression of force times displacement. Instead, an inclusive

definition evaluates work as the change of the energy represented by the total Hamiltonian, including the external influence [34].

The second factor corresponds to the role of the control. Gibbs already stated that the force that induces a given transformation on a system is often affected by the configuration of an external body [35], here the “control system”. The energy needed to manipulate this body should be taken into account when discussing efficiencies, and more so in the context of quantum technologies with a macroscopic control system and a microscopic “primary system”.

Let us combine these factors to propose two useful definitions: *Total work* is the exclusive total energy consumed by the control plus primary system; *Microscopic work* is an inclusive definition for the primary system that disregards the energy cost to set the control parameters. The microscopic work is the definition found in most studies on quantum thermal machines. It is not invariant under gauge transformations that shift in time the zero energy point [32], and thus, according to Cohen-Tannoudji *et al.*, it is not a physical quantity [36]. The gauge, however, may be fixed by the experimental setting to make energy differences physically meaningful [32]. Using the proper gauge the microscopic work may constitute an indicator of the total work if it is proportional to it. This proportionality is not guaranteed, but it indeed occurs, as shown below, for a specific regime in our model.

Ion-in-Paul-trap model. – We consider a one-dimensional quantum harmonic Otto engine whose working medium is a single ion of mass m and electric charge Q . The Hamiltonian for the working medium in the absence of the longitudinal harmonic potential reads $H_{S,0}(x) = \frac{p^2}{2m}$, where p is the momentum of the ion. The ion is trapped in a harmonic potential generated by a segmented linear Paul trap, the control system. Following [27], we model it as a circuit formed by a controllable power source that generates an electromotive force (efm) $\mathcal{E}(t)$ and a low-pass electronic filter formed by a resistor (resistance R) and a capacitor (capacitance C), with Hamiltonian [37] $H_C(q, t) = q^2/2C - \mathcal{E}(t)q$, where q is the charge in the capacitor. Through the modified Hamilton equation $\dot{p}_q = -\frac{\partial H_C}{\partial q} - \frac{\partial \mathcal{F}}{\partial \dot{q}}$, which accounts for friction through Rayleigh’s dissipation function [37] $\mathcal{F} = R\dot{q}^2/2$, we get the dynamics of the control system,

$$\mathcal{E}(t) = \frac{q}{C} + R\dot{q}. \quad (1)$$

The interaction between the control and the ion is $H_{SC}(x, q, t) = Q\phi(x)q/C$, where x is the coordinate of the ion and $\phi(x)$ is a (dimensionless) electrostatic potential that depends on the geometry of the trap [38] given by $\phi(x) = ae^{-x^2/2b^2}$ with a and b constant [27]. The potential is approximately harmonic near the origin with angular frequency $\omega(t)$ determined by $\partial^2 H_{SC}/\partial x^2|_{x=0} = m\omega^2(t)$

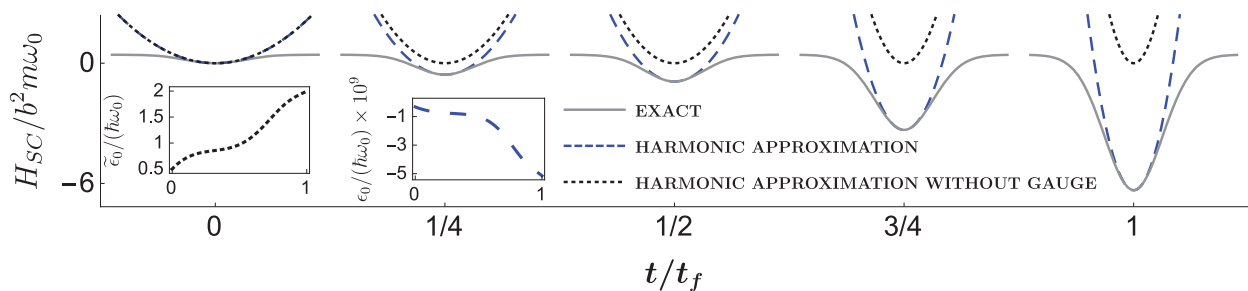


Fig. 1: Evolution of the interaction between ion and control for a compression (left to right) or an expansion (right to left). Exact potential (solid grey line); harmonic approximation (dashed blue line); harmonic potential without the gauge term set by the control (dotted black line). The insets depict the time evolution of the ground energy of the ion in the compression without gauge ($\tilde{\epsilon}_0 = \epsilon_0 + b^2 m \omega^2(t)$) and with gauge term, see eq. (5). $\omega_0 = 1.3 \times 2\pi$ MHz; $\omega_f = 2\omega_0$; mass of $^{40}\text{Ca}^+$; $b = 0.25 \times 10^{-3}$ m; $a = 0.2$; $t_f = 0.2 \mu\text{s}$.

and related to q by

$$q = -\frac{b^2 m C}{a Q} \omega^2(t). \quad (2)$$

Upon Taylor expansion around $x = 0$, the interaction becomes $H_{SC} = m\omega^2(t)x^2/2 - b^2 m \omega^2(t)$. The last term, usually ignored since it does not affect the ion dynamics, fixes the gauge, see fig. 1.

The global Hamiltonian is quadratic,

$$H(x, q, t) = \frac{p^2}{2m} + \frac{m}{2} \omega^2(t) x^2 - b^2 m \omega^2(t) + \frac{1}{2C} q^2 - \mathcal{E}(t) q. \quad (3)$$

It governs the evolution of two interacting degrees of freedom, one of them macroscopic and classical, the charge in the capacitor, and the other microscopic and quantum. The overwhelming difference in scale enables us to make a clear separation and treat the dynamics of the capacitor as effectively independent of the ion dynamics, whereas the dynamics of the quantum system is governed by $H_S = H_{S,0} + H_{SC}$, where $\omega(t)$ is treated as an external parameter, whose evolution is designed in what follows using invariant-based inverse engineering.

This STA technique rests on the parameterization of a quadratic invariant in terms of a scaling factor $\rho(t)$ that determines the state width and satisfies the Ermakov equation [1,5]. The evolution of the control parameter is computed from the Ermakov equation as $\omega^2(t) = \omega_0^2/\rho^4 - \ddot{\rho}/\rho$, where the dots represent time derivatives, and $\rho(t)$ is designed to satisfy the boundary conditions $\rho(0) = 1$, $\rho(t_f) = (\omega_0/\omega_f)^{1/2}$, $\dot{\rho}(t_b) = 0$ and $\ddot{\rho}(t_b) = 0$, with $t_b = 0, t_f$, so that initial eigenstates of $H_S(0)$ evolve according to

$$\psi_n(x, t) = e^{\frac{i m \dot{\rho}}{2 \hbar \rho} x^2} \frac{1}{\sqrt{\rho}} \phi_n\left(\frac{x}{\rho}\right), \quad (4)$$

and become at t_f eigenstates of $H_S(t_f)$. To interpolate we use the ansatz $\rho(t) = \sum_{i=0}^5 \rho_i (t/t_f)^i$, with the ρ_i fixed by the boundary conditions. We will also use the notation $\omega_0 \equiv \omega(0)$ and $\omega_f \equiv \omega(t_f)$.

The expectation value of $H_S(t)$ for the dynamical modes (4) is

$$\epsilon_n(t) = \frac{(2n+1)\hbar}{4\omega_0} \left(\dot{\rho}^2 + \omega^2(t)\rho^2 + \frac{\omega_0^2}{\rho^2} \right) - b^2 m \omega^2(t), \quad (5)$$

see fig. 1, and compare the insets that depict $\tilde{\epsilon}_0 = \epsilon_0 + b^2 m \omega^2(t)$ and ϵ_0 . The gauge term dominates the evolution of $\epsilon_n(t)$ over the vibrational energy of the ion and, moreover, increases the energy of the ion during expansions and decreases it during compressions.

In our inverse engineering protocol, once the desired $\omega(t)$ has been set, the dynamics of the capacitor charge q and the electromotive force \mathcal{E} that we have to implement are found from eqs. (2) and (1).

Work and power. – Work is commonly computed by integrating over time the instantaneous power. The total work considers the evolution of the exclusive instantaneous power \mathcal{P} of the composite unperturbed system driven by $H_0 = H + \mathcal{E}(t)q$. To calculate this total power including the effect of the primary system (backaction) we consider first a fully classical approximation. Later we shall substitute the variables dealing with the quadratic microscopic system by quantum expectation values. For systems described by a Rayleigh dissipation function, the modified Hamilton equations imply that the (exclusive) total power contributes to change the energy of the unperturbed system and to overcome the dissipation, see the appendix. In our model,

$$\mathcal{P} = \mathcal{E}(t)\dot{q} = dH_0/dt + R\dot{q}^2. \quad (6)$$

We can separate it as $\mathcal{P} = \mathcal{P}_C + \mathcal{P}_S$, the power needed to generate the dynamics on the Paul trap (without the ion) and the power to overcome the backaction by the ion,

$$\mathcal{P}_C = \frac{\partial H_{0,C}}{\partial t} + R\dot{q}^2 = (R\dot{q} + q/C)\dot{q}, \quad (7)$$

$$\mathcal{P}_S = \frac{\partial H_S}{\partial t} = \left(1 - \frac{x^2}{2b^2}\right) \frac{aQ}{C} \dot{q}, \quad (8)$$

where $H_{0,C} = q^2/2C$. In \mathcal{P}_S the first term is due to the gauge term. As $q \gg Q$ we expect $|\mathcal{P}_S| \ll |\mathcal{P}_C|$, and

$\mathcal{P} \approx \mathcal{P}_C = \mathcal{E}(t)\dot{q}$, see eq. (1), which holds in all calculations. In fact the dominance of \mathcal{P}_C is needed to set state-independent shortcut protocols.

The possibility to “regenerate” (store and reuse) the energy that flows out of the total system during negative-power time segments is accounted for by a factor $-1 \leq \mu \leq 1$ [26] multiplying the negative power in the total integrated work,

$$W_T = \int_0^t \mathcal{P}_{C_+} dt' + \mu \int_0^t \mathcal{P}_{C_-} dt'. \quad (9)$$

Here $\mathcal{P}_{C_\pm} = \Theta(\pm \mathcal{P}_C) \mathcal{P}_C$, and Θ is the Heaviside function. In the Paul trap both signs need consumption, $\mu = -1$.

The backaction term is in fact the inclusive microscopic work. The quantum version of eq. (8) takes the same form with expectation values, $H_S \rightarrow \langle H_S \rangle$, $x^2 \rightarrow \langle x^2 \rangle$. Defining work at the quantum level is not straightforward [39] and, furthermore, the relation between the system energy and inclusive work holds only if the gauge is appropriately fixed according to the experiment [32,40]. We evaluate the microscopic work for the shortcut process as the difference between final and initial energies determined by H_S . The contribution from each mode is $\langle W_m \rangle = \sum_n p_n^0 \int_0^{t_f} \langle \mathcal{P}_S \rangle_n dt$, where $\langle \mathcal{P}_S \rangle_n = d\epsilon_n/dt = (2n+1)\hbar\rho^2\omega\dot{\omega}/(2\omega_0) - 2b^2m\omega\dot{\omega}$. Assuming an initial thermal distribution with $p_n^0 = e^{-\beta\epsilon_n(0)}/Z$, inverse temperature β , and $Z = \sum_n e^{-\beta\epsilon_n(0)}$, we get

$$\langle W_m \rangle = \frac{\hbar}{2}(\omega_f - \omega_0) \coth\left(\frac{\beta\hbar\omega_0}{2}\right) - b^2m(\omega_f^2 - \omega_0^2). \quad (10)$$

Importantly, for any realistic β , $\langle W_m \rangle$ is negative when $\omega_0 > \omega_f$ and positive when $\omega_0 < \omega_f$. Owing to the gauge term, the microscopic work in each power stroke behaves oppositely to what it is commonly expected when ignoring the physical gauge, see again the inset of fig. 1.

Cost of STA. – The total work in eq. (9) comes from the two terms of \mathcal{P}_C in eq. (7), an Ohmic dissipation $R\dot{q}^2$ and the change in the potential energy of the capacitor. Using the time constant of the circuit (RC) and $q/\dot{q} = \omega/(2\dot{\omega})$ we identify different regimes, dominated by the dissipative term or by the capacitor term. When $\omega/(2\dot{\omega}) \ll RC$, \mathcal{P}_C is dominated by dissipation in the resistor, and, compare eqs. (7) and (8) and note the dominance of the gauge (first term) in eq. (8),

$$\mathcal{P}_C/\dot{q} \approx RC \mathcal{P}_S/(aQ). \quad (11)$$

Alternatively, when $\omega/(2\dot{\omega}) \gg RC$, the instantaneous microscopic power per unit charge is proportional to the control power input per unit charge,

$$\mathcal{P}_C/q \approx \mathcal{P}_S/(aQ). \quad (12)$$

Figure 2 shows the total work consumed by the power strokes in different regimes, for final times that yield a monotonic $\omega(t)$. For an expansion stroke dominated by the capacitor, the consumption decreases first as we reduce

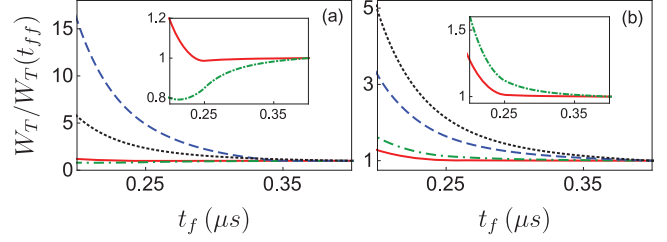


Fig. 2: Normalized total work for (a) an expansion between $\omega_0 = 2 \times 2\pi$ MHz and $\omega_f = 2\pi$ MHz or (b) a reversed compression *vs.* final times of each expansion/compression stroke. W_T is computed with eq. (9). For all curves \mathcal{P}_C is positive for expansions and negative for compressions. The normalization constant is the work for a process time $t_{ff} = 0.4 \mu\text{s}$. Different curves correspond to: $R = 3 \Omega$, $C = 1 \text{ nF}$ (red solid line); $R = 3 \Omega$, $C = 10 \text{ nF}$ (green dash-dotted line); $R = 300 \Omega$, $C = 1 \text{ nF}$ (blue dashed line); $R = 300 \Omega$, $C = 10 \text{ nF}$ (black dotted line). The insets zoom in the first two lines.

t_f (up to $t_f \approx 0.21 \mu\text{s}$ for the green dash-dotted line). For faster protocols, $\omega/(2\dot{\omega}) \gg RC$ becomes unattainable and the total work is dominated by dissipation. We check numerically that for both power strokes, as $t_f \rightarrow 0$, the total work scales as $1/t_f^5$. This scaling agrees with [26,27] and contrasts with Landauer’s estimate of the energy dissipation as being proportional to the “velocity of the process” when studying the cost of computation [41].

Performance of the engine. – The microscopic power output of the engine is calculated along a cycle time τ , adding compression and expansion terms, $P = (\langle W_m^{\text{comp}} \rangle + \langle W_m^{\text{exp}} \rangle)/\tau$. STA protocols increase this quantity by reducing τ and keeping the microscopic work output of adiabatic processes.

Typically, accelerating the thermodynamic cycle increases dissipation, diminishing work output and/or rising the energy required to perform the cycle, reducing efficiency. For a typical engine the input energy is the heat absorbed from the hot bath, $\langle Q \rangle = \hbar\omega_0/2[\coth(\beta_1\hbar\omega_0/2) - \coth(\beta_2\hbar\omega_f/2)]$, with $\beta_{1,2} = 1/k_B T_{1,2}$ and k_B the Boltzmann constant. Since the shortcut does not affect the heat absorbed, it may seem that the efficiency is not affected. Our STA engine, however, is not a typical engine, as the expansion of the piston (in our case the trap expansion) is externally driven rather than being a consequence of the push by the hot working medium. The compression is similarly externally driven with a cost. Thus, the energy used to generate the external driving in eq. (9) constitutes an extra energy demand. We thus redefine the efficiency as microscopic work output divided by the cost¹

$$\eta = \frac{\langle W_m^{\text{comp}} \rangle + \langle W_m^{\text{exp}} \rangle}{\langle Q \rangle + W_T^{\text{exp}} + W_T^{\text{comp}}}, \quad (13)$$

¹Alternative definitions with different physical contents may be also worth considering elsewhere, for example $\eta = (W_T^{\text{comp}} + W_T^{\text{exp}})/\langle Q \rangle$ would give, for the setup and the fast protocols in this work, negative efficiencies instead of vanishing ones.

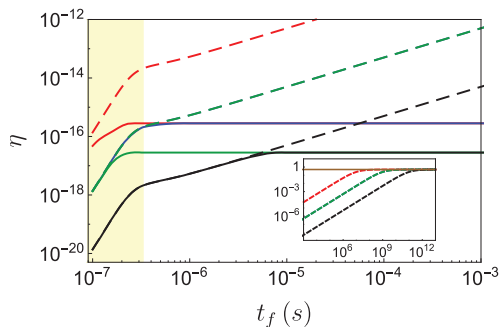


Fig. 3: Efficiency of the harmonic Otto cycle in eq. (13) for $\mu = -1$ (solid lines) and for $\mu = 1$ (dashed lines), *vs.* final times with temperatures $T_1 = 0.5$ K and $T_2 = 0.05$ K. Different colors correspond to: $R = 3 \Omega$, $C = 1$ nF (red); $R = 3 \Omega$, $C = 10$ nF (green); $R = 300 \Omega$, $C = 1$ nF (blue); $R = 300 \Omega$, $C = 10$ nF (black). The inset shows the efficiencies ($\mu = 1$) for longer times, converging to the conventional Otto efficiency (see the main text). The yellow shadowed area corresponds to final times where $\dot{\omega}/\omega^2 < 1$ at all times.

which is negligible ($\eta \approx 0$) for the protocol durations in which STA are of interest due to the scale difference between the working medium and the control. For slower and slower processes (see fig. 3), the dissipation in the control decreases and the efficiency increases thereof, together with a diminishing microscopic power output. If $\mu = -1$, as considered so far, the efficiency increase saturates at the reversible work to charge and discharge the capacitor. For a $\mu = 1$ setting (full regeneration), there is a crossover to a linear growth with t_f around the final time for which $\dot{\omega}/\omega^2 > 1$ during the process, since the dissipated energy diminishes as $\sim t_f^{-1}$, consistently with Landauer’s prediction for long times. Finally it reaches the conventional efficiency of the reversible Otto cycle $\eta = (\langle W_m^{\text{comp}} \rangle + \langle W_m^{\text{exp}} \rangle) / \langle Q \rangle$, as the total work becomes negligible compared with the heat input.

To calculate the engine performance criteria we use the microscopic work in the numerators. Along the cycle the gauge contributions to the microscopic work in each power stroke exactly cancel each other, making engine microscopic power and efficiency truly physical quantities whether we use or do not use the “physical gauge” provided by the experiment. This effect is similar to what happens with the Jarzynski inequality [42], also given in terms of inclusive work.

The idea of finding the optimal time path for the motion of the piston has been present in the field of finite-time thermodynamics for long [43]. However, already Andresen *et al.* pointed out that such trajectory may be optimal for some performance criterion but detrimental for others [9], as we see here in a clear and extreme way.

Discussion and conclusions. – We have studied the energetic cost of performing fast STA expansions/compressions for an ion in a Paul trap. In the context of an Otto cycle, the inclusion of this cost in the “debit” represented by the denominator of the efficiency implies

a vanishing energetic efficiency. The result mirrors the paradigm that slow reversible engines provide maximal efficiencies and zero power. Here the opposite result holds: for the fast STA engine the efficiency vanishes, but microscopic power is enhanced. These findings beg for a more speculative extrapolation and discussion of potential implications in a broader context, beyond the specific model. We shall thus indulge now into arguments that intend to be reasonable rather than based on a formal generic analysis, and suggestive of further research.

A first, preliminary observation is that STA processes on a microscopic system are, in standard applications and from the point of view of the microscopic system, externally driven processes which involve a *semiclassical* Hamiltonian that depends on time-dependent classical parameters, *i.e.*, with a given value at any time. (Applications of STA to optical devices are exceptional since, in the effective Hamiltonian, the position along the optical device plays the role of time, see, *e.g.*, [44] and [2]). The different STA techniques design the time dependence of these classical parameters to take the control-dependent quantum system to the same results of slow adiabatic driving. The semiclassical nature of the Hamiltonian implies a macroscopic object or apparatus that determines the small system dynamics but, at the same time, is quite insensitive to it. These are the conditions in our model and we expect this scenario to be, if not universal, broadly applicable. Even if friction for the microscopic, primary object is evaded by the STA process, changing the classical parameters with the necessary speed involves an energy cost which, to be sure, is system dependent, but will lead to increased macroscopic dissipation for faster speeds. Power input will be required to change inertias of the control parameters and fight dissipation losses. Smart designs for specific systems might minimize the role of inertia and benefit from regeneration mechanisms ($\mu \approx 1$), but never to the point of achieving perpetual cyclic motion of the classical parameters for free. This is quite a fundamental feature that can hardly be ignored when doing energy accounting. A cornerstone of finite-time thermodynamics is that processes without dissipation do not occur in nature if performed in finite time. In particular, the scale difference between macroscopic energy costs, even if small, and the microscopic energies involved makes the prospect for an energetically efficient cycle quite challenging. It also challenges scalability, *i.e.*, the idea that a device that combines many STA quantum engines may outperform a classical engine.

We do not discard the possibility of systems and “sweet spots” where energy balances may be not so unfavorable. Also, a vanishing or small energy efficiency is not necessarily a problem depending on the aim of the STA process. If we are interested in fast adiabatic-like ion cooling by expansion, for example, the energy cost may be worth paying. As for quantum engines, it might be the case that the “quality” of the microscopic work achieved, *i.e.*, the degrees of freedom put in motion when it functions,

is worth the energy expense. A known example of a relatively inefficient but extremely useful device is the laser.

There is also room to explore alternatives to some of the premises applied so far. The microscopic/macrosopic divergence of scales might be absent in some systems. A quantum and macrosopic primary system is a route to explore [2], possibly at the price of making the STA protocol state dependent.

As already stated, the device studied here differs fundamentally from a typical engine. In a typical engine the heated or cooled down working medium moves the piston; in our STA quantum engine, the motion of the element that plays the role of the piston, the harmonic potential, is not at all a consequence of the dynamics of the ion, but an externally controlled evolution which consumes energy. Let us mention in this regard that quantum autonomous engines replicate the behavior of typical engines, because the controller is not driven but it evolves under the action of a time-independent Hamiltonian and the baths. In contrast to our STA engine, there is no need of power input to drive the controller. An experimental implementation was presented in [45]. Here the challenge is to apply STA to a system without time dependence in the Hamiltonian. The work on optics could be a reference about how to do that, this is quite an open and nontrivial issue.

We have also limited the analysis and discussion so far mostly to the power strokes but STA have also been proposed to accelerate the thermalization processes in Markovian [46,47] or non-Markovian regimes [48]. Corresponding energy consumptions should be studied.

We thank A. POLKOVNIKOV for commenting on the paper. This work was supported by the Basque Country Government (Grant No. IT986-16) and PGC2018-101355-B-I00 (MCIU/AEI/FEDER,UE).

Appendix: exclusive power by external force. – Here we prove that the expression in eq. (6) of the main text can be generalized to any system whose dissipation is proportional to the velocity squared, and thus describable by a Hamiltonian complemented by a Rayleigh dissipation function $\mathcal{F} = \frac{1}{2}\gamma\dot{q}^2$. We do it for one dimension in a classical setting, but it can be extended to higher dimensions. We start by separating the total Hamiltonian into the unperturbed system and the external, time-dependent force term, $H(q, p_q, t) = H_0(q, p_q) - F(t)q$. The rate of change of the unperturbed Hamiltonian then reads

$$\frac{dH_0}{dt} = \frac{dH}{dt} + \dot{F}q + F\dot{q}.$$

Rewriting the time derivative of the total Hamiltonian,

$$\frac{dH}{dt} = \frac{\partial H}{\partial t} + \frac{\partial H}{\partial q}\dot{q} + \frac{\partial H}{\partial p}\dot{p},$$

and then using modified Hamilton equations, $\dot{q} = \partial H/\partial p_q$ and $\dot{p}_q = -\partial H/\partial q - \partial \mathcal{F}/\partial \dot{q}$, we get

$$\frac{dH_0}{dt} = \frac{\partial H}{\partial t} - \dot{q}\frac{\partial \mathcal{F}}{\partial \dot{q}} + \dot{F}q + F\dot{q}.$$

Notice that the only explicitly time-dependent element of the Hamiltonian is the external force, and thus $\partial H/\partial t = -\dot{F}q$. Finally, performing the derivative of the Rayleigh function and reordering the terms, we find

$$\frac{dH_0}{dt} + \gamma\dot{q}^2 = F\dot{q}.$$

REFERENCES

- [1] TORRONTGUEI E., IBÁÑEZ S., MARTÍNEZ-GARAOT S., MODUGNO M., DEL CAMPO A., GUÉRY-ODELIN D., RUSCHHAUPT A., CHEN X. and MUGA J. G., *Shortcuts to Adiabaticity, Advances In Atomic, Molecular, and Optical Physics*, Vol. **62** (Elsevier) 2013.
- [2] GUÉRY-ODELIN D., RUSCHHAUPT A., KIELY A., TORRONTGUEI E., MARTÍNEZ-GARAOT S. and MUGA J. G., preprint arXiv:1904.08448v1, to be published in *Rev. Mod. Phys.* (2019).
- [3] KOSLOFF R. and REZEK Y., *Entropy*, **19** (2017) 136.
- [4] ABAH O., ROSSNAGEL J., JACOB G., DEFFNER S., SCHMIDT-KALER F., SINGER K. and LUTZ E., *Phys. Rev. Lett.*, **109** (2012) 203006.
- [5] CHEN X., RUSCHHAUPT A., SCHMIDT S., DEL CAMPO A., GUÉRY-ODELIN D. and MUGA J. G., *Phys. Rev. Lett.*, **104** (2010) 063002.
- [6] SCHAFF J.-F., SONG X.-L., VIGNOLO P. and LABEYRIE G., *Phys. Rev. A*, **82** (2010) 033430.
- [7] SCHAFF J.-F., SONG X.-L., CAPUZZI P., VIGNOLO P. and LABEYRIE G., *EPL*, **93** (2011) 23001.
- [8] BOHM D., *Quantum Theory, Dover Books in Science and Mathematics* (Dover Publications) 1989, <https://books.google.es/books?id=-vhCqN2twGQC>.
- [9] ANDRESEN B., BERRY R. S., ONDRECHEN M. J. and SALAMON P., *Acc. Chem. Res.*, **17** (1984) 266.
- [10] KOSLOFF R. and FELDMANN T., *Phys. Rev. E*, **65** (2002) 055102.
- [11] PLASTINA F., ALECCE A., APOLLARO T. J. G., FALCONE G., FRANCICA G., GALVE F., LO GULLO N. and ZAMBRINI R., *Phys. Rev. Lett.*, **113** (2014) 260601.
- [12] DENG J., WANG Q.-H., LIU Z., HÄNGGI P. and GONG J., *Phys. Rev. E*, **88** (2013) 062122.
- [13] DEL CAMPO A., GOOLD J. and PATERNOSTRO M., *Sci. Rep.*, **4** (2014) 6208.
- [14] ABAH O. and LUTZ E., *Phys. Rev. E*, **98** (2018) 032121.
- [15] SALAMON P., ANDRESEN B., HOFFMANN K. H., NULTON J. D., SEGALL A. M. and ROHWER F. L., *Proceedings of the 240 Conference: Science's Great Challenges, Advances in Chemical Physics Series*, Vol. **157** (Wiley) 2014, p. 43.
- [16] CHEN X. and MUGA J. G., *Phys. Rev. A*, **82** (2010) 053403.
- [17] SANTOS A. C. and SARANDY M. S., *Sci. Rep.*, **5** (2015) 15775.
- [18] SANTOS A. C., SILVA R. D. and SARANDY M. S., *Phys. Rev. A*, **93** (2016) 012311.

- [19] ZHENG Y., CAMPBELL S., DE CHIARA G. and POLETTI D., *Phys. Rev. A*, **94** (2016) 042132.
- [20] FUNO K., ZHANG J.-N., CHATOU C., KIM K., UEDA M. and DEL CAMPO A., *Phys. Rev. Lett.*, **118** (2017) 100602.
- [21] BRAVETTI A. and TAPIAS D., *Phys. Rev. E*, **96** (2017) 052107.
- [22] CALZETTA E., *Phys. Rev. A*, **98** (2018) 032107.
- [23] HERRERA M., SARANDY M. S., DUZZIONI E. I. and SERRA R. M., *Phys. Rev. A*, **89** (2014) 022323.
- [24] COULAMY I. B., SANTOS A. C., HEN I. and SARANDY M. S., *Front. ICT*, **3** (2016) 19.
- [25] CAMPBELL S. and DEFFNER S., *Phys. Rev. Lett.*, **118** (2017) 100601.
- [26] TORRONTGUEI E., LIZUAIN I., GONZÁLEZ-RESINES S., TOBALINA A., RUSCHHAUPT A., KOSLOFF R. and MUGA J. G., *Phys. Rev. A*, **96** (2017) 022133.
- [27] TOBALINA A., ALONSO J. and MUGA J. G., *New J. Phys.*, **20** (2018) 065002.
- [28] ELOUARD C. and JORDAN A. N., *Phys. Rev. Lett.*, **120** (2018) 260601.
- [29] BARRA F., *Sci. Rep.*, **5** (2015) 14873.
- [30] BONANÇA M. V., preprint arXiv:1809.09163 (2018).
- [31] DEFFNER S., *Entropy*, **20** (2018) 875.
- [32] CAMPISI M., HÄNGGI P. and TALKNER P., *Rev. Mod. Phys.*, **83** (2011) 771.
- [33] BOCHKOV G. and KUZOVLEV Y. E., *Zh. Eksp. Teor. Fiz.*, **72** (1977) 238.
- [34] HOROWITZ J. and JARZYNSKI C., *J. Stat. Mech.: Theory Exp.*, **2007** (2007) P11002.
- [35] GIBBS J. W., *Elementary Principles in Statistical Mechanics* (Cambridge University Press) 1902.
- [36] COHEN-TANNOUJDI C., DIU B. and LALOE F., *Quantum Mechanics* (Wiley) 1991.
- [37] GOLDSTEIN H., POOLE C. and SAFKO J., *Classical Mechanics, Addison-Wesley Series in Physics* (Addison Wesley) 2002, <https://books.google.es/books?id=EE-wQgAACAAJ>.
- [38] FÜRST H. A., GOERZ M. H., POSCHINGER U. G., MURPHY M., MONTANGERO S., CALARCO T., SCHMIDT-KALER F., SINGER K. and KOCH C. P., *New J. Phys.*, **16** (2014) 075007.
- [39] TALKNER P., LUTZ E. and HÄNGGI P., *Phys. Rev. E*, **75** (2007) 050102.
- [40] VILAR J. M. G. and RUBI J. M., *Phys. Rev. Lett.*, **100** (2008) 020601.
- [41] LANDAUER R., *Appl. Phys. Lett.*, **51** (1987) 2056.
- [42] JARZYNSKI C., *Phys. Rev. Lett.*, **78** (1997) 2690.
- [43] MOZURKEWICH M. and BERRY R. S., *Proc. Natl. Acad. Sci. U.S.A.*, **78** (1981) 1986.
- [44] MARTÍNEZ-GARAOT S., MUGA J. G. and TSENG S.-Y., *Opt. Express*, **25** (2017) 159.
- [45] ROSSNAGEL J., DAWKINS S. T., TOLAZZI K. N., ABAH O., LUTZ E., SCHMIDT-KALER F. and SINGER K., *Science*, **352** (2016) 325.
- [46] MARTÍNEZ I. A., PETROSYAN A., GUÉRY-ODELIN D., TRIZAC E., BOWLER R. and CILIBERTO S., *Nat. Phys.*, **12** (2016) 843.
- [47] DANN R., TOBALINA A. and KOSLOFF R., *Phys. Rev. Lett.*, **122** (2019) 250402.
- [48] VILLAZON T., POLKOVNIKOV A. and CHANDRAN A., *Phys. Rev. A*, **100** (2019) 012126.

Fast state and trap rotation of a particle in an anisotropic potential

I Lizuain¹ , A Tobalina², A Rodriguez-Prieto³ and J G Muga²

¹ Department of Applied Mathematics, University of the Basque Country UPV/EHU, Donostia-San Sebastián, Spain

² Department of Physical Chemistry, University of the Basque Country UPV/EHU, Apdo. 644, Bilbao, Spain

³ Department of Applied Mathematics, University of the Basque Country UPV/EHU, Bilbao, Spain

E-mail: ion.lizuain@ehu.eus

Received 30 May 2019, revised 6 September 2019

Accepted for publication 2 October 2019

Published 21 October 2019



Abstract

We study the dynamics of a quantum or classical particle in a two-dimensional rotating anisotropic harmonic potential. By a sequence of symplectic transformations for constant rotation velocity we find uncoupled normal generalized coordinates and conjugate momenta in which the Hamiltonian takes the form of two independent harmonic oscillators. The decomposition into normal-mode dynamics enables us to design fast trap-rotation processes to produce a rotated version of an arbitrary initial state, when the two normal frequencies are commensurate.

Keywords: symplectic transformations, quantum control, atom and ion trapping

(Some figures may appear in colour only in the online journal)

1. Introduction

Motivated by existing or developing quantum technologies, much work is currently being devoted to control the motional dynamics of quantum systems. Basic operations such as shuttling, expansions/compressions, merging and separation of atom or ion chains, or rotations of the quantum states are needed to implement interferometers, quantum information applications, or quantum thermodynamical devices. Performing fast operations that do not leave residual excitations is generically of interest not only to save time but to avoid decoherence as well.

Shortcuts to adiabaticity (STA) are proposed as a set of efficient techniques to design such operations [1, 2]. For two or more effective dimensions, shortcut design, by inverse

engineering the control parameters using invariants of motion, is much facilitated by finding *dynamical normal modes* [3]. These modes are independent harmonic motions in the regime of small oscillations corresponding in general to time-dependent harmonic oscillators. Studies on different operations on trapped ions [3–9] made clear that it is not always possible to find a point transformation (a transformation in which the new coordinates only depend on the old ones and not on old momenta) that leads to independent normal modes. The condition that allows to find a point transformation was finally given in [10] for two-dimensional (2D) Hamiltonians: the effective potential can be scaled or translated but it should not rotate. Thus the rotation of a 2D anisotropic trap is the paradigmatic model in which such point transformation cannot be made and it was left as an open question if more general transformations could be used to speed up the rotation [10]. The inertial effect due to the trap rotation can be formally compensated by an effective angular momentum term [10, 11] to leave the particle at rest in the rotating frame. This term though may be difficult to implement, for example if the particle is not charged, so we consider in this paper that the only manipulation available is the rotation of the trap itself, without any additional force. STA for simple 1D-trap rotations, without compensation terms, were described in [8] but STA for the more realistic 2D anisotropic trap had not been described.

The goal of this work is to perform a rotation as represented schematically in figure 1 in the lab frame of coordinates x, y : the trap is at rest for $t < 0$; then it is rotated up to time T ; and finally it remains again at rest for $t > T$. The trap rotation must be designed such that the state at time T is exactly the rotated version of the initial state at time $t = 0$, *for all possible initial states*. Equivalently, from the point of view of the rotating frame, the objective is to get at time T the same state that was prepared at time 0, regardless of what that state may be.

Rotations of condensates or of a few particles are of interest for different reasons, such as reordering chains, redirecting, squeezing [8], or creating artificial magnetism [12, 13]. Here we treat the simplest case of a single particle in a rotating 2D trap. The operation would be instrumental in driving atoms through corners and junctions in a scalable quantum processor [14, 15], and may be regarded as a first step towards the more difficult problem of rotating ion chains [15–17], which would facilitate scalability in linear traps, and be useful to rearrange the chain, e.g. to locate a cooling ion at the right position in the chain [17]. Rotated states have other applications in sensing, metrology, and fundamental physics studies [18].

The treatment and transformations are done first in a classical setting. However, since we deal with a harmonic anisotropic trap the results can be translated into quantum mechanics rather directly. After setting the model in section 2, the independent normal modes will be first defined and characterized by normal frequencies in section 3. Section 4 analyzes the fast rotations that may be achieved at certain process times for configurations in which the normal frequencies are commensurate. The minimal time is identified, examples are given, and a stability analysis is carried out. Finally, section 5 discusses some open questions.

2. Physical model

Our starting point is the Hamiltonian of a particle of mass m in a 2D anisotropic harmonic potential with axial (angular) frequencies ω_1 and ω_2 , which rotates around the z axis perpendicular to the trap plane by an angle θ with an angular velocity $\dot{\theta}$, see figure 1 (dots hereafter represent time derivatives). In the rotating frame of coordinates $\{\tilde{q}_1, \tilde{q}_2\}$ and momenta $\{\tilde{p}_1, \tilde{p}_2\}$ the Hamiltonian is given by, see appendix A,

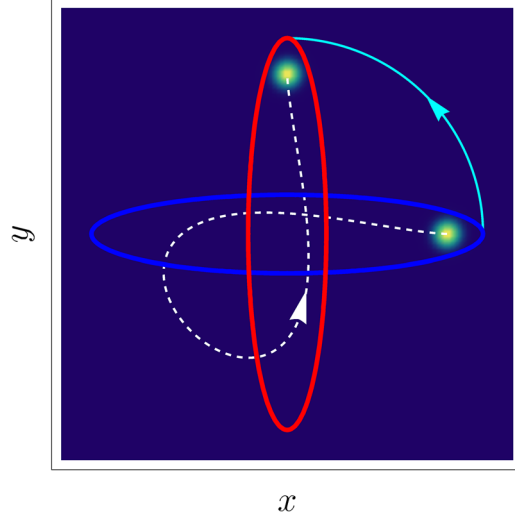


Figure 1. Trap rotation in the lab frame (solid line arrow) and particle dynamics (dashed line arrow). The trap is at rest for $t < 0$ (horizontal ellipse); then it is rotated by $\pi/2$ from $t = 0$ to $t = T$; and finally it remains again at rest for $t > T$ (vertical ellipse). The trap rotation is designed such that the state at time T is the rotated version of the initial state, for all possible—classical or quantum—initial states. Just one of them—chosen arbitrarily—is depicted. The dashed line is the trajectory of the state center along the trap rotation process.

$$H = \frac{\tilde{p}_1^2}{2m} + \frac{\tilde{p}_2^2}{2m} + \frac{1}{2}m\omega_1^2\tilde{q}_1^2 + \frac{1}{2}m\omega_2^2\tilde{q}_2^2 - \dot{\theta}L_z, \quad (1)$$

where $L_z = \tilde{q}_1\tilde{p}_2 - \tilde{q}_2\tilde{p}_1$. H has the form of two harmonic oscillators coupled by an angular momentum L_z that accounts for the inertial effects [19].

By introducing the dimensionless coordinates and momenta

$$q_j = \sqrt{\frac{m\omega_j}{\hbar}}\tilde{q}_j, \quad p_j = \frac{\tilde{p}_j}{\sqrt{m\hbar\omega_j}}, \quad (2)$$

the Hamiltonian (1) can be written ($\hbar = 1$ hereafter) as

$$H = \frac{\omega_1}{2}(p_1^2 + q_1^2) + \frac{\omega_2}{2}(p_2^2 + q_2^2) - \dot{\theta}\left(\frac{1}{\eta}q_1p_2 - \eta q_2p_1\right), \quad (3)$$

where $\eta = \sqrt{\omega_1/\omega_2}$.

This rotating frame Hamiltonian depends only on the angular velocity $\dot{\theta}$ as a control parameter. We shall consider, except in the final discussion, a constant rotation velocity, i.e. a linear-in-time angle $\theta(t) = \dot{\theta}t$ from $t = 0$ to $t = T$. Thus the Hamiltonian in the rotating frame is time independent during the rotation.

The Hamiltonian (3) can be written in compact matrix representation as the quadratic form

$$H = v^T A v, \quad (4)$$

where $v^T = (q_1, q_2, p_1, p_2)$ and A is the symmetric 4×4 matrix

$$A = \frac{1}{2} \begin{pmatrix} \omega_1 & 0 & 0 & -\frac{\dot{\theta}}{\eta} \\ 0 & \omega_2 & \eta\dot{\theta} & 0 \\ 0 & \eta\dot{\theta} & \omega_1 & 0 \\ -\frac{\dot{\theta}}{\eta} & 0 & 0 & \omega_2 \end{pmatrix}. \quad (5)$$

Our first goal is to find a transformation to a frame in which the corresponding effective Hamiltonian is uncoupled in both coordinates and momenta, or, using the four-dimensional matrix formalism, it is characterized by a diagonal matrix. To do so we will use the symplectic approach to canonical transformations.

3. Symplectic diagonalization

In the 4×4 matrix representation presented above, a canonical transformation will be defined by the transformation $v = SV$ to a new set of canonical coordinates $V^T = (Q_1, Q_2, P_1, P_2)$ provided S is a 4×4 symplectic matrix. A symplectic matrix S satisfies $S^T J S = J$, where J is the skew-symmetric matrix [19]

$$J = \begin{pmatrix} 0 & 0 & 1 & 0 \\ 0 & 0 & 0 & 1 \\ -1 & 0 & 0 & 0 \\ 0 & -1 & 0 & 0 \end{pmatrix}. \quad (6)$$

Note that its inverse is simply $J^{-1} = J^T = -J$. As well, $S^{-1} = J^{-1} S^T J$. 4×4 real symplectic matrices form the ten-dimensional symplectic group $Sp(4, \mathbb{R})$ [20]. Applying a symplectic (i.e. canonical) transformation to H amounts to rewrite it as

$$H = v^T A v = V^T (S^T A S) V. \quad (7)$$

Given the matrix A (5) we want to find a symplectic matrix $S \in Sp(4, \mathbb{R})$ so that $S^T A S$ is a diagonal matrix. Such a diagonalizing symplectic matrix S will always exist as long as A is a positive definite matrix. This result is known as Williamson's Theorem [21–23]. The positivity of A imposes an upper bound for the allowed rotation velocity in order to end up with an uncoupled effective Hamiltonian. In particular, the rotation velocity must satisfy

$$\dot{\theta} < \min(\omega_1, \omega_2). \quad (8)$$

For simplicity, and without loss of generality, we will consider $\omega_1 < \omega_2$ (or $0 < \eta < 1$) throughout this work. Therefore, the three (angular) frequencies in our model satisfy the conditions

$$\dot{\theta} < \omega_1 < \omega_2. \quad (9)$$

3.1. Constructing the S matrix

We will construct the S matrix after a four-step sequence of symplectic transformations.

- (i) The first transformation brings the matrix A (5) to a block diagonal form. This is achieved by the symplectic matrix

$$S_0 = \begin{pmatrix} 0 & 0 & -1 & 0 \\ 0 & 1 & 0 & 0 \\ 1 & 0 & 0 & 0 \\ 0 & 0 & 0 & 1 \end{pmatrix}, \quad (10)$$

which leads to

$$A_1 = S_0^T A S_0 = \frac{1}{2} \begin{pmatrix} \omega_1 & \eta\dot{\theta} & 0 & 0 \\ \eta\dot{\theta} & \omega_2 & 0 & 0 \\ 0 & 0 & \omega_1 & \frac{\dot{\theta}}{\eta} \\ 0 & 0 & \frac{\dot{\theta}}{\eta} & \omega_2 \end{pmatrix}. \quad (11)$$

This transformation is not a point transformation since S_0 mixes coordinates and momenta as already noted in [25].

- (ii) The second transformation diagonalizes one of the two blocks in A_1 . We choose the lower one in this case, the ‘momenta block’. If $\omega_1 > \omega_2$ had been assumed, at this point the upper block should be diagonalized instead of the lower one. This transformation is performed by the symplectic matrix

$$S_1 = \begin{pmatrix} 1 & \frac{\dot{\theta}}{\sqrt{\omega_1\omega_2}} & 0 & 0 \\ 0 & 1 & 0 & 0 \\ 0 & 0 & 1 & 0 \\ 0 & 0 & -\frac{\dot{\theta}}{\sqrt{\omega_1\omega_2}} & 1 \end{pmatrix} \quad (12)$$

and leads to

$$A_2 = S_1^T A_1 S_1 = \frac{1}{2} \begin{pmatrix} \omega_1 & 2\eta\dot{\theta} & 0 & 0 \\ 2\eta\dot{\theta} & \frac{3\dot{\theta}^2 + \omega_2^2}{\omega_2} & 0 & 0 \\ 0 & 0 & \frac{\omega_1 - \dot{\theta}^2}{\omega_1} & 0 \\ 0 & 0 & 0 & \omega_2 \end{pmatrix}. \quad (13)$$

- (iii) The third step transforms the block that it is already diagonal (the lower block in our case) into the identity. This is achieved by the symplectic matrix

$$S_2 = \begin{pmatrix} \sqrt{\frac{\omega_1^2 - \dot{\theta}^2}{\omega_1}} & 0 & 0 & 0 \\ 0 & \sqrt{\omega_2} & 0 & 0 \\ 0 & 0 & \sqrt{\frac{\omega_1}{\omega_1^2 - \dot{\theta}^2}} & 0 \\ 0 & 0 & 0 & \frac{1}{\sqrt{\omega_2}} \end{pmatrix}, \quad (14)$$

which transforms A_2 into

$$A_3 = S_2^T A_2 S_2 = \frac{1}{2} \begin{pmatrix} \omega_1^2 - \dot{\theta}^2 & 2\dot{\theta}\sqrt{\omega_1^2 - \dot{\theta}^2} & 0 & 0 \\ 2\dot{\theta}\sqrt{\omega_1^2 - \dot{\theta}^2} & 3\dot{\theta}^2 + \omega_2^2 & 0 & 0 \\ 0 & 0 & 1 & 0 \\ 0 & 0 & 0 & 1 \end{pmatrix}. \quad (15)$$

The transformation requires $\omega_1 > \dot{\theta}$, which is consistent with equation (9).

(iv) Finally, a (formal) rotation of an angle α brings the upper block to a diagonal form, leaving the lower block unaltered,

$$S_3 = \begin{pmatrix} \cos \alpha & -\sin \alpha & 0 & 0 \\ \sin \alpha & \cos \alpha & 0 & 0 \\ 0 & 0 & \cos \alpha & -\sin \alpha \\ 0 & 0 & \sin \alpha & \cos \alpha \end{pmatrix}, \quad (16)$$

with the angle of rotation α given by

$$\tan 2\alpha = \frac{4\dot{\theta}\sqrt{\omega_1^2 - \dot{\theta}^2}}{\omega_1^2 - \omega_2^2 - 4\dot{\theta}^2}. \quad (17)$$

This last transformation, leads to our objective, a diagonal matrix

$$A_4 = S_3^T A_3 S_3 = \frac{1}{2} \begin{pmatrix} \Omega_1^2 & 0 & 0 & 0 \\ 0 & \Omega_2^2 & 0 & 0 \\ 0 & 0 & 1 & 0 \\ 0 & 0 & 0 & 1 \end{pmatrix}, \quad (18)$$

where the $\Omega_{1,2}$ are the normal mode frequencies with squares

$$\begin{aligned} \Omega_1^2 &= \dot{\theta}^2 + \frac{\omega_1^2 + \omega_2^2}{2} - \frac{1}{2} \sqrt{8\dot{\theta}^2 (\omega_1^2 + \omega_2^2) + (\omega_1^2 - \omega_2^2)^2}, \\ \Omega_2^2 &= \dot{\theta}^2 + \frac{\omega_1^2 + \omega_2^2}{2} + \frac{1}{2} \sqrt{8\dot{\theta}^2 (\omega_1^2 + \omega_2^2) + (\omega_1^2 - \omega_2^2)^2}, \end{aligned} \quad (19)$$

see a plot of these frequencies as a function of $\dot{\theta}$ in figure 2. These eigenfrequencies have been found before by Bialynicki-Birula using a different approach [24]. Our four-step method is sketched in [25], although the eigenfrequencies and explicit transformations were not given there.

3.2. Uncoupled Hamiltonian and normal modes

After the sequence of four different transformations, the symplectic matrix we were looking for can be written as (the product of symplectic matrices is symplectic)

$$S = S_0 S_1 S_2 S_3. \quad (20)$$

S diagonalizes the initial A matrix by the relation $A_4 = S^T A S$ and relates old coordinates and momenta in the rotating-frame and new coordinates and momenta in the transformed frame by the transformation $v = S V$ or

$$\begin{pmatrix} q_1 \\ q_2 \\ p_1 \\ p_2 \end{pmatrix} = S \begin{pmatrix} Q_1 \\ Q_2 \\ P_1 \\ P_2 \end{pmatrix}. \quad (21)$$

By inverting this relation, we can give explicit expressions for the new frame coordinates and momenta in terms of the original ones,

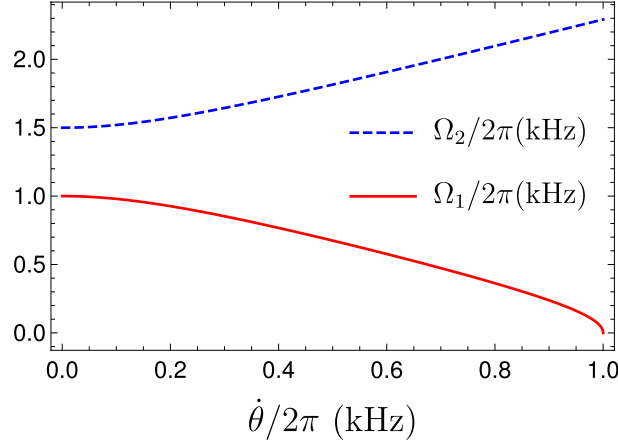


Figure 2. Normal mode frequencies Ω_1 (red solid) and Ω_2 (blue dashed) as a function of the rotation angular velocity for axial frequencies $\omega_1 = 2\pi \times 1$ kHz and $\omega_2 = 1.5\omega_1$. There is a maximum allowed $\dot{\theta}$, when one of the normal mode frequencies (Ω_1 in this case) becomes complex $\dot{\theta}_{\max} = \omega_1$, see equation (9). For a non-rotating trap ($\dot{\theta} = 0$), these frequencies are simply the axial frequencies $\omega_{1,2}$.

$$\begin{cases} Q_1 = q_2 \frac{\sqrt{\delta} \sin \alpha - \dot{\theta} \cos \alpha}{\sqrt{\delta \omega_2}} + p_1 \sqrt{\frac{\omega_1}{\delta}} \cos \alpha \\ Q_2 = q_2 \frac{\sqrt{\delta} \cos \alpha + \dot{\theta} \sin \alpha}{\sqrt{\delta \omega_2}} - p_1 \sqrt{\frac{\omega_1}{\delta}} \sin \alpha \\ P_1 = -q_1 \frac{\sqrt{\delta} \cos \alpha + \dot{\theta} \sin \alpha}{\sqrt{\omega_1}} + p_2 \sqrt{\omega_2} \sin \alpha \\ P_2 = q_1 \frac{\sqrt{\delta} \sin \alpha - \dot{\theta} \cos \alpha}{\sqrt{\omega_1}} + p_2 \sqrt{\omega_2} \cos \alpha \end{cases}, \quad (22)$$

with $\delta = \omega_1^2 - \dot{\theta}^2$, which makes clear that this is not a point transformation. The Hamiltonian written in normal-mode coordinates and momenta takes the simple form of two independent harmonic oscillators with normal frequencies $\Omega_{1,2}$,

$$H = v^T A v = V^T S^T A S V = V^T A_4 V = \frac{1}{2} (P_1^2 + P_2^2 + \Omega_1^2 Q_1^2 + \Omega_2^2 Q_2^2). \quad (23)$$

As discussed in appendix B, these transformations are identical for a quantum Hamiltonian and can be related to quantum unitary transformations. Therefore, the Hamiltonian (23) can be quantized by substituting the generalized coordinate and momenta by the corresponding operators. Since the Hamiltonian is quadratic, we may equivalently rely on a phase-space description of the quantum state dynamics in Wigner representation. The dynamics of the Wigner function is governed by a classical Liouville equation; equivalently, a phase-space point is driven by classical Hamiltonian dynamics.

4. Fast rotations

4.1. Commensurate anisotropic oscillator

The time evolution generated by the Hamiltonian (23) is governed by two independent harmonic oscillators. In this frame, the corresponding classical trajectories will be given by Lissajous-like orbits, that will only be closed when the ratio between the $\Omega_{1,2}$ frequencies is

a rational number, i.e. when they are commensurate. Let us suppose that $n_{1,2}$ are two integers ($1 \leq n_1 < n_2$). Then, if the condition

$$\frac{\Omega_2}{\Omega_1} = \frac{n_2}{n_1} \quad (24)$$

is satisfied, the full period of the dynamics is given by

$$T = \frac{2\pi n_1}{\Omega_1} = \frac{2\pi n_2}{\Omega_2}. \quad (25)$$

If a rotation is performed in a time T , the system will end up in the same initial state in the rotating frame: the first oscillator performs n_1 oscillations, and the second one n_2 full oscillations.

To perform a rotation of an angle $\theta_f = \dot{\theta}T$ (assuming an initial angle $\theta_i = 0$) at a constant angular velocity $\dot{\theta}$ in time T , the above relation may be written as

$$T = \frac{\theta_f}{\dot{\theta}} = \frac{2\pi n_1}{\Omega_1(\dot{\theta}, \omega_1, \omega_2)} = \frac{2\pi n_2}{\Omega_2(\dot{\theta}, \omega_1, \omega_2)}. \quad (26)$$

For some fixed values of θ_f , n_1 and n_2 , these equalities do not have a unique solution since there are two equations but three different parameters (rotation velocity $\dot{\theta}$, and frequencies ω_1 and ω_2). Using equation (26) we may write two of the frequencies in terms of a third one, for instance

$$\begin{aligned} \omega_1 &= \kappa_- \dot{\theta}, \\ \omega_2 &= \kappa_+ \dot{\theta}, \end{aligned} \quad (27)$$

where

$$\kappa_{\pm} = \left(-1 + \frac{2\pi^2 \delta_{\pm}}{\theta_f^2} \pm \frac{2\sqrt{\pi^4 \delta_-^2 - 2\pi^2 \delta_+ \theta_f^2 + \theta_f^4}}{\theta_f^2} \right)^{1/2} \quad (28)$$

with $\delta_{\pm} = n_1^2 \pm n_2^2$. Once one of the frequencies is fixed, the remaining two will be determined by equation (27). In the following, the value of the smallest axial frequency ω_1 will be fixed, but a similar analysis could be done if any of the two remaining ones is fixed: also of interest is the setting where ω_1 and ω_2 are given, i.e. we do not assume that their values can be controlled. Then $\dot{\theta}$ for different n_1, n_2 should be adjusted to satisfy the last equality in equation (26). Since T is fixed by the last two ratios in equation (26), only a set of discrete values of θ_f are allowed in this scenario.

For a given value of ω_1 , relation (27) determines $\dot{\theta}$ and ω_2 , and using equation (26) the time duration of the rotation operation is

$$T_{n_1, n_2} = \frac{\kappa_- \theta_f}{\omega_1}, \quad (29)$$

which, for some fixed values of ω_1 and θ_f , is just a function of the integers n_1 and n_2 . See some numerical values of $T_{1,2}$ for a $\pi/2$ rotation in table 1.

4.2. Fast rotations

In principle, the values of n_1 and n_2 can be chosen arbitrarily as long as $n_1 < n_2$: the time duration of a given rotation (for given θ_f and ω_1) will be completely determined by the factor κ_- .

Table 1. Some numerical values of the trapping frequencies ω_1 and ω_2 , rotation angular velocity $\dot{\theta}$ and time duration T of the rotation operation calculated according to equations (26)–(29). $\theta_f = \pi/2$, $n_1 = 1$, and $n_2 = 2$.

ω_1 (kHz)	ω_2 (kHz)	$\dot{\theta}$ (kHz)	$T_{1,2} = \theta_f/\dot{\theta}$ (ms)
$2\pi \times 1$	$2\pi \times 1.79$	$2\pi \times 0.23$	1.08
$2\pi \times 2$	$2\pi \times 3.59$	$2\pi \times 0.46$	0.54
$2\pi \times 5$	$2\pi \times 8.96$	$2\pi \times 1.16$	0.22
$2\pi \times 10$	$2\pi \times 17.93$	$2\pi \times 2.32$	0.11

As it is shown in figures 3(a) and (b), the fastest possible rotation (minimum value of κ_-) is found with the values $n_1 = 1$ and $n_2 \rightarrow \infty$. This means that the minimum rotation time T_{\min} corresponds to a single oscillation of the first (slow) normal mode oscillator and to infinitely many oscillations of the second one,

$$T_{\min} = T_{1,\infty} = \sqrt{\frac{\theta_f^2 + 4\pi^2}{\omega_1^2}}. \quad (30)$$

This minimal time corresponds to the $\omega_1 \ll \omega_2$ limit (i.e. an infinitely narrow trap) as shown in figure 3(c).

Of course this limit is an idealization and in practice ω_2 will have some maximal value. To illustrate features of a generic case ($n_2 \neq \infty$) we choose $n_1 = 1$ and $n_2 = 2$ in numerical calculations.

4.3. Time evolution of states and observables

In the reference system of the normal modes, $\{\mathcal{Q}_1, \mathcal{Q}_2\}$, a general wave function takes the form

$$\psi(\mathcal{Q}_1, \mathcal{Q}_2, t) = \sum_{j=0}^{\infty} \sum_{j'=0}^{\infty} c_{jj'} \phi_j^{(1)}(\mathcal{Q}_1) e^{-i\Omega_1(j+\frac{1}{2})t} \phi_{j'}^{(2)}(\mathcal{Q}_2) e^{-i\Omega_2(j'+\frac{1}{2})t}, \quad (31)$$

where the $c_{jj'}$ are constant coefficients set by the initial conditions and $\phi_j^{(1,2)}(\mathcal{Q}_{1,2})$ are the usual stationary eigenfunctions of the harmonic oscillators. If the rotation continues indefinitely, at a time $t + T$ with T given in equation (25), one gets

$$\begin{aligned} \psi(\mathcal{Q}_1, \mathcal{Q}_2, t + T) &= \sum_{j=0}^{\infty} \sum_{j'=0}^{\infty} c_{jj'} \phi_j^{(1)}(\mathcal{Q}_1) e^{-i\Omega_1(j+\frac{1}{2})(t+\frac{2\pi n_1}{\Omega_1})} \\ &\quad \times \phi_{j'}^{(2)}(\mathcal{Q}_2) e^{-i\Omega_2(j'+\frac{1}{2})(t+\frac{2\pi n_2}{\Omega_2})} \\ &= (-1)^{n_1+n_2} \psi(\mathcal{Q}_1, \mathcal{Q}_2, t), \end{aligned} \quad (32)$$

i.e. the wave function one period T earlier, with an overall phase that depends on $n_1 + n_2$. The quantum system is said to experience ‘exact revivals’ at intervals of T [26]. Here we are interested in setting $t = 0$ and the corresponding revival at T .

In the numerical examples the dynamics is solved entirely in a truncated Fock space for the interaction-free part (two harmonic oscillators) which is enlarged until converge is achieved.

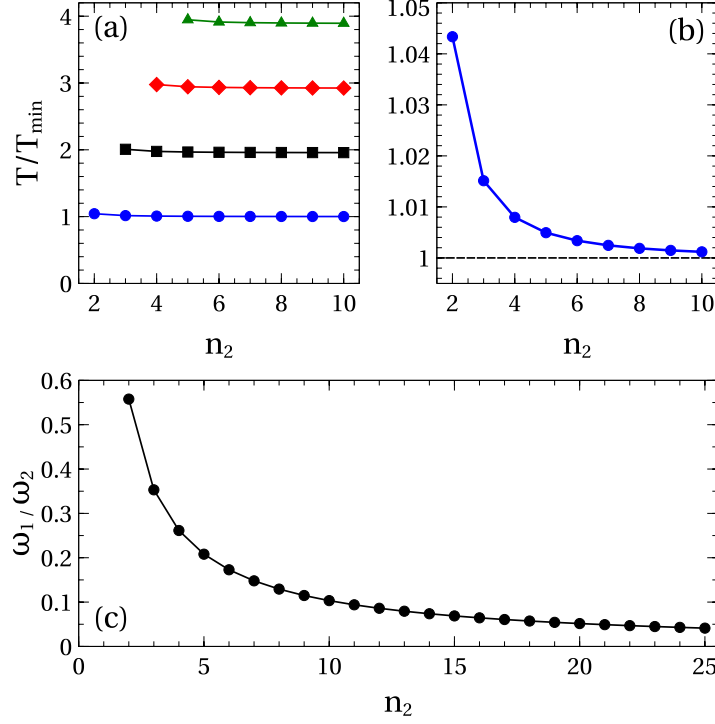


Figure 3. (a) Time T to perform a rotation of $\pi/2$ without final excitation as a function of n_2 for different values of n_1 : $n_1 = 1$ blue circles, $n_1 = 2$ black squares, $n_1 = 3$ red diamonds and $n_1 = 4$ green triangles. The fastest possible rotation corresponds to $n_1 = 1$ and $n_2 \rightarrow \infty$. (b) Closer look at the $n_1 = 1$ series. (c) Ratio between axial frequencies $\omega_1/\omega_2 = \kappa_-/\kappa_+$ for $n_1 = 1$. As n_2 increases the trap gets narrower. The fastest possible rotation, at the $n_2 \rightarrow \infty$ limit, occurs for an infinitely narrow trap $\omega_1 \ll \omega_2$.

4.3.1. Periodic orbits in the rotating frame. In the normal-mode frame, the classical trajectories or corresponding center of a wavepacket describe closed Lissajous orbits for commensurate normal frequencies. In the rotating frame we find also corresponding closed orbits.

To visualize them let us suppose that the system is initially in the two-mode coherent state $|\psi(0)\rangle = |\alpha_1, \alpha_2\rangle$. The state $|\alpha_1, \alpha_2\rangle$ may be expanded in terms of number states of the harmonic oscillators with frequencies $\omega_{1,2}$,

$$|\alpha_1, \alpha_2\rangle = e^{-\frac{1}{2}(|\alpha_1|^2 + |\alpha_2|^2)} \sum_{n_1, n_2=0}^{\infty} \frac{\alpha_1^{n_1} \alpha_2^{n_2}}{\sqrt{n_1! n_2!}} |n_1, n_2\rangle,$$

with $\alpha_j = |\alpha_j|e^{i\varphi}$ and

$$\langle q_1, q_2 | n_1, n_2 \rangle = \frac{e^{-\frac{q_1^2 + q_2^2}{2}} H_{n_1}(q_1) H_{n_2}(q_2)}{\sqrt{2^{n_1 + n_2} n_1! n_2! \pi}}, \quad (33)$$

where $H_n(q)$ is the n th order Hermite polynomial. The time-evolved two-mode coherent state in coordinate representation will be given by the wave function

$$\langle q_1, q_2 | \psi(t) \rangle = \langle q_1, q_2 | e^{-iHt} | \alpha_1, \alpha_2 \rangle. \quad (34)$$

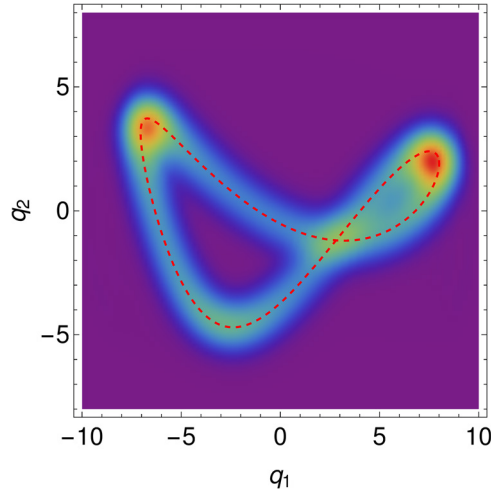


Figure 4. Wavepacket track $\mathcal{P}(q_1, q_2)$ of the two mode coherent state $|\alpha_1, \alpha_2\rangle$ for the values (initial conditions) $\alpha_1 = 8/\sqrt{2}$ and $\alpha_2 = 2/\sqrt{2}$ during a rotation of an angle of $\pi/2$. Red dashed line: corresponding classical trajectory with initial conditions $q_1(0) = \sqrt{2}|\alpha_1| = 8$, $q_2(0) = \sqrt{2}|\alpha_2| = 2$ and $p_1(0) = p_2(0) = 0$. The trap and rotation parameters are those in the first row of table 1. Dimensionless spatial coordinates q_1 and q_2 have been used as explained in the text.

By integrating the probability density over a full period T ,

$$\mathcal{P}(q_1, q_2) = \int_0^T |\langle q_1, q_2 | \psi(t) \rangle|^2 dt, \tag{35}$$

a track of the wave-packet is found, see figure 4, which is more intense where the motion is slow. The center of the wave-packet follows the classical closed Lissajous-like orbits, ending in its initial configuration after a full rotation is performed.

4.3.2. Mean number of excitations, survival probability. We will now consider the mean vibrational number as a function of time in the rotating frame,

$$\langle N(t) \rangle = \langle \psi(t) | a_1^\dagger a_1 + a_2^\dagger a_2 | \psi(t) \rangle, \tag{36}$$

where the creation and annihilation operators in each direction are defined in terms of position and momentum operators as usual,

$$a_j = \frac{1}{\sqrt{2}}(\hat{q}_j + i\hat{p}_j), \quad a_j^\dagger = \frac{1}{\sqrt{2}}(\hat{q}_j - i\hat{p}_j), \tag{37}$$

for $j = 1, 2$. In the first column of figure 5, the time evolution of the mean number of excitations during $\pi/2$ rotations designed without final excitation using the first row of table 1 ($n_1 = 1, n_2 = 2$) is shown for different initial states: the ground state of the non-rotating trap, an entangled state, and a coherent state. Interestingly, figure 5 (first column) demonstrates that the mean excitation can actually decrease, at least temporarily, with respect to the initial value. Of course for all states the final value coincides with the initial value.

The rotation process has been chosen so that the survival probability in the rotating frame $P(t) = |\langle \psi(t) | \psi(0) \rangle|^2$ satisfies the condition $P(0) = P(T)$, due to commensurability. In the second column of figure 5, the probability of finding the system in its initial state is calculated

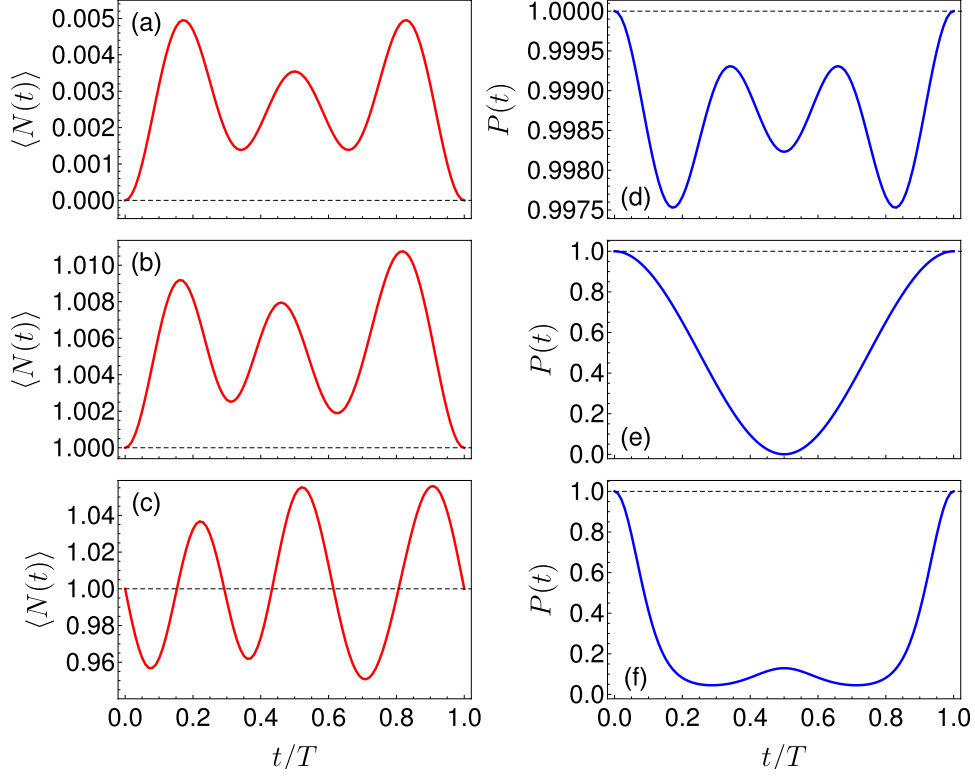


Figure 5. Time evolution of different observables during a $\theta_f = \pi/2$ rotation. In the left column the evolution of the average number of excitations $\langle N(t) \rangle$ is plotted as a function of time, while in the second the survival probability $P(t) = |\langle \psi(t) | \psi(0) \rangle|^2$ of finding the system in its initial state (in the rotating frame) is plotted. Different initial states are considered for each figure: in (a) and (d), the initial state is the ground state of a 2D oscillator $|v(0)\rangle = |0,0\rangle$ with $\langle N(0) \rangle = 0$. In (b) and (e), the initial state is an entangled state $|v(0)\rangle = \frac{1}{\sqrt{2}}(|0,1\rangle + |1,0\rangle)$ with $\langle N(0) \rangle = 1$. In (c) and (f), the initial state is a coherent state $|v(0)\rangle = |\alpha_1, \alpha_2\rangle$ with $\alpha_1 = \alpha_2 = 1/\sqrt{2}$ (i.e. a minimum uncertainty wave packet centered at $q_1 = q_2 = 1$ with mean number of excitations $\langle N(0) \rangle = |\alpha_1|^2 + |\alpha_2|^2 = 1$). Trap and rotation parameters are those in the first row of table 1.

for different initial quantum states. The revivals are seen clearly in all three cases. The survival of the coherent and entangled states decays at intermediate times much more severely than the one for the ground state. Indeed, a classical particle set initially at rest at the bottom of the trap would not be affected by the trap rotation.

4.4. Stability

As already pointed out in section 4.2, the fastest allowed rotations are found for $n_1 = 1$ and $n_2 \gg 1$, which imply very narrow quasi-1D traps with $\omega_2 \gg \omega_1$. However, fast rotations come with a price, since as n_2 increases the ideal result becomes more unstable. This can be intuitively understood: for larger n_2 the second normal oscillator oscillates faster so it is easier to

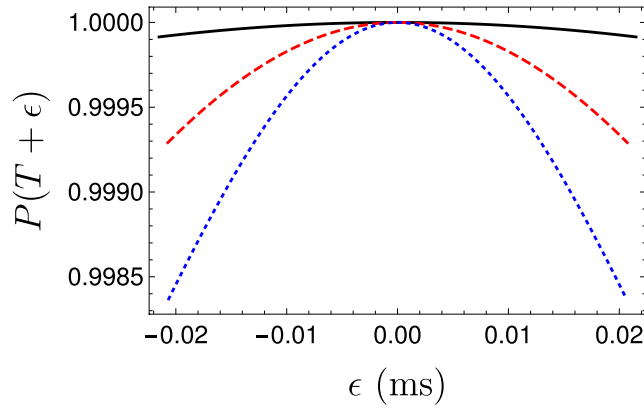


Figure 6. Stability when the rotation lasts $T + \epsilon$. The survival probability is plotted as a function of ϵ for the example shown in figure 5(d) ($\pi/2$ rotation of the ground state) for $n_1 = 1$ and different integer values of n_2 : $n_2 = 2$ (black-solid line), $n_2 = 5$ (red-dashed line), and $n_2 = 10$ (blue-dotted line).

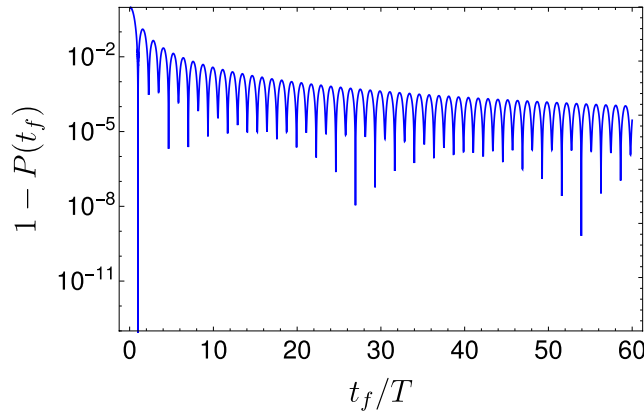


Figure 7. One minus the survival probability at final time t_f (logarithmic scale) in the rotating frame for a $\theta_f = \pi/2$ rotation versus the scaled total process time t_f/T , with $T = 1.08$ ms being the process time using our fast protocol. The initial state is the excited state $|0, 1\rangle$. The trap frequencies ω_1 and ω_2 are fixed with the values in the first row of table 1.

miss the exact final state due to some small timing error. This is confirmed in figure 6, which depicts the survival probability as a function ϵ , a small deviation from the nominal operation time T . For larger n_2 the survival becomes less robust.

This effect can be quantified by approximating the survival probability to second order in ϵ as

$$P(T + \epsilon) \approx 1 - \Delta H^2 \epsilon^2 \quad (38)$$

with

$$\Delta H^2 = \langle \psi(0) | H^2 | \psi(0) \rangle - \langle \psi(0) | H | \psi(0) \rangle^2. \quad (39)$$

ΔH^2 depends on the considered initial state as figure 5 (right column) illustrates. The survival probability of the ground state, in particular, decays with ϵ^2 at a rate

$$\Delta H^2 = \frac{\dot{\theta}^2(\omega_1 - \omega_2)^2}{4\omega_1\omega_2}, \quad (40)$$

which, for a given ω_1 , increases for faster rotations (larger $\dot{\theta}$ and ω_2).

4.5. Comparison with slow adiabatic rotations

An example to see how much faster the process may be compared to a slow adiabatic rotation is depicted in figure 7. The trap is set with the angular frequencies fixed for a $n_1 = 1, n_2 = 2$ configuration and a $\theta_f = \pi/2$ rotation, see the first line in table 1. The time $T = 1.08$ ms satisfying (26) is the scale used to compare the final error to find the ideal rotated state by keeping ω_1 and ω_2 fixed but varying the final process time t_f and therefore the rotation speed as $\dot{\theta} = \theta_f/t_f$. We use an initial state of interest in a quantum information scenario, $|0, 1\rangle$. This state is initially stationary and will remain stationary after the ideal rotation that takes a time $t_f = T$, which gives by construction a perfect fidelity. For some special larger times the conditions where t_f is an integer number of both normal-mode periods are almost (but not exactly) fulfilled. We note that a 10^{-4} error value for the upper envelop of the error curve needs about $t_f > 60T$.

5. Discussion

Controlling the motion of quantum particles is needed to manipulate them for fundamental science studies and to develop different quantum technologies. In particular, operations which are fast, robust, and do not leave residual excitations are typically preferred. Here we focused on rotating arbitrary states of a single particle in an anisotropic harmonic trap using the rotation speed and rotation time as the only control parameters. By ‘rotating’ a state here we mean to end at a time $t = T$ with a particle and trap configuration which is identical to the one at time $t = 0$ but rotated by some angle θ_f in the laboratory frame. As an inverse problem, even such a simple system and operation involves considerable complexities. Since normal modes cannot be found by a point transformation, we have first performed a non point (but canonical) transformation to find the normal modes for constant rotation speed. Based on the normal mode analysis we apply a protocol in which any initial state becomes its rotated version in the final trap. Minimal times are found and a stability analysis with respect to time errors is performed.

We may envision several worthwhile and natural extensions of this work such as considering anharmonicities, two or more interacting particles in the trap, or, to achieve further flexibility in the rotation times, time-dependent rotation speeds $\dot{\theta}(t)$. This time-dependence makes the $A(t)$ matrix in the Hamiltonian of the rotating frame time dependent, and following the steps in the main text and appendix B we may perform a time-dependent symplectic transformation and find that the interaction picture effective Hamiltonian will be given by $H_I = v^T[S^T(A - \dot{G})S]v$, where G is the real symmetric matrix that generates the symplectic matrix S , $S = e^{2JG}$, see appendix B. Finding the time-dependent symplectic transformation S that makes the 4×4 matrix $A' = S^T(A - \dot{G})S$ diagonal is a challenging open question, since it involves a highly non-linear system of coupled differential equations to determine the elements of G (and therefore S).

We cannot fail to point out an analogy between the structure of A' and the effective Hamiltonian used in superadiabatic iterations to achieve shortcuts [27, 28]. If S is set to diagonalize A , rather than the whole matrix A' , two uncoupling strategies are: to ignore the inertial term $\mathcal{I} = -S^T \dot{G} S$ because it is small (this is analogous to an adiabatic approximation), or to compensate it exactly with $-\mathcal{I}$ (this is analogous to counter-diabatic driving). However implementing such a compensating term is often difficult in practice, in this case it implies crossed operator terms. A third route is to apply the next ‘superadiabatic’ iteration, i.e. to find an S' that makes $S'^T A' S'$ diagonal, which produces a term $\mathcal{I}' = -S'^T \dot{G} S'$ in the new Hamiltonian. Further iterations would repeat the same scheme but they do not need to converge so there may be an optimal iteration. Alternatively the coupling term may be approximated to achieve convergence [29]. All this is very intriguing and will be explored elsewhere.

Acknowledgments

We are grateful to K Takahashi for discussions in the early stages of the work. This work was supported by the Basque Country Government (Grant No. IT986-16) and PGC2018-101355-B-I00 (MCIU/AEI/FEDER,UE).

Appendix A. Laboratory frame

The Hamiltonian for a particle of mass m in a two-dimensional anisotropic harmonic potential with axial frequencies ω_1 and ω_2 and with a time varying orientation angle $\theta(t)$ (i.e. which is rotating around the z axis with angular velocity $\dot{\theta}(t)$) is given in laboratory $\{x, y\}$ frame by

$$H_{\text{lab}} = \frac{p_x^2}{2m} + \frac{p_y^2}{2m} + \frac{m\omega_1^2}{2} [x \cos \theta(t) + y \sin \theta(t)]^2 + \frac{m\omega_2^2}{2} [-x \sin \theta(t) + y \cos \theta(t)]^2. \quad (\text{A.1})$$

Defining the rotated coordinates and momenta by the relations

$$\begin{pmatrix} \tilde{q}_1 \\ \tilde{q}_2 \end{pmatrix} = R(t) \begin{pmatrix} x \\ y \end{pmatrix}; \quad \begin{pmatrix} \tilde{p}_1 \\ \tilde{p}_2 \end{pmatrix} = R(t) \begin{pmatrix} p_x \\ p_y \end{pmatrix} \quad (\text{A.2})$$

with $R(t)$ being the usual rotation matrix

$$R(t) = \begin{pmatrix} \cos \theta(t) & \sin \theta(t) \\ -\sin \theta(t) & \cos \theta(t) \end{pmatrix}, \quad (\text{A.3})$$

the new Hamiltonian is given by

$$H = \frac{\tilde{p}_1^2}{2m} + \frac{\tilde{p}_2^2}{2m} + \frac{1}{2} m\omega_1^2 \tilde{q}_1^2 + \frac{1}{2} m\omega_2^2 \tilde{q}_2^2 - \dot{\theta} L_z, \quad (\text{A.4})$$

with $L_z = \tilde{q}_1 \tilde{p}_2 - \tilde{q}_2 \tilde{p}_1$. This last term, which couples coordinates and momenta, accounts for the inertial effects that arise due to the time-dependent canonical transformation applied.

Appendix B. Quantum unitary transformations

It is also instructive to set a quantum description by means of a unitary transformation of the Hamiltonian. As it is well known from group theory, the generators of symplectic matrices

are symmetric matrices in the sense that any symplectic matrix S can be written in terms of its generator G as $S = e^{2JG}$, G being a symmetric matrix and J the symplectic matrix (6). Let us define the unitary operator

$$\mathcal{U} = e^{iv^T G v}, \quad (\text{B.1})$$

where v^T is now regarded as a vector of operators $v^T = (\widehat{q}_1, \widehat{q}_2, \widehat{p}_1, \widehat{p}_2)$. The unitarily transformed, interaction picture Hamiltonian will be given by

$$H_I = \mathcal{U} H \mathcal{U}^\dagger + i\dot{\mathcal{U}} \mathcal{U}^\dagger, \quad (\text{B.2})$$

where the last term arises due to the possible time dependence of the unitary transformation. For a quadratic Hamiltonian with the form $H = v^T A v$, see equation (4), and the unitary operator \mathcal{U} defined by (B.1), it can be shown that the above effective Hamiltonian is given by

$$H_I = v^T [S^T (A - \dot{G}) S] v. \quad (\text{B.3})$$

Details of this calculation are given in appendix C.

In a time independent scenario, where $\dot{G} = \dot{S} = 0$, we have an uncoupled (i.e. without cross terms) effective interaction picture Hamiltonian

$$H_I = v^T (S^T A S) v \quad (\text{B.4})$$

since $S^T A S$ is a diagonal matrix as shown in section 3. Indeed, the inverse unitary transformation $\mathcal{U}^\dagger(\dots)\mathcal{U}$ maps all the components v_j to V_j ,

$$\mathcal{U}^\dagger v_j \mathcal{U} = (S^{-1} v)_j = V_j, \quad (\text{B.5})$$

so that H is recovered,

$$H = \mathcal{U}^\dagger H_I \mathcal{U} = v^T (S^T A S) v = v^T A v. \quad (\text{B.6})$$

In summary, the same symplectic transformation that diagonalizes the classical Hamiltonian matrix provides as well a quantum Hamiltonian written as a sum of quadratic operators without cross terms.

If the symplectic transformation S depends on time, the extra term $-v^T (S^T \dot{G} S) v$ has to be included in the effective Hamiltonian to account for the inertial effects. For a time dependent transformation, one would have to symplectically diagonalize the full matrix $A - \dot{G}$.

Appendix C. Detailed calculation of equation (B.3)

Let \mathcal{A} and \mathcal{B} be two real symmetric matrices. Taking into account that the position-momentum commutators $[q_j, p_k] = i\delta_{jk}$ can be summarized as $[v_j, v_k] = iJ_{jk}$, one can find the relation

$$\sum_{n=0}^{\infty} \frac{[v^T \mathcal{B} v, v^T \mathcal{A} v]_n}{n!} = v^T (e^{2i\mathcal{B}J} \mathcal{A} e^{-2iJ\mathcal{B}}) v, \quad (\text{C.1})$$

where $[v^T \mathcal{B} v, v^T \mathcal{A} v]_n = [v^T \mathcal{B} v, v^T \mathcal{B} v, \dots, v^T \mathcal{B} v, v^T \mathcal{A} v]$ denotes the n th nested commutator between the involved operators. Using this result, the two terms in the effective Hamiltonian (B.2) will be calculated separately:

- (i) The first term $\mathcal{U} H \mathcal{U}^\dagger$ can be calculated using the Baker–Campbell–Hausdorff (BCH) formula and the previous result (C.1) to sum the series expansion. For the unitary operator defined in (B.1) and a Hamiltonian with the form (4) we have

$$\begin{aligned} \mathcal{U}\mathcal{H}\mathcal{U}^\dagger &= e^{iv^T Gv} (v^T A v) e^{-iv^T Gv} = \sum_{n=0}^{\infty} \frac{[iv^T Gv, v^T A v]_n}{n!} \\ &= v^T (e^{-2GJ} A e^{2JG}) v = v^T (S^T A S) v. \end{aligned} \quad (\text{C.2})$$

(ii) To calculate the second term $i\dot{\mathcal{U}}\mathcal{U}^\dagger$, we must be careful when computing the time derivative of \mathcal{U} , since it involves not-commuting operators [30],

$$\begin{aligned} i\dot{\mathcal{U}}\mathcal{U}^\dagger &= i \sum_{n=0}^{\infty} \frac{[iv^T Gv, iv^T \dot{G}v]_n}{n!} = -v^T (e^{-2GJ} \dot{G} e^{2JG}) v \\ &= -v^T (S^T \dot{G} S) v. \end{aligned} \quad (\text{C.3})$$

Here, again, equation (C.1) has been used to sum the series expansion.

The sum of these two terms leads finally to the interaction picture effective Hamiltonian (B.3)

$$H_I = \mathcal{U}\mathcal{H}\mathcal{U}^\dagger + i\dot{\mathcal{U}}\mathcal{U}^\dagger = v^T [S^T (A - \dot{G}) S] v. \quad (\text{C.4})$$

ORCID iDs

I Lizuain  <https://orcid.org/0000-0001-9207-4493>

References

- [1] Torrontegui E *et al* 2013 *Adv. At. Mol. Phys.* **62** 117
- [2] Guéry-Odelin D, Ruschhaupt A, Kiely A, Torrontegui E, Martínez-Garaot S and Muga J G 2019 *Rev. Mod. Phys.* (accepted) (arXiv: [1904.08448](https://arxiv.org/abs/1904.08448))
- [3] Palmero M, Bowler R, Gaebler J P, Leibfried D and Muga J G 2014 *Phys. Rev. A* **90** 053408
- [4] Palmero M, Torrontegui E, Guéry-Odelin D and Muga J G 2013 *Phys. Rev. A* **88** 053423
- [5] Palmero M, Martínez-Garaot S, Alonso J, Home J P and Muga J G 2015 *Phys. Rev. A* **91** 053411
- [6] Palmero M, Martínez-Garaot S, Poschinger U G, Ruschhaupt A and Muga J G 2015 *New J. Phys.* **17** 093031
- [7] Lu X J, Palmero M, Ruschhaupt A, Chen X and Muga J G 2015 *Phys. Scr.* **90** 074038
- [8] Palmero M, Wang S, Guéry-Odelin D, Li J-S and Muga J G 2016 *New J. Phys.* **18** 043014
- [9] Palmero M, Martínez-Garaot S, Leibfried D, Wineland D J and Muga J G 2017 *Phys. Rev. A* **95** 022328
- [10] Lizuain I, Palmero M and Muga J G 2017 *Phys. Rev. A* **95** 022130
- [11] Masuda S and Rice S A 2015 *J. Phys. Chem. B* **119** 11079
- [12] Fetter A L 2009 *Rev. Mod. Phys.* **81** 647
- [13] Dalibard J, Gerbier F, Juzeliūnas G and Öhberg P 2011 *Rev. Mod. Phys.* **83** 1523
- [14] Amini J M, Uys H, Wesenberg J H, Seidelin S, Britton J, Bollinger J J, Leibfried D, Ospelkaus C, VanDevender A P and Wineland D J 2010 *New J. Phys.* **12** 033031
- [15] Hensinger W K *et al* 2006 *Appl. Phys. Lett.* **88** 034101
- [16] Blakestad R B, VanDevender A P, Ospelkaus C, Amini J M, Britton J, Leibfried D and Wineland D J 2009 *Phys. Rev. Lett.* **102** 153002
- [17] Splatt F, Harlander M, Brownutt M, Zähringer F, Blatt R and Hänsel W 2006 *New J. Phys.* **11** 103008
- [18] Urban E, Glikin N, Mouradian S, Krimmel K, Hemmerling B and Haeffner H 2019 *Phys. Rev. Lett.* **123** 133202
- [19] Goldstein H, Poole C and Safko J 2001 *Classical Mechanics* 3rd edn (Reading, MA: Addison-Wesley)
- [20] Simon R 2000 *Phys. Rev. Lett.* **84** 2726
- [21] Williamson J 1936 *Am. J. Math.* **58** 141
- [22] Pirandola S, Serafini A and Lloyd S 2009 *Phys. Rev. A* **79** 052327

- [23] de Gosson M 2006 *Symplectic Geometry and Quantum Mechanics* (Basel: Springer)
- [24] Bialynicki-Birula I and Bialynicka-Birula Z 1997 *Phys. Rev. Lett.* **78** 2539
- [25] Leyraz F, Man'ko V I and Seligman T H 1996 *Phys. Lett. A* **210** 26
- [26] Razi Naqvi K and Waldenström S 2000 *Phys. Scr.* **62** 12
- [27] Demirplak M and Rice S A 2008 *J. Chem. Phys.* **129** 154111
- [28] Ibáñez S, Chen X and Muga J G 2013 *Phys. Rev. A* **87** 043402
- [29] Theis L S, Motzoi F, Machnes S and Wilhelm F K 2018 *Europhys. Lett.* **123** 60001
- [30] Hall B C 2015 *Lie Groups, Lie Algebras, and Representations: an Elementary Introduction (Graduate Texts in Mathematics)* (Berlin: Springer)

Invariant-based inverse engineering of time-dependent, coupled harmonic oscillatorsA. Tobalina,^{1,*} E. Torrontegui,^{2,3} I. Lizuain,⁴ M. Palmero,^{5,6} and J. G. Muga¹¹*Department of Physical Chemistry, University of the Basque Country UPV/EHU, Apdo 644, Bilbao, Spain*²*Departamento de Física, Universidad Carlos III de Madrid, Avda. de la Universidad 30, 28911 Leganés (Madrid), Spain*³*Instituto de Física Fundamental IFF-CSIC, Calle Serrano 113b, 28006 Madrid, Spain*⁴*Department of Applied Mathematics, University of the Basque Country UPV/EHU, 20018 Donostia-San Sebastian, Spain*⁵*Department of Applied Physics I, University of the Basque Country, UPV/EHU, 48013 Bilbao, Spain*⁶*Science and Math Cluster, Singapore University of Technology and Design, 8 Somapah Road, 487372 Singapore*

(Received 27 July 2020; accepted 28 October 2020; published 14 December 2020)

Two-dimensional (2D) systems with time-dependent controls admit a quadratic Hamiltonian modeling near potential minima. Independent, dynamical normal modes facilitate inverse Hamiltonian engineering to control the system dynamics, but some systems are not separable into independent modes by a point transformation. For these “coupled systems” 2D invariants may still guide the Hamiltonian design. The theory to perform the inversion and two application examples are provided: (i) We control the deflection of wave packets in transversally harmonic wave guides and (ii) we design the state transfer from one coupled oscillator to another.

DOI: [10.1103/PhysRevA.102.063112](https://doi.org/10.1103/PhysRevA.102.063112)**I. INTRODUCTION**

Controlling the motional dynamics of quantum systems is of paramount importance for fundamental science and quantum-based technologies [1]. In particular, controlling the evolution of interacting quantum systems is crucial to design logic gates, one of the key elements of a quantum computer [2]. Often the external driving needs to be fast, but also gentle, to avoid excitations. Slow adiabatic driving is gentle in this sense, but it exposes the system for long times to control noise, heating, and perturbations. Shortcuts to adiabaticity (STA) are techniques to reach, via fast nonadiabatic routes, the results of slow adiabatic processes [3,4].

A distinction can be made between STA methods that keep the structure of some Hamiltonian form and design the time dependence of the controls, e.g., using invariants [5] and those techniques that add new terms, e.g., counterdiabatic driving [6]. Both may be useful depending on system-dependent practical considerations. A frequent problem with added terms is the difficulty to implement them, whereas a limitation of structure-preserving, invariant-based methods is that they need Hamiltonian-invariant pairs with specific forms, such as the Lewis-Leach family of Hamiltonian-invariant pairs [7], to go beyond brute-force parameter optimization [3,4].

Here we shall deal with two-dimensional (2D) systems with quadratic Hamiltonians, found in particular in small-oscillation regimes of ultracold atom physics. In fact quadratic Hamiltonians are ubiquitous as they represent the systems

near potential minima [8]. So far, invariant based STA have only been developed for 2D systems with independent “dynamical normal modes” [9]. When the two dynamical-mode motions separate, inverse engineering the dynamics to perform some fast operation free from final excitations is relatively easy: each of the time-dependent effective oscillators implies a one-dimensional Hamiltonian-invariant “Lewis-Leach” pair [7] for which inverse engineering can be performed. The two oscillators have to be driven simultaneously with common controls but, among the plethora of parameter trajectories, it is possible to find the ones that satisfy simultaneously the boundary conditions imposed on both oscillators. This strategy has been successfully applied to design the driving of different operations on two trapped ions such as transport or expansions [9,10], separation of two equal ions in double wells [11], phase gates [12], or dynamical exchange cooling [13].

This decomposition though, may not always be possible. Lizuain *et al.* [14] described the condition for which a point transformation of coordinates decouples the instantaneous modes leading to truly independent dynamical normal modes for two time-dependent harmonic oscillators: the principal axes of the potential should not rotate in the 2D space.

This work extends the domain of systems and processes that can be controlled by invariant-based inverse engineering to those problems where the effective 2D potential rotates and the normal mode motions remain coupled. Solutions to the ensuing control problem exist that depend on the system and/or the operation, such as taking refuge in a perturbative regime [12], adding terms to cancel the inertial effects [14], increasing the number of time-dependent controls to uncouple the modes [13], or using more complex, nonpoint transformations to find independent modes [15]. Here we explore instead the use of 2D dynamical invariants associated with the coupled Hamiltonian.

*ander.tobalina@ehu.eus

Published by the American Physical Society under the terms of the [Creative Commons Attribution 4.0 International](https://creativecommons.org/licenses/by/4.0/) license. Further distribution of this work must maintain attribution to the author(s) and the published article's title, journal citation, and DOI.

The paper is organized as follows: First we introduce the model and its dynamical normal modes in Sec. II. Then we present the invariant we will use to inverse engineer the control fields in Sec. III. The first application, in Sec. IV, is the control of longitudinal energy in 2D deflected wave guides. Section V describes further control possibilities for 2D waveguides, and Sec. VI deals with a second type of application: controlled state transfer between oscillators. The paper ends with a discussion in Sec. VII.

II. HAMILTONIAN MODEL

Consider the Hamiltonian

$$H(t) = \frac{p_1^2}{2} + \frac{p_2^2}{2} + \frac{1}{2}\omega_1^2(t)q_1^2 + \frac{1}{2}\omega_2^2(t)q_2^2 - \gamma(t)q_1q_2. \quad (1)$$

We use throughout dimensionless variables such that no mass factors or \hbar appear explicitly. Equation (1) describes different physical systems, such as a single particle in a 2D potential, or two coupled harmonic oscillators on a line. Other systems different from (one or two) particles but driven by Hamiltonians of the form (1) are, e.g., coupled superconducting qubits [16–20] or optomechanical oscillators [21–23]. All these systems are analogous to each other but, arguably, the single particle in a 2D potential is easiest to visualize so we shall use a terminology (such as longitudinal and transversal directions for principal axes, rotations...) borrowed from that system. Indeed, our first example, see below, deals with a single particle.

The Hamiltonian (1) may be instantaneously diagonalized by “rotated” variables [14]

$$\begin{pmatrix} q_l \\ q_t \end{pmatrix} = A(t) \begin{pmatrix} q_1 \\ q_2 \end{pmatrix}, \quad \begin{pmatrix} p_l \\ p_t \end{pmatrix} = A(t) \begin{pmatrix} p_1 \\ p_2 \end{pmatrix}, \quad (2)$$

where $A(t) = \begin{pmatrix} \cos \theta(t) & \sin \theta(t) \\ -\sin \theta(t) & \cos \theta(t) \end{pmatrix}$, and

$$\theta(t) = \frac{1}{2} \arctan \left(\frac{2\gamma(t)}{\omega_2^2(t) - \omega_1^2(t)} \right). \quad (3)$$

Subscripts l and t stand for “longitudinal” and “transversal”. The original Hamiltonian, expressed in terms of the new variables, is

$$H = \frac{p_l^2}{2} + \frac{p_t^2}{2} + \frac{1}{2}\Omega_l^2 q_l^2 + \frac{1}{2}\Omega_t^2 q_t^2, \quad (4)$$

$$\Omega_l^2 = (\omega_1^2 + \omega_2^2 - \Lambda)/2, \quad \Omega_t^2 = (\omega_1^2 + \omega_2^2 + \Lambda)/2, \quad (5)$$

where $\Lambda(t) = \sqrt{4\gamma^2(t) + [\omega_2^2(t) - \omega_1^2(t)]^2}$.

The formal decoupling in Eq. (4) is a mirage. H is not the Hamiltonian that describes the dynamics in the rotated variables $\{p_l, p_t, q_l, q_t\}$ [14,24]. In general the dependence of $A(t)$ on time couples dynamically the “instantaneous normal modes”, i.e., the normal modes that would separate the motion if the Hamiltonian kept for all times the values that the parameters have at a particular instant. In the moving frame the oscillators are coupled by a term proportional to $\dot{\theta} = d\theta/dt$ [14]. Some peculiar, but physically significant relations between $\omega_1(t)$, $\omega_2(t)$, and $\gamma(t)$ can make $\theta(t)$ time independent. Here we consider instead the scenario where

$\theta(t)$ changes with time. This is unavoidable if the process we want to implement implies boundary conditions for the parameters such that $\theta(0) \neq \theta(t_f)$, as in the examples below.

III. 2D INVARIANT

Urzúa *et al.* [8], generalizing previous results in 1D [25,26] and the work in Ref. [27] for classical coupled oscillators, see also Ref. [28], have recently found that the linear combination of operators (dots stand for time derivatives hereafter)

$$G(t) = u_1(t)p_1 - \dot{u}_1(t)q_1 + u_2(t)p_2 - \dot{u}_2(t)q_2, \quad (6)$$

satisfies the invariant equation $i\partial G/\partial t - [H, G] = 0$, provided u_1 and u_2 satisfy

$$\ddot{u}_1 + \omega_1^2(t)u_1 = \gamma(t)u_2, \quad \ddot{u}_2 + \omega_2^2(t)u_2 = \gamma(t)u_1, \quad (7)$$

which are classical equations of motion driven by a Hamiltonian (1). For any state driven by $H(t)$, $\langle G(t) \rangle$ is the sum of two Wronskians $W_1[u_1(t), \langle q_1 \rangle(t)] + W_2[u_2(t), \langle q_2 \rangle(t)]$, where all functions in their arguments evolve as Eq. (7). The geometrical meaning of $W_i(t)$ is an “oriented” phase-space area formed by phase-space points $U_i(t) = \{u_i(0), \dot{u}_i(t)\}$, $Q_i(t) = \{\langle q_i \rangle(t), \langle p_i \rangle(t)\}$ and the origin $O_i = \{0_i, 0_i\}$. We consider two phase spaces, $i = 1, 2$, one for each oscillator. $W_i(t)$ is plus or minus the area $A_i(t)$ of the triangle formed by U_i, Q_i and O_i for each phase space, depending on whether going from U_i to Q_i needs an anticlockwise or clockwise displacement. For $\gamma = 0$, the two areas (and Wronskians) remain constant in time. When $\gamma \neq 0$ the individual Wronskians are not conserved. The conserved quantities are now $W_i(t) - \int_0^t \dot{W}_i(t')dt' = W_i(0)$, i.e., the initial phase-space oriented areas. The added terms cancel each other, namely, $\dot{W}_1 = -\dot{W}_2 = (u_1 \langle q_2 \rangle - \langle q_1 \rangle u_2)\gamma$, so that the sum $W_1(t) + W_2(t)$ is the sum of oriented areas and it is constant. This result is a particular case of the preservation of sums of oriented areas in classical Hamiltonian systems [29].

We construct from G a quadratic invariant that may become proportional to some relevant energy at boundary times by choosing specific boundary conditions for the u_i and \dot{u}_i , $I = \frac{1}{2}G^\dagger G$. Designing the u_i we may manipulate the invariants and therefore the dynamics. From the u_i we can as well get the Hamiltonian as demonstrated in the following application examples.

IV. CONTROLLED DEFLECTION

A single particle is launched along a potential “wave guide”, which is harmonic in the transversal direction. Our goal is to deflect it, that is, manipulate the potential to change the waveguide direction, controlling the input/output scaling factor of the longitudinal velocity. To have waveguide potentials at the boundary times $t_b = 0, t_f$ we impose

$$\gamma(t_b) = \omega_1(t_b)\omega_2(t_b). \quad (8)$$

As a consequence, $\Omega_l(t_b) = 0$ and $\Omega_t(t_b) = [\omega_1^2(t_b) + \omega_2^2(t_b)]^{1/2}$. Thus, at boundary times, the potential is a harmonic “waveguide” with longitudinal direction defined by the angle $\theta(t_b) = \arctan[\omega_1(t_b)/\omega_2(t_b)]$. The deflection angle $\Delta\theta = \theta(t_f) - \theta(0)$ can take any value between 0 and $\pi/2$ for $\theta(t_f) \geq \theta(0)$. The condition (8) in Eq. (7) implies that

TABLE I. Initial and final frequencies and angles defining the wave guides for γ -constant and ω_2 -constant protocols. The deflection angle $\Delta\theta = \theta(t_f) - \theta(0)$ determines the ratio $\omega_2(0)/\omega_1(0)$.

	Initial wave guide	Final wave guide
γ const.	$\omega_1(0)$	$\omega_1(t_f) = \omega_2(0)$
	$\omega_2(0)$	$\omega_2(t_f) = \omega_1(0)$
	$\Omega_t(0)$	$\Omega_t(t_f) = \Omega_t(0)$
ω_2 const.	$\omega_1(0)$	$\omega_1(t_f) = \omega_2^2(0)/\omega_1(0)$
	$\omega_2(0)$	$\omega_2(t_f) = \omega_2(0)$
	$\Omega_t(0)$	$\Omega_t(t_f) = \frac{\omega_2(0)}{\omega_1(0)}\Omega_t(0)$

$\ddot{u}_{1,2}(t_b) = 0$, which also gives

$$u_1(t_b)\omega_1(t_b) = u_2(t_b)\omega_2(t_b), \quad (9)$$

i.e., the reference trajectories must start and end at $q_t(t_b) = 0$, on the axis of the waveguide. If the frequencies at t_b are fixed, either $q_l(t_b)$, or one of the $u_i(t_b)$ can still be chosen freely.

Rewriting the invariant G in terms of the rotated variables $\{q_t, q_l\}$ and imposing $\dot{u}_{1,2}(t_b) = 0$ we find that

$$G(t_b) = \frac{u_2(t_b)}{\sin\theta(t_b)}p_l, \quad I(t_b) = \left[\frac{u_2(t_b)}{\sin\theta(t_b)} \right]^2 \frac{p_l^2}{2}, \quad (10)$$

i.e., $I(t_b)$ is proportional to the longitudinal energy.

With Eq. (10) we get

$$\langle p_l(t_f) \rangle = F \langle p_l(0) \rangle, \quad E_l(t_f) = F^2 E_l(0), \quad (11)$$

where $F = \frac{u_2(0)}{u_2(t_f)} \frac{\sin\theta(t_f)}{\sin\theta(0)}$ and $E_l = \langle p_l^2/2 \rangle$. For some chosen deflection angle $\Delta\theta$ and waveguide frequencies $\Omega_t(t_b)$ we may impose any scaling factor F by manipulating the ratio $u_2(0)/u_2(t_f)$, which allows us to set any desired velocity scaling, that is, any ratio between the incoming and the outgoing average velocity of the wave packet. This scaling factor will affect all wave packets, and the deflection angle $\Delta\theta$ and the waveguide compression/expansion factors [ratio between $\Omega_t(0)$ and $\Omega_t(t_f)$] can be chosen independently.

The Hamiltonian parameters are found inversely from Eq. (7). We choose $u_{1,2} = \sum_{k=0}^5 \alpha_k^{(1,2)} (t/t_f)^k$, with coefficients fixed so that $\dot{u}_{1,2}(t_b) = \ddot{u}_{1,2}(t_b) = 0$, and the $u_{1,2}(t_b)$ are consistent with Eq. (9).

There are three external parameters, $\omega_1(t)$, $\omega_2(t)$, and $\gamma(t)$, but two coupled equations in Eq. (7). Thus we may fix one of the external parameters or some combination. We consider two simple, not exhaustive, possibilities: (i) γ constant, so initial and final Ω_t coincide; and (ii) ω_2 constant, which implies a compression (transverse focusing useful to avoid transversal excitation) of the final wave guide with respect to the initial one, see Table I.

The initial state chosen for the numerical examples is a product of the ground state of the transversal harmonic oscillator and a minimum-uncertainty-product Gaussian in the longitudinal direction centered at q_{l0} , with initial momentum p_{l0} , $\psi_l(q_l, t=0) = [\sigma\sqrt{2\pi}]^{-1/2} e^{ip_{l0}q_l} e^{-(q_l - q_{l0})^2/(4\sigma^2)}$. Firstly, we design a process that interchanges $\omega_1(t)$ and $\omega_2(t)$ with $\Delta\theta = \pi/4$ and constant γ , conceived to preserve the initial longitudinal velocities in the outgoing waveguide,

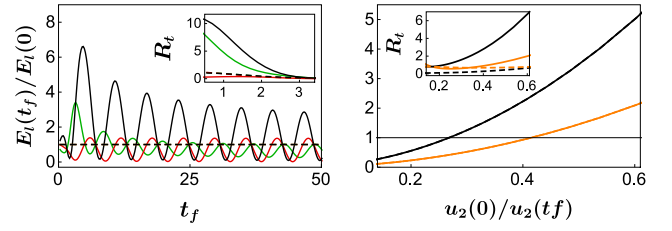


FIG. 1. Ratio of final to initial longitudinal energy for different process times t_f (a) and for different scaling factors $u_2(0)/u_2(t_f)$ (b). The insets show the scaled transversal excitation $R_t = \Delta E_t/\Omega_t(t_f)$. (a) initial longitudinal Gaussian wave packet with $2^{1/2}\sigma = 1$, $p_{l0} = 1$, and $q_{l0} = -4$ (green), $q_{l0} = 0$ (red), and $q_{l0} = 4$ (black). $\Delta\theta = \pi/4$ starting from $\omega_1(0) = 1$ and $\omega_2(0) = 2.41$, using linear ramps (solid lines) and an invariant-based protocol for γ constant that produces $E_l(t_f) = E_l(0)$ (dashed lines). (b) Initial longitudinal Gaussian wave packet centered at the origin with $p_{l0} = 1$ and $2^{1/2}\sigma = 1$. $\Delta\theta = \pi/4$ with $\omega_1(0) = 1$ and $\omega_2(0) = 2.41$ (orange curves), and $\Delta\theta = \pi/3$ with $\omega_1(0) = 1$ and $\omega_2(0) = 3.73$ (black curves) for constant- γ processes (solid lines) and constant- ω_2 processes (dashed lines, overlapping with solid lines in main figure). See Table I for values at $t = t_f$.

$E_l(t_f) = E_l(0)$, and use linear ramps (a control field that evolves linearly between the boundary values) for the same boundary waveguides as a benchmark to compare the performance of the invariant-based protocol.

Figure 1(a) depicts the final longitudinal energy. For the linear ramps it oscillates with operation time. The envelope for the minima is at zero but the maximum tends for long times to some value that depends on the initial wave packet. Contrast this with the full stability of the invariant-lead processes. They guarantee a fixed result, the final longitudinal energy being identical to the initial one for any initial wave packet. The transversal excitation by the linear ramps in fast processes increases considerably as the initial wave packet deviates from the origin, while the transversal excitation in the invariant-based protocol is, in general, small and much more stable.

Figure 1(b) verifies that, for some chosen deflection angle, we can scale the final longitudinal energy at will in both scenarios (γ or ω_2 constant). Since the invariant does not control the transversal direction, the transversal energy may be excited, but it still depends on the design of the $u_i(t)$, see the inset of Fig. 1(b). Such dependence may be exploited to minimize the transversal excitation and even suppress it in some cases (notice that the $\pi/3$ rotation with constant ω_2 produces zero transversal excitation for a given relation between the boundary values of u_2). Figure 2 provides snapshots of

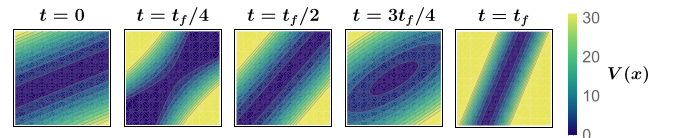


FIG. 2. Snapshots of the top view of the 2D potential for $E_l(t_f) = E_l(0)/2$ with constant ω_2 . $\omega_1(0) = 1$ and $\omega_2 = 2.41$, deflection angle $\Delta\theta = \pi/4$ ($\omega_1(t_f) = 2.41^2$) and process time $t_f = 1$. The transversal frequency is compressed 2.41 times, from $\Omega_t(0) = 2.61$ to $\Omega_t(t_f) = 6.29$, see Table I.

the evolution of the 2D potential for a ω_2 -constant processes that slows down the particle by a factor of 2 with deflection $\Delta\theta = \pi/4$.

V. COMMUTATION OF $H(t_b)$ AND $I(t_b)$ AND OTHER BOUNDARY CONDITIONS

Note that the necessary condition for the Hamiltonian and the invariant to commute at boundary times is precisely the waveguide condition in Eq. (8) (together with the auxiliary equations in Eq. (7)). In the case of a potential waveguide, however, the eigenvectors of $I(t_b)$ are highly degenerate, since a longitudinal plane wave multiplied by an arbitrary function of q_i is a valid eigenvector with the same eigenvalue. This means that even if $I(t_b)$ commutes with $H(t_b)$ and shares some eigenvectors with $H(t_b)$ the vast majority of them are not eigenvectors of $H(t_b)$. This phenomenon, i.e., the existence of eigenvectors of one operator not shared with the other one, is well known and is explained in detail in Ref. [30].

Thus, commutativity of $H(t_b)$ and $I(t_b)$ plays a lesser role in the 2D scenario, compared to the use of invariants for inverse engineering in 1D [4], and may in fact be abandoned for different applications. For example, note the following alternative sets of boundary conditions and corresponding quadratic invariants:

$$\begin{aligned} \dot{u}_i(t_b) &= 0, u_1(t_b)\omega_2(t_b) = -u_2(t_b)\omega_1(t_b), \\ I(t_b) &= \frac{u_2^2(t_b)}{\cos^2\theta(t_b)} \frac{p_i^2}{2}, \end{aligned} \quad (12)$$

where $i = 1, 2$ and the invariant at the boundary time t_b is proportional to the transversal kinetic energy. With these boundary conditions we could control and scale the transverse kinetic energy. As well,

$$\begin{aligned} u_i(t_b) &= 0, \dot{u}_1(t_b)\omega_1(t_b) = \dot{u}_2(t_b)\omega_2(t_b), \\ I(t_b) &= \frac{\dot{u}_2^2(t_b)}{\sin^2\theta(t_b)} \frac{q_i^2}{2}, \end{aligned} \quad (13)$$

which allows us to scale the longitudinal coordinate, e.g., to focus or defocus, or

$$\begin{aligned} u_i(t_b) &= 0, \dot{u}_1(t_b)\omega_2(t_b) = -\dot{u}_2(t_b)\omega_1(t_b), \\ I(t_b) &= \frac{\dot{u}_2^2(t_b)}{\cos^2\theta(t_b)} \frac{q_i^2}{2}, \end{aligned} \quad (14)$$

where the invariant at the boundary is proportional to the transverse potential energy.

Even more generally, the boundary conditions imposed on the $u_i(t)$ and their derivatives do not need to be of the same type at $t = 0$ and t_f , i.e., for longitudinal momenta or positions at both boundary times, or for transverse momenta or positions at both boundary times. Designing $u_i(t)$ so as to satisfy at $t = 0$ and t_f different boundary condition types opens several control possibilities such as, for example, driving the initial longitudinal energy into final transversal kinetic energy or vice versa.

VI. STATE TRANSFER

Up to now we have considered real $u_j(t)$, but the coupled Newton's equations admit purely real and purely imaginary solutions combined into complex solutions. Exploiting this

complex structure, $u_i = u_i^R + iu_i^I$, leads to interesting forms of the invariant. In particular the invariant may become proportional to the uncoupled Hamiltonians at boundary times, enabling energy transfer from one oscillator to the other. Processes that exchange the state, or some property of it, between coupled systems are highly relevant for the development of quantum technologies. They have been extensively studied in the context of quantum computation and communication [31,32] and also addressed in experiments [33,34]. State transfer between coupled harmonic oscillators has also been thoroughly explored [35–37]. Here we develop a protocol that induces energy exchange between oscillators by inverse engineering the control fields that govern the system.

Let us first drop the waveguide condition (8) and go back to the laboratory frame variables $\{q_1, q_2\}$. Defining annihilation operators in the usual manner, $a_i(t) = \sqrt{\omega_i(t)/2} q_i + ip_i/\sqrt{2\omega_i(t)}$, $i = 1, 2$, G in Eq. (6) may become a_1 or a_2 by certain choices of the u_j . Let us choose at initial time

$$u_1(0) = ic_0/\sqrt{2\omega_1(0)}, \quad \dot{u}_1(0) = -c_0\sqrt{\omega_1(0)}/2, \quad (15)$$

and $u_2(0) = \dot{u}_2(0) = 0$ with c_0 real. This implies $G(0) = c_0 a_1(0)$, and $I(0) = c_0^2 a_1^\dagger(0) a_1(0)/2$. Instead, at final time we impose

$$u_2(t_f) = ic_0/\sqrt{2\omega_2(t_f)}, \quad \dot{u}_2(t_f) = -c_0\sqrt{\omega_2(t_f)}/2, \quad (16)$$

together with $u_1(t_f) = \dot{u}_1(t_f) = 0$, so that $G(t_f) = c_0 a_2(t_f)$, and $I(t_f) = c_0^2 a_2^\dagger(t_f) a_2(t_f)/2$. The same constant c_0 appears in Eqs. (15) and (16) because the solutions of Eq. (7) must satisfy $\frac{d}{dt} \{\text{Im}[u_1^*(t)\dot{u}_1(t) + u_2^*(t)\dot{u}_2(t)]\} = 0$ [27].

The choice $c_0^2/2 = \omega_1(0)$, together with the mentioned boundary conditions give $I(0) = H_1(0)$ and $I(t_f) = [\omega_1(0)/\omega_2(t_f)]H_2(t_f)$, where we define the ‘‘uncoupled Hamiltonians’’ $H_j(t) \equiv \omega_j(t)a_j^\dagger(t)a_j(t)$. Eigenstates of $H_1(0)$ may thus be mapped into eigenstates of $H_2(t_f)$ by proper inverse engineering of the $u_j(t)$. If $\omega_1(0) = \omega_2(t_f)$,

$$\langle H_1(0) \rangle = \langle I(0) \rangle = \langle I(t_f) \rangle = \langle H_2(t_f) \rangle \quad (17)$$

for all initial wave packets. (Any other scale factor may be chosen.) The system (7), which now involves four real functions, $u_1^R(t), u_1^I(t), u_2^R(t), u_2^I(t)$, has to be solved inversely for $\omega_1(t), \omega_2(t)$ and $\gamma(t)$. The inversion is done following techniques developed for trapped ions [12] or systems [38]. Assuming that the values of the control parameters at boundary times are set, we start by designing a $\gamma(t)$ that satisfies the boundary values $\gamma(t_b)$ and that has zero first and second derivatives at the boundaries for smoothness. We use a sum-of-cosines ansatz

$$\gamma(t) = \sum_{k=0}^4 a_k \cos\left(\frac{k\pi t}{t_f}\right), \quad (18)$$

which meets the boundary conditions with just five terms. The coefficient a_4 is left free for now. Then we design the imaginary part of the dynamics, again using sums of cosines

$$\begin{aligned} u_1^I(t) &= \sum_{i=0}^6 b_i \cos\left(\frac{i\pi t}{t_f}\right), \\ u_2^I(t) &= \sum_{j=0}^6 c_j \cos\left(\frac{j\pi t}{t_f}\right). \end{aligned} \quad (19)$$

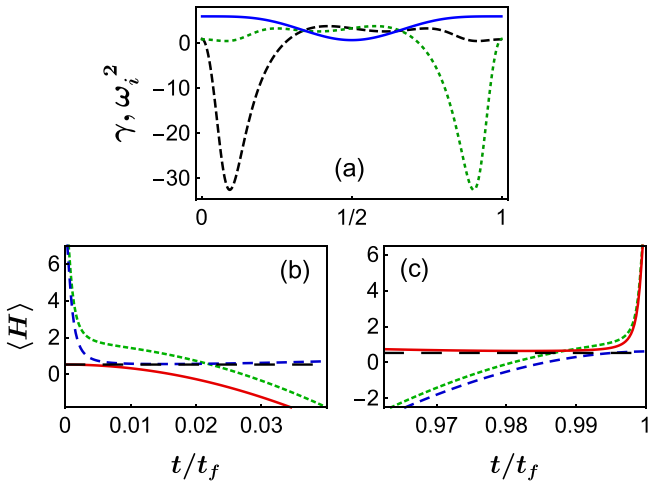


FIG. 3. (a) Control parameters, ω_1^2 (dashed black), ω_2^2 (short-dashed green) and γ (solid blue) vs t/t_f , for an energy transfer from oscillator 1 to 2. $\langle H_1 \rangle$ in solid red, $\langle H_2 \rangle$ in dashed blue, $\langle H \rangle$ in short-dashed green, and $\langle I \rangle$ in long-dashed black, for initial (b) and final (c) parts of the process. $\omega_1(0)^2 = \omega_2(t_f)^2 = 1$, $\omega_2(0)^2 = \omega_1(t_f)^2 = 0.9$ and $\gamma(0) = \gamma(t_f) = 6$; $t_f = 4$; the system starts in a (tensor) product state between the ground states of the uncoupled oscillators H_1 and H_2 , not an eigenstate of the total Hamiltonian (1).

Coefficients $\{b, c\}_{1-5}$ are fixed so that the real reference trajectories satisfy the boundary conditions for $u_{1,2}(t_b)$ and its derivatives, and so that the frequencies $\omega_i(t)$ have the desired boundary values, which amounts to satisfying

$$\begin{aligned} \ddot{u}_1^l(0) &= -\omega_1(0)^2, & \ddot{u}_1^l(t_f) &= \gamma(t_f) \sqrt{\frac{\omega_1(0)}{\omega_2(t_f)}}, \\ \ddot{u}_2^l(0) &= \gamma(0), & \ddot{u}_2^l(t_f) &= \omega_2(t_f) \sqrt{\omega_1(0)\omega_2(t_f)}. \end{aligned} \quad (20)$$

Note, from the expression of the frequencies

$$\omega_{1,2}(t)^2 = \frac{\gamma(t)u_{2,1}^l(t) - \ddot{u}_{1,2}^l(t)}{u_{1,2}^l(t)}, \quad (21)$$

that, even if the conditions in Eq. (20) are fulfilled, we may encounter indeterminacies at boundary times (some $u_{1,2}(t_b)$ become 0). Thus, we have to impose additional boundary conditions for consistency using L'Hopital's rule,

$$\begin{aligned} u_1^{l(3)}(t_f) &= 0, \\ u_1^{l(4)}(t_f) &= -\gamma(t_f) \sqrt{\frac{\omega_1(0)}{\omega_2(t_f)}} [\omega_1(t_f)^2 + \omega_2(t_f)^2], \\ u_2^{l(3)}(0) &= 0, \\ u_2^{l(4)}(0) &= -\gamma(0) [\omega_1(0)^2 + \omega_2(0)^2]. \end{aligned} \quad (22)$$

Coefficients $\{b, c\}_6$ are left yet undetermined. In the next step, we numerically solve the real equations of motion with the already designed control parameters for the initial conditions and find, again, numerically, the value of the coefficients that have been left free to satisfy the final boundary conditions.

Figure 3(a) displays the resulting evolution of the control parameters for a specific example in which the frequencies ω_i swap their boundary values and $\gamma(0) = \gamma(t_f)$. Figure 3(b) shows the expectation values of the total and the uncoupled Hamiltonians near the time boundaries, together with the constant expectation value of the invariant. Indeed $\langle H_2(t_f) \rangle = \langle H_1(0) \rangle$, thus proving that our protocol transfers the state from one uncoupled oscillator at the initial time to the other one at the final time. Similarly to what happens with the transversal energy in the wave guide, the invariant does not impose the value of the final total energy, which does not necessarily coincide with the initial one.

VII. DISCUSSION

In some multidimensional systems with time-dependent control there are no point transformations that lead to uncoupled normal modes. Our main point here is that in these “coupled systems”, invariants of motion may still guide us to inversely design the time dependence of the controls for driving specific dynamics.

This inversion procedure extends the domain of invariant-based engineering, which had been applied so far to 1D or uncoupled systems [4]. An important difference with respect to uncoupled systems is the diminished role of commutativity of Hamiltonian and invariant at boundary times. Commutativity, because of degeneracy, does not guarantee one-to-one mapping of eigenstates of the total Hamiltonian from initial to final configurations. One should then focus on the invariant itself for applications, and, if required, rely on design freedom to keep other variables, e.g., the total energy, controlled. An alternative to be explored is to make use of a second invariant corresponding to a linearly independent set of classical solutions of Eq. (7), $\{u_1^l(t), u_2^l(t)\}$, linearly independent with respect to $\{u_1(t), u_2(t)\}$ [27]. Imposing boundary conditions to the second set we would aim to control the second invariant as well, but the inversion problem becomes more demanding, as the number of conditions double, while the number of (common) controls remains the same.

As for further open questions, invariant-based engineering is known to be related to other STA approaches such as counterdiabatic driving for single oscillators [39]. It would be of interest to connect the current work with counterdiabatic driving for coupled oscillators [40,41]. Finally, other boundary conditions on the u_j would allow to control other processes, different from the ones examined here.

ACKNOWLEDGMENTS

This work was supported by the Basque Country Government (Grant No. IT986-16), and by PGC2018-101355-B-I00 (MCIU/AEI/FEDER,UE). E.T. acknowledges support from PGC2018-094792-B-I00 (MCIU/AEI/FEDER,UE), CSIC Research Platform PTI-001, and CAM/FEDER No. S2018/TCS- 4342 (QUITEMAD-CM).

- [1] J. P. Dowling and G. J. Milburn, Quantum technology: the second quantum revolution, *Philos. Trans. R. Soc. London Ser. A* **361**, 1655 (2003).
- [2] D. Kielpinski, C. Monroe, and D. J. Wineland, Architecture for a large-scale ion-trap quantum computer, *Nature (London)* **417**, 709 (2002).
- [3] E. Torrontegui, S. Ibáñez, S. Martínez-Garaot, M. Modugno, A. del Campo, D. Guéry-Odelin, A. Ruschhaupt, X. Chen, and J. G. Muga, *Shortcuts to Adiabaticity*, volume 62 of *Advances In Atomic, Molecular, and Optical Physics* (Elsevier, Amsterdam, 2013), p. 117.
- [4] D. Guéry-Odelin, A. Ruschhaupt, A. Kiely, E. Torrontegui, S. Martínez-Garaot, and J. G. Muga, Shortcuts to adiabaticity: Concepts, methods, and applications, *Rev. Mod. Phys.* **91**, 045001 (2019).
- [5] X. Chen, A. Ruschhaupt, S. Schmidt, A. del Campo, D. Guéry-Odelin, and J. G. Muga, Fast Optimal Frictionless Atom Cooling in Harmonic Traps: Shortcut to Adiabaticity, *Phys. Rev. Lett.* **104**, 063002 (2010).
- [6] M. Demirplak and S. A. Rice, Adiabatic population transfer with control fields, *J. Phys. Chem. A* **107**, 9937 (2003).
- [7] H. R. Lewis and P. G. L. Leach, A direct approach to finding exact invariants for one-dimensional time-dependent classical Hamiltonians, *J. Math. Phys.* **23**, 2371 (1982).
- [8] A. R. Urzúa, I. Ramos-Prieto, M. Fernández-Guasti, and H. M. Moya-Cessa, Solution to the time-dependent coupled harmonic oscillators hamiltonian with arbitrary interactions, *Quant. Rep.* **1**, 82 (2019).
- [9] M. Palmero, R. Bowler, J. P. Gaebler, D. Leibfried, and J. G. Muga, Fast transport of mixed-species ion chains within a Paul trap, *Phys. Rev. A* **90**, 053408 (2014).
- [10] M. Palmero, S. Martínez-Garaot, J. Alonso, J. P. Home, and J. G. Muga, Fast expansions and compressions of trapped-ion chains, *Phys. Rev. A* **91**, 053411 (2015).
- [11] M. Palmero, S. Martínez-Garaot, U. G. Poschinger, A. Ruschhaupt, and J. G. Muga, Fast separation of two trapped ions, *New J. Phys.* **17**, 093031 (2015).
- [12] M. Palmero, S. Martínez-Garaot, D. Leibfried, D. J. Wineland, and J. G. Muga, Fast phase gates with trapped ions, *Phys. Rev. A* **95**, 022328 (2017).
- [13] T. Sägger, R. Matt, R. Oswald, and J. P. Home, Robust dynamical exchange cooling with trapped ions, *New J. Phys.* **22**, 073069 (2020).
- [14] I. Lizuain, M. Palmero, and J. G. Muga, Dynamical normal modes for time-dependent Hamiltonians in two dimensions, *Phys. Rev. A* **95**, 022130 (2017).
- [15] I. Lizuain, A. Tobalina, A. Rodríguez-Prieto, and J. G. Muga, Fast state and trap rotation of a particle in an anisotropic potential, *J. Phys. A* **52**, 465301 (2019).
- [16] R. Barends, J. Kelly, A. Megrant, D. Sank, E. Jeffrey, Y. Chen, Y. Yin, B. Chiaro, J. Mutus, C. Neill, P. O'Malley, P. Roushan, J. Wenner, T. C. White, A. N. Cleland, and J. M. Martinis, Coherent Josephson Qubit Suitable for Scalable Quantum Integrated Circuits, *Phys. Rev. Lett.* **111**, 080502 (2013).
- [17] M. A. Rol, F. Battistel, F. K. Malinowski, C. C. Bultink, B. M. Tarasinski, R. Vollmer, N. Haider, N. Muthusubramanian, A. Bruno, B. M. Terhal, and L. DiCarlo, Fast, High-Fidelity Conditional-Phase Gate Exploiting Leakage Interference in Weakly Anharmonic Superconducting Qubits, *Phys. Rev. Lett.* **123**, 120502 (2019).
- [18] B. Peropadre, D. Zueco, F. Wulchner, F. Deppe, A. Marx, R. Gross, and J. J. García-Ripoll, Tunable coupling engineering between superconducting resonators: From sidebands to effective gauge fields, *Phys. Rev. B* **87**, 134504 (2013).
- [19] J. J. García-Ripoll, A. Ruiz-Chamorro, and E. Torrontegui, Quantum Control of Frequency-Tunable Transmon Superconducting Qubits, *Phys. Rev. Appl.* **14**, 044035 (2020).
- [20] Y. Chen, C. Neill, P. Roushan, N. Leung, M. Fang, R. Barends, J. Kelly, B. Campbell, Z. Chen, B. Chiaro, A. Dunsworth, E. Jeffrey, A. Megrant, J. Y. Mutus, P. J. J. O'Malley, C. M. Quintana, D. Sank, A. Vainsencher, J. Wenner, T. C. White, M. R. Geller, A. N. Cleland, and J. M. Martinis, Qubit Architecture with High Coherence and Fast Tunable Coupling, *Phys. Rev. Lett.* **113**, 220502 (2014).
- [21] D. Kleckner, B. Pepper, E. Jeffrey, P. Sonin, S. M. Thon, and D. Bouwmeester, Optomechanical trampoline resonators, *Opt. Express* **19**, 19708 (2011).
- [22] K. Zhang, F. Bariani, and P. Meystre, Quantum Optomechanical Heat Engine, *Phys. Rev. Lett.* **112**, 150602 (2014).
- [23] M. Aspelmeyer, T. J. Kippenberg, and F. Marquardt, Cavity optomechanics, *Rev. Mod. Phys.* **86**, 1391 (2014).
- [24] H. Goldstein, C. Poole, and J. Safko, *Classical Mechanics* (Addison-Wesley, Reading, MA, 2002).
- [25] M. Fernández-Guasti and A. Gil-Villegas, Orthogonal functions invariant for the time-dependent harmonic oscillator, *Phys. Lett. A* **292**, 243 (2002).
- [26] M. Fernández-Guasti and H. Moya-Cessa, Solution of the Schrödinger equation for time-dependent 1D harmonic oscillators using the orthogonal functions invariant, *J. Phys. A* **36**, 2069 (2003).
- [27] K.-E. Thylwe and H. J. Korsch, The 'Ermakov-Lewis' invariants for coupled linear oscillators, *J. Phys. A* **31**, L279 (1998).
- [28] O. Castanos, R. Lopez-Pena, and V. I. Man'ko, Noether's theorem and time-dependent quantum invariants, *J. Phys. A* **27**, 1751 (1994).
- [29] V. I. Arnold, *Mathematical Methods of Classical Mechanics*, 2nd ed. (Springer-Verlag, Berlin, 1989).
- [30] C. Cohen-Tannoudji, B. Diu, and F. Laloe, *Quantum Mechanics* (Wiley, New York, 1991).
- [31] J. I. Cirac, P. Zoller, H. J. Kimble, and H. Mabuchi, Quantum State Transfer and Entanglement Distribution among Distant Nodes in a Quantum Network, *Phys. Rev. Lett.* **78**, 3221 (1997).
- [32] M. Christandl, N. Datta, A. Ekert, and A. J. Landahl, Perfect State Transfer in Quantum Spin Networks, *Phys. Rev. Lett.* **92**, 187902 (2004).
- [33] D. N. Matsukevich and A. Kuzmich, Quantum state transfer between matter and light, *Science* **306**, 663 (2004).
- [34] P. Kurpiers, P. Magnard, T. Walter, B. Royer, M. Pechal, J. Heinsoo, Y. Salathé, A. Akin, S. Storz, J. Besse, S. Gasparinetti, A. Blais, and A. Wallraff, Deterministic quantum state transfer and remote entanglement using microwave photons, *Nature (London)* **558**, 264 (2018).

- [35] A. S. M. de Castro and V. V. Dodonov, Squeezing exchange and entanglement between resonantly coupled modes, *J. Russ. Laser Res.* **23**, 93 (2002).
- [36] A. S. M. de Castro, V. V. Dodonov, and S. S. Mizrahi, Quantum state exchange between coupled modes, *J. Opt. B* **4**, S191 (2002).
- [37] A. S. M. de Castro and V. V. Dodonov, Purity and squeezing exchange between coupled bosonic modes, *Phys. Rev. A* **73**, 065801 (2006).
- [38] S. González-Resines, D. Guéry-Odelin, A. Tobalina, I. Lizuain, E. Torrontegui, and J. G. Muga, Invariant-Based Inverse Engineering of Crane Control Parameters, *Phys. Rev. Appl.* **8**, 054008 (2017).
- [39] X. Chen, E. Torrontegui, and J. G. Muga, Lewis-Riesenfeld invariants and transitionless quantum driving, *Phys. Rev. A* **83**, 062116 (2011).
- [40] C. W. Duncan and A. del Campo, Shortcuts to adiabaticity assisted by counterdiabatic Born–Oppenheimer dynamics, *New J. Phys.* **20**, 085003 (2018).
- [41] T. Villazon, A. Polkovnikov, and A. Chandran, Swift heat transfer by fast-forward driving in open quantum systems, *Phys. Rev. A* **100**, 012126 (2019).

Time-dependent harmonic potentials for momentum or position scalingJ. G. Muga¹, S. Martínez-Garaot¹, M. Pons², M. Palmero² and A. Tobalina¹¹*Department of Physical Chemistry, University of the Basque Country UPV/EHU, Apartado 644, 48080 Bilbao, Spain*²*Department of Applied Physics I, University of the Basque Country, UPV/EHU, 48013 Bilbao, Spain*

(Received 20 July 2020; accepted 7 September 2020; published 30 October 2020)

Cooling methods and particle slowers as well as accelerators are basic tools for fundamental research and applications in different fields and systems. We put forward a generic mechanism to scale the momentum of a particle, regardless of its initial position and momentum, by means of a transient harmonic potential. The design of the time-dependent frequency makes use of a linear invariant and inverse techniques drawn from “shortcuts to adiabaticity.” The timing of the process may be decided beforehand, and its influence on the system evolution and final features is analyzed. We address quantum systems, but the protocols found are also valid for classical particles. Similar processes are possible as well for position scaling.

DOI: [10.1103/PhysRevResearch.2.043162](https://doi.org/10.1103/PhysRevResearch.2.043162)**I. INTRODUCTION**

Particle slowers and accelerators are basic tools for fundamental research and applications in different fields covering a huge range of systems, from high-energy physics to atomic and molecular physics. Zeeman [1] or Stark slowers [2], optical slowers [3], magnetic inverse coil guns [4,5], and delta-kick cooling (DKC) [6], for example, have played a central role in the development of cold and ultracold physics, while accelerators are needed to launch beams for controlled collisions, deposition [7], or implantation [8] at chosen speeds. For such a vast domain of systems and conditions many different techniques have been developed. A broad family of methods applies electromagnetic fields adapted to the particle type and the operation, taking into account if the particle is charged, its magnetic moment, its dipole moment, its polarizability, or if it allows for cyclic transitions. The results often depend heavily on the initial states, initial location, velocity, or spreads, and methods that could suppress or mitigate these dependences are of general interest.

In this paper we find a simple, generic mechanism, and work out protocols, to scale the momentum of a classical particle or of a quantum wave packet. The scaling can speed up or slow down the particle by a predetermined factor; this factor could even be negative, to produce a “momentum mirror.” The main features of this mechanism are system independent; the only formal requirement is that the particle is subjected to a transient harmonic potential with time-dependent frequency during a prearranged duration. The specific system

will determine the practical details as to how the harmonic potential is implemented, using optical, magnetic, electrical, or mechanical means. An astonishing property of the protocols described below is that the scale factor is the same for all initial conditions, i.e., for arbitrary quantum wave packets or for all initial positions and momenta of the classical particles. While, in principle, information on the exact initial condition is not needed to perform the scaling, practical considerations will of course set limits. These limits are not fundamental, but depend on the spatial, energetic, and temporal domain in which the needed harmonic potential can be effectively implemented in some specific setting.

The theory behind the time-dependent protocols for the harmonic potential makes use of an invariant of motion linear in position and momentum. Basically, we deal with an inverse problem, where the Hamiltonian is found from the desired dynamics encoded in the invariant, along the lines of the set of inverse techniques known as “shortcuts to adiabaticity” [9,10]. The theory is worked out here for a quantum particle represented by a wave packet, but the resulting protocols apply equally well to classical particles since, as is well known, harmonic potentials lead to classical equations of motion for the expectation values of position and momentum. In fact the dynamics of an arbitrary wave packet can be exactly reproduced by swarms of classical particles using the Wigner representation to fix the (possibly negative) “weighting factors” [11].

We shall first present the theory and deduce the protocols. Then we provide expressions for the time dependence of expectation values of position and momentum for a chosen scale factor, as well as expressions for second-order moments for positions and momenta in terms of the initial values. This is valuable information to set both practical limits and design details depending on the intended target and resources available. We end the paper by considering related processes, in particular, the scaling of positions, i.e., focusing or antifocusing.

Published by the American Physical Society under the terms of the Creative Commons Attribution 4.0 International license. Further distribution of this work must maintain attribution to the author(s) and the published article’s title, journal citation, and DOI.

II. LINEAR INVARIANTS

Lewis-Riesenfeld “time-dependent invariants” are operators whose expectation values remain constant for states driven by the associated time-dependent Hamiltonian [12]. The time-dependent eigenvectors of the invariant form a convenient basis, since their probabilities remain constant along the evolution. The phases can be chosen to make each eigenvector a solution of the time-dependent Schrödinger equation. This structure has been used systematically to inverse engineer Hamiltonians from desired faster-than-adiabatic dynamics since Ref. [13], for operations to control internal or motional states. Specifically in harmonic systems, most applications have made use of quadratic invariants in positions and momenta. The existence of linear invariants was known [14–16] but has not been exploited for inverse engineering. The bias towards quadratic invariants in most inverse engineering applications is in part explained by the fact that an “Ermakov” quadratic invariant (see further details in Sec. III D) may be set to commute with the harmonic-oscillator Hamiltonian at initial and final process times [13]. Thus fast expansions, transport, rotations, or splittings between initial and final traps can be designed so that the final total energy is the same as if the process had been very slow, i.e., adiabatic [10]. Instead, the linear invariants provide the natural frame to control (scale) other observables, such as the momentum or the position. Moreover, the linear invariant eigenvectors provide continuum representations well adapted to processes where the initial and final harmonic frequencies vanish, a challenging limit for the discrete representations associated with the conventional Ermakov invariant.

The Hamiltonian of a particle subjected to a harmonic potential with its center fixed at the origin and time-varying frequency is given by

$$H(t) = \frac{p^2}{2m} + \frac{m}{2}\omega^2(t)q^2. \quad (1)$$

Here, we consider q and p noncommuting operators (but the same symbols may represent c numbers in wave-function representations, or conjugate variables of a classical particle). The context should avoid any confusion. The linear combination of operators (dots stand for time derivatives hereafter) [14,15,17],

$$G(t) = u(t)p - m\dot{u}(t)q, \quad (2)$$

satisfies the invariant equation $i\hbar\partial G/\partial t - [H, G] = 0$, provided the reference trajectory u satisfies

$$\ddot{u} + \omega^2(t)u = 0, \quad (3)$$

which is a classical equation of motion for a particle driven by a Hamiltonian (1). Here, we shall consider only real solutions u . For any quantum state evolving with $H(t)$, the expectation value of $G(t)$ at time t is the Wronskian $W(t) = W[u(t), \langle q \rangle(t)]$ times m , where both functions in the argument evolve classically, i.e., following a harmonic-oscillator equation (3), according to Ehrenfest’s theorem [18]. $\langle G \rangle$ is indeed invariant as $\dot{W}(t) = 0$ using Eq. (3). This result does not depend on the particular state, so the expectation values can be substituted by operators in Eq. (2).

A corresponding quadratic invariant takes the form (up to a multiplication constant that can be chosen for convenience)

$$I = \frac{1}{2m}G^\dagger G = \frac{u^2 p^2}{2m} + \frac{m}{2}\dot{u}^2 q^2 - \frac{1}{2}u\dot{u}(pq + qp). \quad (4)$$

By imposing the boundary conditions at initial and final times $t_b = 0, t_f$,

$$\omega(t_b) = 0, \quad \dot{u}(t_b) = 0, \quad (5)$$

which also imply $\ddot{u}(t_b) = 0$ [see Eq. (3)], we find $G(t_b) = u(t_b)p$, proportional to the momentum. Thus the final and initial momenta are proportional to each other for any wave packet, with a corresponding relation for kinetic energies due to the associated quadratic invariant,

$$\begin{aligned} \langle p \rangle_f &= (u_0/u_f)\langle p \rangle_0, \\ E_f &= (u_0/u_f)^2 E_0, \end{aligned} \quad (6)$$

where we use shorthand notations $u_0 = u(0)$, $u_f = u(t_f)$ and generally subscripts f and 0 for final and initial times, respectively. The scaling affects not only expectation values but also each momentum component as we shall see. To design a harmonic slower or accelerator, we first choose the scaling factor u_0/u_f and a $u(t)$ that satisfies the boundary conditions (5) and the scaling factor. $\omega(t)$ is found from Eq. (3) as

$$\omega^2(t) = -\ddot{u}(t)/u(t). \quad (7)$$

With the chosen boundary conditions the eigenvectors of $G(t_b)$ or $I(t_b)$ are plane waves, i.e., not square integrable, but they form a valid and useful basis. The (constant-in-time) eigenvalues of $G(t)$ can be conveniently computed at time 0 as $\lambda = u_0 p_0$. The initial plane-wave momentum p_0 will play the role of integration variable to expand the wave functions. At an arbitrary time the eigenvectors of $G(t)$, $G(t)|\phi_{p_0}(t)\rangle = u_0 p_0 |\phi_{p_0}(t)\rangle$, may be calculated as

$$\phi_{p_0}(q, t) = \frac{e^{i\varphi_{p_0}(t)}}{h^{1/2}} e^{i(u_0 p_0 q + m\dot{u}_0 q^2/2)/(\hbar u_t)}. \quad (8)$$

The phase $\varphi_{p_0}(t)$ is chosen so that Eq. (8) represents a solution of the time-dependent Schrödinger equation, and it is found by inserting Eq. (8) into the Schrödinger equation,

$$e^{i\varphi_{p_0}(t)} = \left(\frac{u_0}{u_t}\right)^{1/2} e^{-i\frac{p_0^2}{2m\hbar}\mathcal{I}_t}, \quad (9)$$

where

$$\mathcal{I}_t = \int_0^t dt' u_0^2/u_t'^2 \quad (10)$$

and in general we use the subscript t as a shorthand for the argument (t). The factor $h^{-1/2}$ in the eigenvector (8) is chosen to have delta-normalized momentum plane waves at time $t = 0$, $\langle q|\phi_{p_0}(0)\rangle = \langle q|p_0\rangle$, i.e., $\langle p_0|p'_0\rangle = \delta(p_0 - p'_0)$. Instead, at the final time, $\langle x|\phi_{p_0}(t_f)\rangle = e^{i\varphi_{p_0}(t_f)}\langle q|p_0 u_0/u_f\rangle$. The invariant eigenstate that starts as a plane wave with momentum p_0 ends being proportional to a plane wave with momentum $p_f = p_0 u_0/u_f$. An arbitrary wave function may be expanded

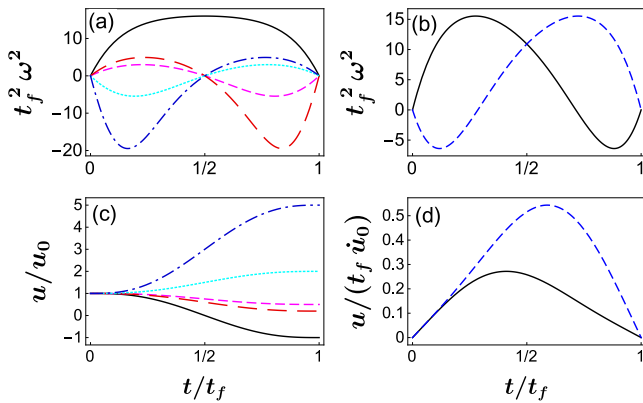


FIG. 1. (a) $\omega^2(t)$ for momentum scaling and (c) corresponding $u(t)$. (b) $\omega^2(t)$ for position scaling and (d) corresponding $u(t)$. Momentum scaling is designed with Eq. (12) and scaling factors $u_0/u_f = 5$ (long-dashed red), $u_0/u_f = 2$ (dashed magenta), $u_0/u_f = 1/2$ (dotted cyan), $u_0/u_f = 1/5$ (dotted-dashed blue), and $u_0/u_f = -1$ (solid black, a momentum-reversing process). Spatial scaling uses a different polynomial for $u(t)$, to satisfy $u(t_b) = \ddot{u}(t_b) = 0$, $\dot{u}(0) = \dot{u}_0$, and $\dot{u}(t_f) = \dot{u}_f$. We depict a focusing protocol, $\dot{u}_0/\dot{u}_f = -1/2$ (dashed blue), and a spreading protocol, $\dot{u}_0/\dot{u}_f = -2$ (solid black). $\omega(t_b) = 0$ in all cases.

on the basis of functions (8) as

$$\psi(q, t) = \left(\frac{u_0}{\hbar u_t}\right)^{1/2} \int dp_0 \exp\left[\frac{i}{\hbar u_t}(u_0 p_0 q + m i q^2/2)\right] \times \exp\left(-i \frac{p_0^2}{2m\hbar} \mathcal{I}_t\right) \langle p_0 | \psi(0) \rangle. \quad (11)$$

Integrating first over q in the (implicit) triple integral $\int dq |\psi(q, t)|^2$ gives a delta function in momentum so $\int dq |\psi(q, t)|^2 = \int dp_0 |\langle p_0 | \psi(0) \rangle|^2$, i.e., the norm is conserved at all times.

Here, we choose polynomial trajectories for simplicity, with the coefficients fixed so that $\dot{u}(t_b) = \ddot{u}(t_b) = 0$, $u(0) = u_0$, $u(t_f) = u_f$,

$$u(t) = u_0 + (u_f - u_0)s^3(10 - 15s + 6s^2), \quad (12)$$

where $s = t/t_f$. See Fig. 1 for examples of this function and the corresponding $\omega^2(t)$. $u(t)$ in Eq. (12) goes from u_0 to u_f monotonously and possesses the symmetry $u(t_f/2 + \tau) + u(t_f/2 - \tau) = u_f + u_0$.

The following first-order moments are calculated from Eq. (11) by using triple integrals and delta-function derivatives. Since $u(t)$ appears only in the form of the ratio $U_t = u_t/u_0$, we can work out all expressions in terms of U_t ,

$$\begin{aligned} \langle q \rangle_t &= \langle q \rangle_0 U_t + \langle p \rangle_0 \frac{U_t}{m} \mathcal{I}_t, \\ \langle p \rangle_t &= \langle q \rangle_0 m \dot{U}_t + \langle p \rangle_0 \frac{\mathcal{A}_t}{U_t}, \end{aligned} \quad (13)$$

where $\mathcal{A}_t = 1 + U_t \dot{U}_t \mathcal{I}_t$. Similarly, the second-order moments are

$$\langle q^2 \rangle_t = \langle p^2 \rangle_0 \left(\frac{U_t \mathcal{I}_t}{m}\right)^2 + \langle qp + pq \rangle_0 \frac{U_t^2 \mathcal{I}_t}{m} + \langle q^2 \rangle_0 U_t^2, \quad (14)$$

$$\begin{aligned} \langle pq + qp \rangle_t &= \langle pq + qp \rangle_0 (1 + 2\dot{U}_t U_t \mathcal{I}_t) \\ &\quad + \langle p^2 \rangle_0 \frac{2\mathcal{I}_t}{m} \mathcal{A}_t + \langle q^2 \rangle_0 2m U_t \dot{U}_t, \end{aligned} \quad (15)$$

$$\begin{aligned} \langle p^2 \rangle_t &= \langle p^2 \rangle_0 \frac{1}{U_t^2} \mathcal{A}_t^2 \\ &\quad + \langle pq + qp \rangle_0 \frac{m \dot{U}_t}{U_t} \mathcal{A}_t + \langle q^2 \rangle_0 (m \dot{U}_t)^2. \end{aligned} \quad (16)$$

The above first- and second-order moments are consistent with the invariants G and I , in the sense that the expectation values of G and I are indeed constant with them. The variances for position and momentum take the form

$$\begin{aligned} (\Delta q)_t^2 &= (\Delta p)_0^2 \left(\frac{U_t \mathcal{I}_t}{m}\right)^2 + (\Delta q)_0^2 U_t^2 \\ &\quad + (\langle qp + pq \rangle_0 - 2\langle q \rangle_0 \langle p \rangle_0) \frac{U_t^2 \mathcal{I}_t}{m}, \end{aligned} \quad (17)$$

$$\begin{aligned} (\Delta p)_t^2 &= (\Delta p)_0^2 \frac{1}{U_t^2} \mathcal{A}_t^2 + (\Delta q)_0^2 (m \dot{U}_t)^2 \\ &\quad + (\langle qp + pq \rangle_0 - 2\langle q \rangle_0 \langle p \rangle_0) \frac{m \dot{U}_t \mathcal{A}_t}{U_t}. \end{aligned} \quad (18)$$

Considering that $\mathcal{A}_f = 1$, we get at t_f that

$$(\Delta p)_f^2 = (\Delta p)_0^2 / U_f^2 \quad (19)$$

for any state. Moreover, $\mathcal{I}_t = t_f \int_0^1 ds / \tilde{U}(s)^2 \sim t_f$, where $\tilde{U}(s) = U(t = st_f)$. For a packet without initial position-momentum correlations $(\Delta q)_f^2 = (\Delta q)_0^2 U_f^2 + \mathcal{O}(t_f^2)$, in other words, a very fast process in which the t_f^2 term is neglected performs the momentum scaling preserving the uncertainty product $\Delta p_f \Delta q_f \approx \Delta p_0 \Delta q_0$. This comes at a price, as the maximal transient value of $|\omega^2|$ (and thus of the absolute value of the potential energy) scales as $\sim t_f^{-2}$ for short times. In other words, demanding shorter and shorter process times requires the ability to implement the harmonic-oscillator potential for energies growing as t_f^{-2} . The practical limitations of the opposite, large time limit are due to the the first term in $\langle q^2 \rangle_t$, which grows as t_f^2 . Thus large process times need a potential implemented over a large spatial range. Similar limitations concern the first moments; in particular, $\langle q \rangle_t$ should not exceed the region where the potential may be implemented. In a realistic setting the harmonic potential will be realized within a temporal, spatial, and energetic domain, which will determine the range of values allowed for the initial (first or second) moments so that the final and/or transient moments do not exceed the set limits.

“Cooling,” conserving phase-space volume, is an obvious application of the above by setting a large factor U_f . Notice that some of the constraints of delta-kick cooling do not apply here; specifically, in DKC [6,19–21] the initial state must be centered at the origin in phase space, so that a free expansion elongates the state along a given well-defined angle (phase line) and a transient harmonic trap rotates the state to the horizontal (position) axis. The present method, instead, does not require any condition for the initial state, other than those imposed by the geometry of the actual setting and technical

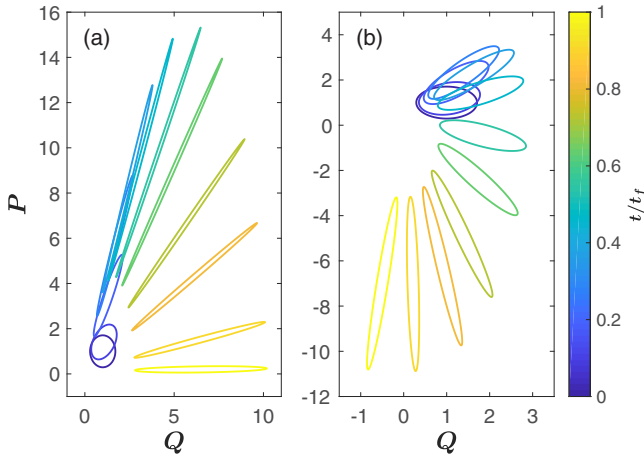


FIG. 2. Evolution of a Gaussian state from $t = 0$ to t_f in phase space. Twelve snapshots at equal time intervals of a Wigner-function contour line. The color sidebar helps to follow the time ordering from $t = 0$ (purple) to t_f (yellow). The dimensionless units are explained in the main text. The initial “off-center” state is a minimum-uncertainty-product state. In the initial state the principal semiaxes are $\Delta Q = \Delta P = 2^{-1/2}$. $\langle P \rangle_0 = \langle Q \rangle_0 = 1$. (a) Momentum scaling, $u_0/u_f = 1/5$. (b) Position scaling, $\dot{u}_0/\dot{u}_f = -1/2$. See corresponding $\omega^2(t)$ in Fig. 1.

limits to implement the harmonic potential. Figure 2(a) shows the evolution of a state in phase space, initially a minimum-uncertainty-product state which is initially “off center.”

There is one more (partial) precedent for stopping all particles regardless of the initial velocity [22]: Classical particles may be stopped by displacing a hard wall away from the origin proportionally to the square root of time. However, in that approach all particles must again depart from the origin at the same time, and the result does not have an exact quantum counterpart [22]. By contrast the current method scales down all momenta for any initial condition both classically and quantumly.

In the simulations and figures we use dimensionless variables for coordinates, times, or momenta, defined from dimensional ones as

$$Q = q/l, \quad s = t/t_f, \quad P = pl/\hbar, \quad (20)$$

where $l = (\hbar t_f/m)^{1/2}$. The Schrödinger equation becomes

$$i\partial\Psi(Q, s)/\partial s = [P^2/2 + \Omega(s)^2 Q^2/2]\Psi(Q, s), \quad (21)$$

where

$$\Omega(s) = t_f\omega(t), \quad \Psi(Q, s) = l^{-1/2}\psi(q, t), \quad P = -i\partial/\partial Q. \quad (22)$$

III. MOMENTUM MIRRORS, POSITION FOCUSING, AND MORE

A. Negative scaling factors

We may consider as well negative scaling factors with a $u(t)$ designed to avoid singularities in $\omega(t)$. The simplest case is $U_f = -1$, which provides a momentum mirror, inverting all momenta regardless of their initial sign and the initial state.

The $u(t)$ function in Eq. (12) is valid for this purpose as the zero of u at $t_f/2$ is canceled by a zero of $\ddot{u}(t_f/2)$; see Fig. 1.

Zeros of $u(t)$ at some intermediate time $t_0 > 0$ might seem to imply singularities in the wave function $\psi(q, t)$ even if $\omega^2(t)$ remains finite. A detailed analysis though shows that cancellations occur, e.g., due to the asymptotic property $\lim_{t \rightarrow t_0} u(t)\mathcal{I}_t = -u_0^2/\dot{u}_{t_0}$, so that the singularities are in fact avoided. A simple example is a Gaussian state for which the momentum integral in Eq. (11) can be done formally.

B. Position focusing or antifocusing

A second extension of the current methodology is “position focusing” or antifocusing, namely, to scale positions rather than momenta. Formally the procedure is very similar, with a different design for $u(t)$ so that $u(t_b) = 0$. Thus the linear invariant (2) is at initial and final times proportional to q . The process scaling is of the form $q_f = q_0\dot{u}_0/\dot{u}_f$. In parallel with Eqs. (8) and (11) we work out the eigenvectors of $G(t)$ in momentum representation with eigenvalues $-m\dot{u}_0q_0$,

$$\phi_{q_0}(p, t) = \left(\frac{\dot{u}_0}{\hbar\dot{u}_t}\right)^{1/2} e^{-\frac{i}{m\dot{u}_t\hbar}(mq_0\dot{u}_0+u_t p^2/2)} e^{-\frac{imq_0^2\mathcal{J}_t}{2\hbar}}, \quad (23)$$

where

$$\mathcal{J}_t = \int_0^t dt' \omega_{t'}^2 \dot{u}_0^2/\dot{u}_{t'}^2, \quad (24)$$

and a corresponding representation for arbitrary wave functions,

$$\psi(p, t) = \int dq_0 \phi_{q_0}(p, t) \langle q_0 | \psi(0) \rangle. \quad (25)$$

The invariant eigenvector and solution of the Schrödinger equation $\phi_{q_0}(t)$ evolves from an eigenvector of position, $\phi_{q_0}(p, 0) = \langle p | q_0 \rangle$, to a scaled version

$$\phi_{q_0}(p, t_f) = (\dot{u}_0/\dot{u}_t)^{1/2} \exp[-imq_0^2\mathcal{J}_t/(2\hbar)] \langle p | q_0 \dot{u}_0/\dot{u}_t \rangle. \quad (26)$$

For completeness, the first moments are

$$\begin{aligned} \langle p \rangle_t &= (-m\mathcal{J}_t \langle q \rangle_0 + \langle p \rangle_0) (\dot{u}_t/\dot{u}_0), \\ \langle q \rangle_t &= \langle p \rangle_0 u_t / (m\dot{u}_0) + \langle q \rangle_0 [\dot{u}_0/\dot{u}_t - (u_t/\dot{u}_0)\mathcal{J}_t]. \end{aligned} \quad (27)$$

These processes may lead to position focusing or to position expansions that can be combined with side inversions if the scaling factor \dot{u}_0/\dot{u}_f is made negative (see Fig. 1). Again, the initial state is arbitrary. A process for focusing with side inversion is depicted in Fig. 2 for an initially off-center state.

C. Arbitrary values for initial and final frequencies

So far we have considered, in all examples and boundary conditions, processes from free motion to free motion, i.e., $\omega(t_b) = 0$. In fact the frequencies at the boundaries may have any desired value by choosing $u(t_b)$ and its derivatives consistently. Specifically for momentum scaling, $G(t_b) = u(t_b)p$ is valid as long as $\dot{u}(t_b) = 0$, so $\omega(t_b) = 0$ is not necessary. Thus the approach can be adapted to scale the momenta from a trap with $\omega_0 = \omega(0)$ to a trap with $\omega_f = \omega(t_f)$. Also the kinetic energy is scaled but not necessarily the total energy. A possible application could be to control the temperature if its final desired value does not correspond to that of an adiabatic

process. The momentum does not commute with $H(t_b)$ for nonzero $\omega(t_b)$, so the final momenta will not be conserved for $t > t_f$ unless the trap is switched off abruptly at t_f . As for position scaling, its combination with a nonzero $\omega(t_b) = 0$ provides a way to scale the potential energy at will, since the quadratic invariant I becomes proportional to the potential energy at boundary times in these protocols.

D. Relation to Ermakov invariants

Note that the quadratic invariant (4) does not have the general form of the Ermakov quadratic invariant I_E [10,12],

$$I_E = \frac{1}{2m} \left[\left(\frac{Kq}{\rho} \right)^2 + (\rho p - m\dot{\rho}q)^2 \right], \quad (28)$$

where K is a constant and ρ (here with dimensions of length) satisfies the Ermakov equation

$$\ddot{\rho} + \omega^2(t)\rho = \frac{K^2}{\rho^3}. \quad (29)$$

To get the generic Ermakov quadratic invariant from a linear invariant of the form (2), u has to be made complex (see, e.g., Refs. [17,18]). However, if we take $u = \rho$ to be real and set $K = 0$, then $I = I_E$. This particular form may explain why the possibility to scale momenta or positions has been overlooked so far when using the Ermakov invariants for inverse engineering. I_E is typically applied choosing $K = \omega_0\rho(0)^2 \neq 0$ for processes where both ω_0 and ω_f are nonzero [9,10,13]. Then I_E can be made proportional to initial and final oscillator

Hamiltonians, and the basis spanned by its eigenstates is a discrete one.

IV. DISCUSSION

Spreads of momentum or velocity of initial particles often lead to particle loss and inefficiencies in focusing, slowing, or acceleration processes. Shortcuts to adiabaticity techniques can be made very robust with respect to initial conditions or protocol imperfections. This feature and the possibility to choose and shorten the process time make them powerful tools to design cooling [13,23,24], even for open systems [25–28], launching [29], or compression and expansion protocols [9,10]. This work, in particular, demonstrates that by making use of linear invariants, momentum or position scaling, irrespective of initial conditions of the particle, can be achieved. The proposed methodology can be adapted to sequential interactions for beam control or for trapped particles, for example, providing a robust alternative to DKC to reach picokelvin temperatures. A simple extension of the present framework making use of moving potentials gives further control possibilities, e.g., to create a narrow momentum band around a desired “launching” momentum value (other than zero).

ACKNOWLEDGMENTS

This work was supported by the Basque Country Government (Grant No. IT986-16) and by Grants No. PGC2018-101355-B-I00 (MCIU/AEI/FEDER,UE) and No. FIS2016-80681P.

-
- [1] W. D. Phillips and H. Metcalf, Laser Deceleration of an Atomic Beam, *Phys. Rev. Lett.* **48**, 596 (1982).
 - [2] H. L. Bethlem, G. Berden, and G. Meijer, Decelerating Neutral Dipolar Molecules, *Phys. Rev. Lett.* **83**, 1558 (1999).
 - [3] R. Fulton, A. I. Bishop, and P. F. Barker, Optical Stark Decelerator for Molecules, *Phys. Rev. Lett.* **93**, 243004 (2004).
 - [4] E. Narevicius, C. G. Parthey, A. Libson, M. F. Riedel, U. Even, and M. G. Raizen, Towards magnetic slowing of atoms and molecules, *New J. Phys.* **9**, 96 (2007).
 - [5] K. Dulitz, M. Motsch, N. Vanhaecke, and T. P. Softley, Getting a grip on the transverse motion in a Zeeman decelerator, *J. Chem. Phys.* **140**, 104201 (2014).
 - [6] S. Chu, J. E. Bjorkholm, A. Ashkin, J. P. Gordon, and L. W. Hollberg, Proposal for optically cooling atoms to temperatures of the order of 10–6 K, *Opt. Lett.* **11**, 73 (1986).
 - [7] K. Yagi, S. Tamura, and T. Tokuyama, Germanium and silicon film growth by low-energy ion beam deposition, *Jpn. J. Appl. Phys.* **16**, 245 (1977).
 - [8] *Industrial Accelerators and Their Applications*, edited by R. W. Hamm and M. E. Hamm (World Scientific, Hackensack, NJ, 2012).
 - [9] E. Torrontegui, S. Ibáñez, S. Martínez-Garaot, M. Modugno, A. del Campo, D. Guéry-Odelin, A. Ruschhaupt, X. Chen, and J. G. Muga, Shortcuts to adiabaticity, in *Advances in Atomic, Molecular, and Optical Physics* (Elsevier, Amsterdam, 2013), Vol. 62, Chap. 2, pp. 117–169.
 - [10] D. Guéry-Odelin, A. Ruschhaupt, A. Kiely, E. Torrontegui, S. Martínez-Garaot, and J. G. Muga, Shortcuts to adiabaticity: concepts, methods, and applications, *Rev. Mod. Phys.* **91**, 045001 (2019).
 - [11] J. G. Muga, R. Sala, and R. F. Snider, Comparison of classical and quantal evolution of phase space distribution functions, *Phys. Scr.* **47**, 732 (1993).
 - [12] H. R. Lewis and W. B. Riesenfeld, An exact quantum theory of the time-dependent harmonic oscillator and of a charged particle in a time-dependent electromagnetic field, *J. Math. Phys.* **10**, 1458 (1969).
 - [13] X. Chen, A. Ruschhaupt, S. Schmidt, A. del Campo, D. Guéry-Odelin, and J. G. Muga, Fast Optimal Frictionless Atom Cooling in Harmonic Traps: Shortcut to Adiabaticity, *Phys. Rev. Lett.* **104**, 063002 (2010).
 - [14] O. Castanos, R. Lopez-Pena, and V. I. Man’ko, Noether’s theorem and time-dependent quantum invariants, *J. Phys. A: Math. Gen.* **27**, 1751 (1994).
 - [15] M. Fernández-Guasti and H. Moya-Cessa, Solution of the Schrödinger equation for time-dependent 1D harmonic oscillators using the orthogonal functions invariant, *J. Phys. A: Math. Gen.* **36**, 2069 (2003).
 - [16] M. Lohe, Exact time dependence of solutions to the time-dependent Schrödinger equation, *J. Phys. A: Math. Theor.* **42**, 035307 (2009).

- [17] M. Fernández-Guasti and A. Gil-Villegas, Orthogonal functions invariant for the time-dependent harmonic oscillator, *Phys. Lett. A* **292**, 243 (2002).
- [18] A. Tobalina, E. Torrontegui, I. Lizuain, M. Palmero, and J. G. Muga, Invariant-based inverse engineering of time-dependent, coupled harmonic oscillators, [arXiv:2007.15055](https://arxiv.org/abs/2007.15055).
- [19] H. Ammann and N. Christensen, Delta Kick Cooling: A New Method for Cooling Atoms, *Phys. Rev. Lett.* **78**, 2088 (1997).
- [20] H. Myrskog, J. K. Fox, H. S. Moon, J. B. Kim, and A. M. Steinberg, “Modified delta-kick cooling” using magnetic field gradients, *Phys. Rev. A* **61**, 053412 (2000).
- [21] T. Kovachy, J. M. Hogan, A. Sugarbaker, S. M. Dickerson, C. A. Donnelly, C. Overstreet, and M. A. Kasevich, Matter Wave Lensing to Picokelvin Temperatures, *Phys. Rev. Lett.* **114**, 143004 (2015).
- [22] S. Schmidt, J. G. Muga, and A. Ruschhaupt, Stopping particles of arbitrary velocities with an accelerated wall, *Phys. Rev. A* **80**, 023406 (2009).
- [23] T. Sägerser, R. Matt, R. Oswald, and J. P. Home, Robust dynamical exchange cooling with trapped ions, *New J. Phys.* **22**, 073069 (2020).
- [24] J. P. Bartolotta, J. T. Reilly, and M. J. Holland, Speeding up particle slowing using shortcuts to adiabaticity, *Phys. Rev. A* **102**, 043107 (2020).
- [25] I. A. Martínez, A. Petrosyan, D. Guéry-Odelin, E. Trizac, and S. Ciliberto, Engineered swift equilibration of a Brownian particle, *Nat. Phys.* **12**, 843 (2016).
- [26] T. Villazon, A. Polkovnikov, and A. Chandran, Swift heat transfer by fast-forward driving in open quantum systems, *Phys. Rev. A* **100**, 012126 (2019).
- [27] R. Dann, A. Tobalina, and R. Kosloff, Shortcut to Equilibration of an Open Quantum System, *Phys. Rev. Lett.* **122**, 250402 (2019).
- [28] S. Alipour, A. Chenu, A. Rezakhani, and A. del Campo, Shortcuts to adiabaticity in driven open quantum systems: Balanced gain and loss and non-Markovian evolution, *Quantum* **4**, 336 (2020).
- [29] A. Tobalina, M. Palmero, S. Martínez-Garaot, and J. G. Muga, Fast atom transport and launching in a nonrigid trap, *Sci. Rep.* **7**, 5753 (2017).